

NTIS # PB2009-

SSC-457

**INVESTIGATION OF PLASTIC LIMIT
STATES FOR DESIGN OF SHIP HULL
STRUCTURES**



This document has been approved
For public release and sale; its
Distribution is unlimited

SHIP STRUCTURE COMMITTEE
2009

Ship Structure Committee

RADM Brian M. Salerno
U. S. Coast Guard Assistant Commandant,
Assistant Commandant for Marine Safety, Security and Stewardship
Chairman, Ship Structure Committee

{Name}
{Title}
Naval Sea Systems Command

Mr. Christopher McMahon
Director, Office of Ship Construction
Maritime Administration

Mr. Kevin Baetsen
Director of Engineering
Military Sealift Command

UNITED STATES COAST GUARD
Mr. Jeffrey Lantz,
Commercial Regulations and Standards for the
Assistant Commandant for Marine Safety, Security
and Stewardship
Mr. Jeffery Orner
Deputy Assistant Commandant for Engineering and
Logistics

Dr. Roger Basu
Senior Vice President
American Bureau of Shipping

Mr. Donald Roussel
Director General, Marine Safety,
Safety & Security
Transport Canada

Dr. Neil Pegg
Group Leader - Structural Mechanics
Defence Research & Development Canada - Atlantic

EXECUTIVE DIRECTOR
Lieutenant Commander, Jason Smith
U. S. Coast Guard

ADMINISTRATIVE ASSISTANT
Ms. Jeannette Y. Grant
U. S. Coast Guard

SHIP STRUCTURE SUB-COMMITTEE

AMERICAN BUREAU OF SHIPPING (ABS)

Mr. Glenn Ashe
Mr. Derek Novak
Mr. Phil Rynn
Mr. Balji Menon

MARITIME ADMINISTRATION (MARAD)

Mr. Chao Lin
Mr. Carl Setterstrom
Mr. Richard Sonnenschein

NAVY/ONR / NAVSEA/NSWCCD

{Name}
{Name}
{Name}
{Name}

UNITED STATES COAST GUARD

CDR Charles Rawson
Mr. James Person
CAPT Paul Roden
Mr. Rubin Sheinberg

DEFENCE RESEARCH & DEVELOPMENT CANADA ATLANTIC

Dr. David Stredulinsky
Mr. John Porter

MILITARY SEALIFT COMMAND (MSC)

Mr. Michael W. Touma
Mr. Paul Handler

TRANSPORT CANADA

Paul Denis Vallee

SOCIETY OF NAVAL ARCHITECTS AND MARINE ENGINEERS (SNAME)

Mr. Jaideep Sirkar
Mr. Al Rowen
Mr. Norman Hammer

Member Agencies:

*American Bureau of Shipping
Defence Research and Development Canada
Maritime Administration
Military Sealift Command
Naval Sea Systems Command
Society of Naval Architects & Marine Engineers
Transport Canada
United States Coast Guard*



Ship
Structure
Committee

Address Correspondence to:

COMMANDANT (CG-5212/SSC)
ATTN (EXECUTIVE DIRECTOR/SHIP
STRUCTURE COMMITTEE)
US COAST GUARD
2100 2ND ST SW STOP 7126
WASHINGTON DC 20593-7126
Website: <http://www.shipstructure.org>

SSC – 457
SR –1442

SEPTEMBER 12, 2009

**SHIP FRAME RESEARCH PROGRAM - AN EXPERIMENTAL STUDY OF SHIP FRAMES
AND GRILLAGES SUBJECTED TO PATCH LOADS**

The research described here was conducted as part of a comprehensive study of the ultimate strength of ships frames. This report's focus is on frames subject to intense local lateral loads, such as ice loads. The experimental investigation of single frames, small grillages, and two large grillages subjected to these loads was conducted.

This report presents a summary and overview of the experimental work along with a description of the results. Findings from the experimental study imply that post yield response is initially linear and is practically indistinguishable from elastic response. The magnitude of this type of behavior depends on the section shape. This pseudo-elastic behavior is quite small for symmetric I beams but is quite large for flat bar stiffeners in ships.

A handwritten signature in black ink, appearing to read 'B. Salerno', with a long, sweeping underline that extends to the right.

BRIAN M. SALERNO
Rear Admiral, U.S. Coast Guard
Chairman, Ship Structure Committee

1. Report No. SSC-457		2. Government Accession No.		3. Recipient's Catalog No.	
4. Title and Subtitle Ship Frame Research Program- A Experimental Study of Ship Frames and Grillages Subjected to Patch Loads				5. Report Date	
				6. Performing Organization Code	
7. Author(s) Daley, C. and Hermanski, G.				8. Performing Organization Report No. SR-1442	
9. Performing Organization Name and Address Memorial University of Newfoundland / Nat'l Research Council of Canada Ocean Engineering Research Center / Institute for Ocean Technology				10. Work Unit No. (TRAIS)	
				11. Contract or Grant No.	
12. Sponsoring Agency Name and Address Ship Structure Committee U.S. Coast Guard (CG-5212/SSC) 2100 Second Street, SW Washington, DC 20593				13. Type of Report and Period Covered Final Report	
				14. Sponsoring Agency Code CG-5	
15. Supplementary Notes Sponsored by the Ship Structure Committee. Jointly funded by its member agencies.					
<p>16. Abstract</p> <p>Continuing improvements in materials and ship construction technology are encouraging change. An increasingly sensitive public has lead to demands on the governments, shipping companies and classification societies to find way to make ships safer.</p> <p>As part of this trend, new ship structural rules are going beyond the traditional approach of using yielding as the design criterion. The ice class rules developed during the 1980's and 1990's have all been formulated using plastic limit states for the sizing of plating and framing.</p> <p>This research program began with the aim of validating the limit state equations for single frames, determining any limits to the validity, and exploring the way frames interact in grillages.</p>					
17. Key Words			18. Distribution Statement Distribution is available to the public through: National Technical Information Service U.S. Department of Commerce Springfield, VA 22151 Ph. (703) 487-4650		
19. Security Classif. (of this report) Unclassified		20. Security Classif. (of this page) Unclassified		21. No. of Pages	22. Price

CONVERSION FACTORS
(Approximate conversions to metric measures)

To convert from	to	Function	Value
LENGTH			
inches	meters	divide	39.3701
inches	millimeters	multiply by	25.4000
feet	meters	divide by	3.2808
VOLUME			
cubic feet	cubic meters	divide by	35.3149
cubic inches	cubic meters	divide by	61,024
SECTION MODULUS			
inches ² feet ²	centimeters ² meters ²	multiply by	1.9665
inches ² feet ²	centimeters ³	multiply by	196.6448
inches ⁴	centimeters ³	multiply by	16.3871
MOMENT OF INERTIA			
inches ² feet ²	centimeters ² meters	divide by	1.6684
inches ² feet ²	centimeters ⁴	multiply by	5993.73
inches ⁴	centimeters ⁴	multiply by	41.623
FORCE OR MASS			
long tons	tonne	multiply by	1.0160
long tons	kilograms	multiply by	1016.047
pounds	tonnes	divide by	2204.62
pounds	kilograms	divide by	2.2046
pounds	Newtons	multiply by	4.4482
PRESSURE OR STRESS			
pounds/inch ²	Newtons/meter ² (Pascals)	multiply by	6894.757
kilo pounds/inch ²	mega Newtons/meter ² (mega Pascals)	multiply by	6.8947
BENDING OR TORQUE			
foot tons	meter tons	divide by	3.2291
foot pounds	kilogram meters	divide by	7.23285
foot pounds	Newton meters	multiply by	1.35582
ENERGY			
foot pounds	Joules	multiply by	1.355826
STRESS INTENSITY			
kilo pound/inch ² inch ^{1/2} (ksi√in)	mega Newton MNm ^{3/2}	multiply by	1.0998
J-INTEGRAL			
kilo pound/inch	Joules/mm ²	multiply by	0.1753
kilo pound/inch	kilo Joules/m ²	multiply by	175.3

TABLE OF CONTENTS: VOLUME 1

Table of Figures

Table of Tables

Symbols and Notation

Acknowledgement

1	Introduction	1
2	Background and Discussion	2
3	Overview and Data Collection.....	4
3.1	Overview of Experiments.....	4
3.2	Data Collection	4
4	Single Frame Tests.....	6
4.1	Description of Single Frame Experiments.....	6
4.2	Data, Plots and Photos of the Single Frame Tests	9
4.3	Discussion of the Single Frame Tests	11
5	Large Grillage Tests	13
5.1	Description of Large Grillage Experiments	13
5.2	Load-Deflection Results for the Large Grillage	16
5.3	Photographs of the Large Grillage Tests	18
5.4	Discussion of Large Grillage Tests	29
6	Material Test Data	30
7	Conclusions	31
8	Recommendations.....	32
9	References	33

Appendix A – Single Frame Experimental Data Tables and Plots

Appendix B – Single Frame Material Test Data Tables and Plots

Appendix C – Large Grillage Test Data Tables and Plots

Table of Figures

Figure 1: Idealized load-deflection curve for a frame subjected to a lateral patch load..... 3

Figure 2: Frame Sections 4

Figure 3: Data Collection components..... 5

Figure 4: Single Frame Tests (first six) 6

Figure 5: Single Frame Test L75c..... 6

Figure 6: Single Frame L75e 7

Figure 7: Single Frame Tests (for T50c and Fc) 7

Figure 8: Single Frame Test (Fc) 8

Figure 9: Load-Displacement plot for single frame flatbar test (Fc) 8

Figure 10: Load-Displacement plot for single frame flatbar test (Fc) 9

Figure 10: Comparison of T50c and Fc tests. 10

Figure 11: Large Grillage Test Setup..... 13

Figure 12: Large Grillage Test 1 Setup..... 14

Figure 13: Large Grillage Test 2 Setup..... 14

Figure 14: Large Grillage Test Arrangement 15

Figure 15: Load-Deflection for Large Grillage 1 (additional plots in Appendix C) 16

Figure 16: Load-Deflection for Large Grillage 2 (additional plots in Appendix C) 17

Figure 17: LG1_2 test prior to load 18

Figure 18: LG1_1 prior to test..... 19

Figure 19: LG1_1 test overview..... 19

Figure 20: LG1_1 test: MicroScribe measurements at 271kips (1205kN)..... 20

Figure 21: LG1_1 test: web deformation at 281kips (1250 kN)..... 20

Figure 22: LG1_1 test web deformation at 291kips (1294 kN)..... 21

Figure 23: LG1_1 View of ram on plate 21

Figure 24: LG1_1 view of ram after test (note imprint)..... 22

Figure 25: LG1_2 test: MicroScribe measurements at 330 kips (1468 kN)..... 22

Figure 26: LG1_2 test: web deformation at 330kips (1468 kN)..... 23

Figure 27: LG1_2 test: close-up of web deformation at 330kips (1468 kN) 23

Figure 28: LG1_2: ram after test (note imbedded platen and small tear)..... 24

Figure 29: LG1_2 test, web distortion 24

Figure 30: LG1_3 at 198 kips (note: load is at center, with prior shear damage at end) 25

Figure 31: LG2_2 side view 25

Figure 32: LG2_2 at 202kips 26

Figure 33: LG2_2: End after prior center load. 26

Figure 34: Large Grillage end clamp arrangement. 27

Figure 35: Large Grillage test overview. 27

Figure 36: LG2_1 - Partial Image Sequence 28

Figure 37: Load vs. deflection for three of the single frame tests..... 30

Table of Tables

Table 1: Single Frame Tests Conducted.....	7
Table 2: Large Grillage Tests Conducted	15

Symbols and Notation

IACS	International Association of Classification Societies
a	length of shear panel
A_f	area of the flange
A_w	area of the web
b	height of the ice load patch
h_w	height of the web
k_w	area ratio
k_z	ratio of z_p to Z_p
L	length of frame
P_{3h}	pressure causing collapse for case of 2 fixed supports
P_s	pressure causing collapse for end load case
S	frame spacing
tw	thickness of web
Z_p	plastic section modulus
z_p	sum of plastic section moduli of plate and flange
Z_{pns}	a non-dimensional modulus
σ_y	yield stress
L1800nb_W11/308_P20_F16/95	This refers to an L section frame, 1800mm long, with a Web 11mm thick, 308mm high, with 20mm shell Plate, and a 16 by 95mm Flange.

Acknowledgement

The work was made possible with the support of funding from a number of organizations sponsoring this research program. These include Ship Structures Committee and its member agencies. The close interaction with the representatives of Transport Canada, Defense Research and Development Canada (Atlantic), and the US Coast Guard is acknowledged. In particular we acknowledge the input and support from Mr. Jacek Dubiel (TC), Mr. Dave Stredulinsky (DRDC) and Mr. Alfred Tunik (USCG). Sadly, Mr. Jacek Dubiel passed away in 2008.

1 Introduction

The design of ship structures is undergoing considerable change. The reasons for the change are numerous. New and larger ships are continuing to address new commercial opportunities. Continuing improvements in materials and ship construction technology are encouraging change. The constant improvement of computational power is letting researchers and designers contemplate and execute ever more sophisticated simulations of ship structural behavior (loads and failure mechanisms). An increasingly sensitive public has led to demands on the governments, shipping companies and classification societies to find way to make ships safer. The International Maritime Organization (IMO) is the focal point for much of the discussion and debate.

As part of this trend, new ship structural rules are going beyond the traditional approach of using yielding as the design criterion. The ice class rules developed during the 1980s and 90s (Transport Canada 1995, IACS 2006) have all been formulated using plastic limit states for the sizing of plating and framing. The new IACS Common Structural Rules (IACS 2005) have included certain assessment of plastic limit states in their formulations.

The research described here is being conducted as part of a comprehensive study of the ultimate strength of ships frames (Pavic, Daley, Hussein and Hermanski, 2004; Daley and Hermanski, 2005). The current focus is on frames subject to intense local lateral loads, such as ice loads. The work was begun with support from Transport Canada to study single frames. Eight single frames were tested. The US Coast Guard then joined the project and enabled an expansion of the experimental and numerical analysis. The experimental program was then further expanded with the support of the Ship Structures Committee, which funded the experimental investigation of two large grillages.

This report represents a summary and overview of the experimental work along with a description of the results.

2 Background and Discussion

The Ocean Engineering Research Center and the Institute for Ocean Technology have conducted a research program to study the plastic behavior and ultimate limit states of ship frames and grillages subject to lateral loads. This work began as the result of the development of the new IACS Unified Requirement for Polar Ship Construction (IACS/URI2 or Polar Rules). The Polar Rules contain limit state equations for ship frames subject to lateral loads (ice loads) [3]. The limit state equations were derived on the basis of energy methods (plastic work) [4]. This research program began with the aim of validating the limit state equations for single frames, determining any limits to the validity, and exploring the way frames interact in grillages. The problem under study also applies to cases of hydrodynamic impact and other types of collisions. As a result, the research applies to most ship structures and many types of offshore structures.

The first phase of the experiments focused on single frames in isolation and was the first attempt to experimentally assess the validity of the IACS/URI2 equations. URI2 contains a set of requirements that are based on 3 distinct limit states. URI2 contains a formula for the required minimum shear area and the required modulus. The required shear area and modulus are considered together. In this way the interaction between bending and shear is accounted for. These are explained in [4,5,6]. Also given are related capacity equations that give the patch pressure that will cause the limit state to occur in both 3 hinge bending (for a central load), and end shear collapse (for an end load). Equation (1) gives the central load capacity value. The terms are defined in the nomenclature. A full explanation is given in [4,5].

$$P_{3h} = \frac{(2 - kw) + kw \sqrt{1 - 48 \cdot Zpns \cdot (1 - kw)}}{12 \cdot Zpns \cdot kw^2 + 1} \cdot \frac{Zp \cdot \sigma_y \cdot 4}{\left[S \cdot b \cdot L \cdot \left(1 - \frac{b}{2 \cdot L} \right) \right]} \quad (1)$$

The experimental work was supported by extensive finite element analysis, [1,2].

Figure 1 sketches the typical load deflection pattern that was observed in the test frames. The deflection plotted is the maximum deflection of the web under at the plate-web connection. The UR limit state (equation 1) represents a capacity comparable to that labeled “plastic mechanism” in Figure 1. This is only the first plastic mechanism. It may be the only mechanism, or it may be the first of many local plastic mechanisms. Prior to that point ‘P’, the load-deflection curve is essentially linear and follows the original elastic slope. Yielding occurs well before point ‘P’. This is followed by the expansion of the plastic zone, during which stress redistribution takes place. Once the plastic zone fills one or more critical cross sections, the initial plastic mechanism forms, allowing large and permanent deformations. The first plastic mechanism might be called ‘collapse’, though this term is not exactly correct. Subsequent to point ‘P’, while the frame is ‘collapsing’ in bending, membrane forces tend to rise and support the growing load. Further along this curve, additional mechanisms can occur, including various plastic folding mechanisms, possibly buckling (though this is rare for the cases studies) and fracture (which was also quite rare). In the analyses in this report, some frames experienced a kind of local plastic buckling after

the first mechanism. These behaviors were never sudden and were probably not analogous to 'Euler' buckling. In most case the frames would exhibit monotonically increasing capacity, even as the permanent deflections grow very large.

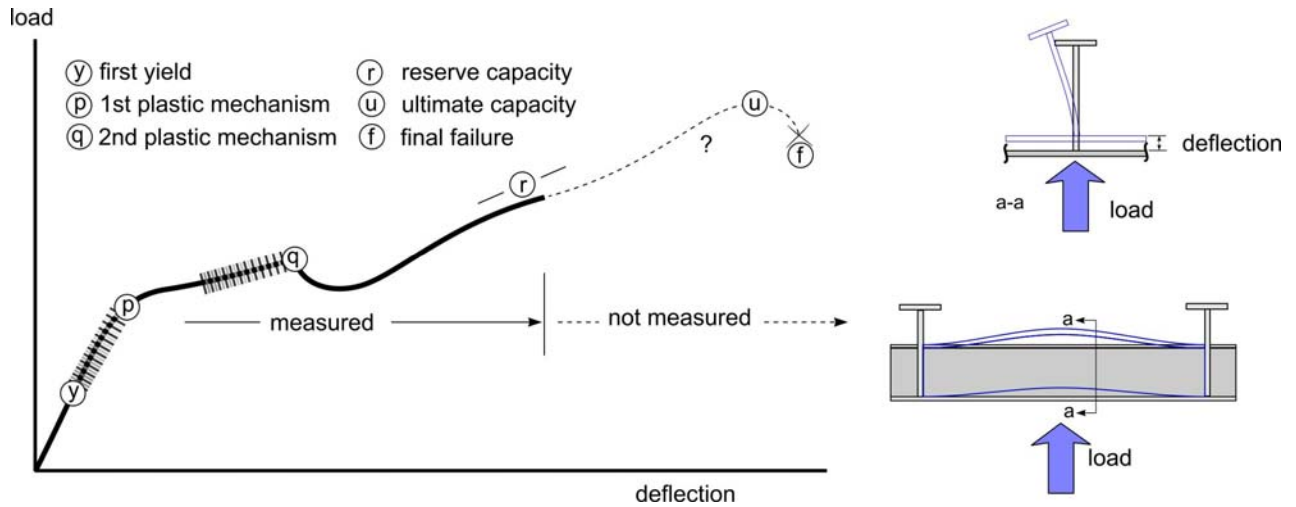


Figure 1: Idealized load-deflection curve for a frame subjected to a lateral patch load.

3 Overview and Data Collection

3.1 Overview of Experiments

The experimental program has provided empirical evidence to support the numerical and analytical investigations. The experiments explored the influence of frame geometry (for single frames), load position (central and end) and frame boundary conditions. In ships, any single frame is joined laterally to neighboring frames through the shell plating. At their ends, frames typically continue to the next bay, through a supporting stringer (or similar). The experiments examined a range of frame support conditions. In the single frame tests, the frame ends are held rigidly (as rigidly as possible), while the sides were free. In the large grillage the frames continued through a stringer and on to a remote fixed support. Also, on both sides of the central frame, there were neighboring frames and a heavy side bar, designed to approximate additional frames. Thus in the large grillage, both the side and end conditions (for the central frame) are realistic. Figure 2 shows the cross sections of the frames tested. The grillages were all made with the T75 frame section.

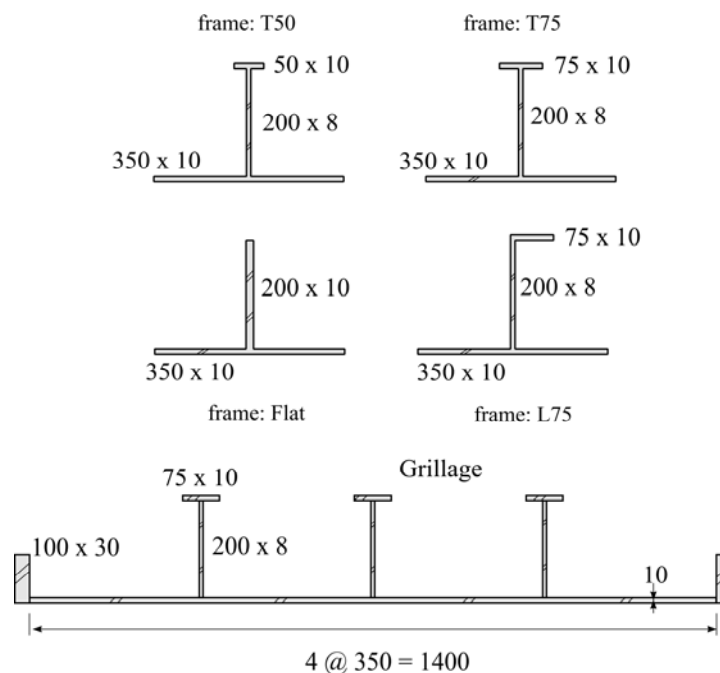


Figure 2: Frame Sections

3.2 Data Collection

The components of the data collection system are shown in Figure 3. The data collection system was very similar for all tests conducted. In the first six single frame tests, the load was measured

with a load cell, in line with the actuator. In the later tests, the load was determined by measuring the hydraulic pressure in the load jack. The system was calibrated in a press, to ensure that the calculated and measured loads were in agreement. Strain was measured with a set of resistance strain gauges. The strain gauges were long-elongation gauges, chosen to give values well up into the plastic strain region. Deflections were measured with a set of wire-reel extensometers ('yo-yo' pots.). The strain, deflection and loads were all gathered Local deformations were also recorded automatically throughout the test using hardware and software (LabView™) from National Instruments. In addition, a 3D coordinate measurement device (microscribe from Immersion Corporation) was used to determine the distortion of the frame under load. The microscribe was connected to a computer running Rhinoceros (from McNeel and Associates), where the 3D deformation data was recorded . At each load step, the microscribe was used to manually measure the x,y,z coordinates of about 15 points on the cross section above the load.

In addition to the numerical data, digital still and video images of the tests have been recorded. One 6mp still camera was used to gather time-lapse images of the later tests. These images can be viewed individually or as a motion video. The digital video used DV format tapes.

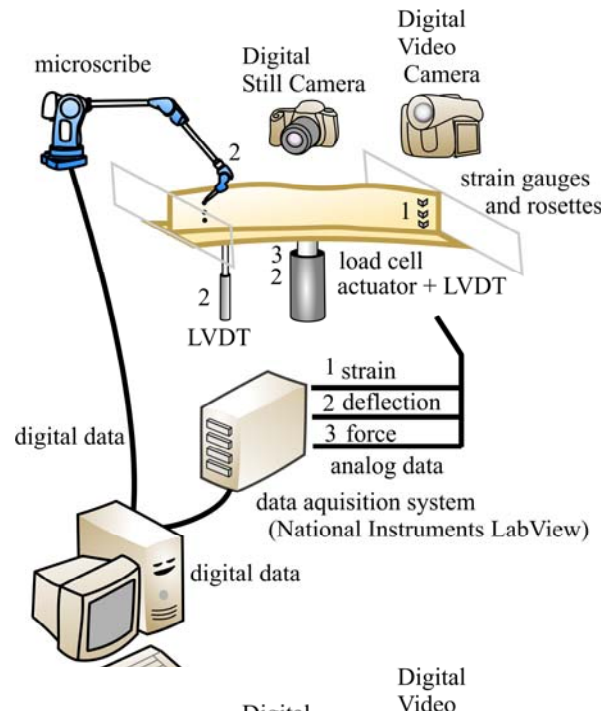


Figure 3: Data Collection components

4 Single Frame Tests

4.1 Description of Single Frame Experiments

The first six single frame tests were conducted using the support frame illustrated in Figure 4. Photos of two tests are shown in Figure 5 and Figure 6. At first, a 350x350mm (14"x14") silicon filled loading pillow was used to apply the load (see Figure 5). This proved to be problematic, so that after two tests, the load was applied through a 102x102mm (4"x4") square steel block (Figure 6).

After the first six single frame tests were complete, the new grillage test apparatus was ready for use. This large support structure was then used to test that last two of the single frames (Figure 7 and Figure 8). Table 1 summarizes the eight single frame tests that have been conducted.

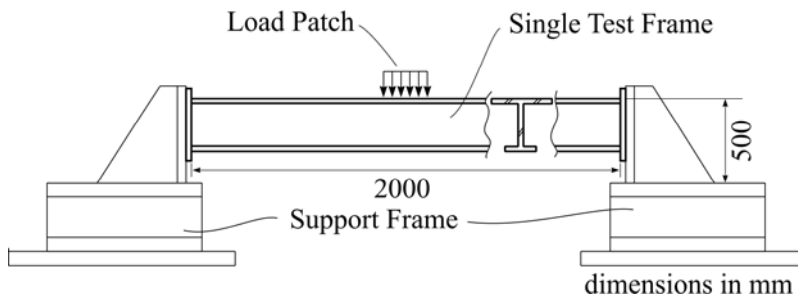


Figure 4: Single Frame Tests (first six)



Figure 5: Single Frame Test L75c

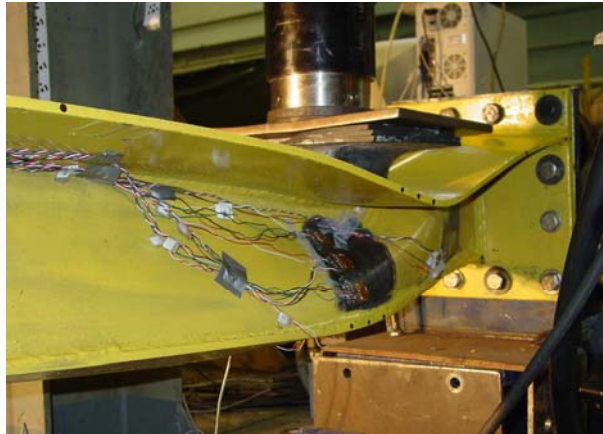


Figure 6: Single Frame L75e

Table 1: Single Frame Tests Conducted

Test Name	Load Position	Test Date	Frame Description*
L75e	End	8/18/2004	200x8,75x10 L
L75c	Center	10/7/2004	200x8,75x10 L
T75e	End	5/19/2004	200x8,75x10 T
T75c	Center	8/12/2004	200x8,75x10 T
T50e	End	7/16/2004	200x8,50x10 T
T50c	Center	6/16/2005	200x8,50x10 T
Fe	End	7/28/2004	200x10 Fl
Fc	Center	6/6/2005	200x10 Fl

*dimensions in mm.

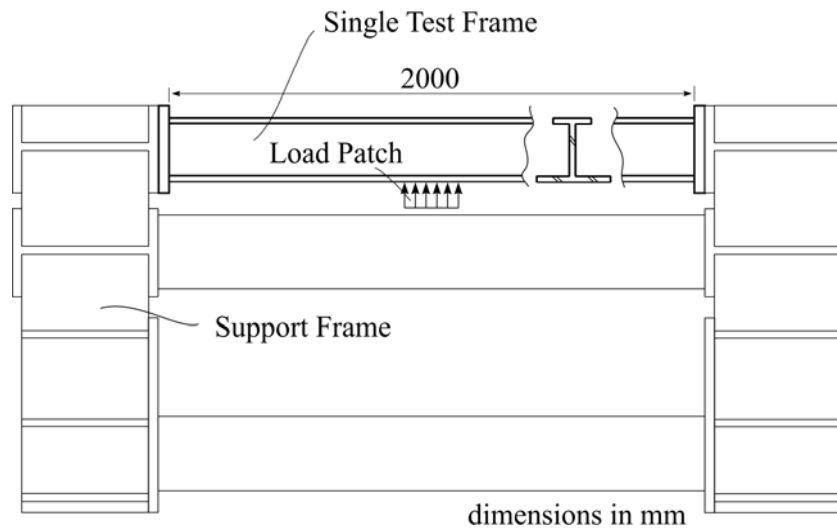


Figure 7: Single Frame Tests (for T50c and Fc)



Figure 8: Single Frame Test (Fc)

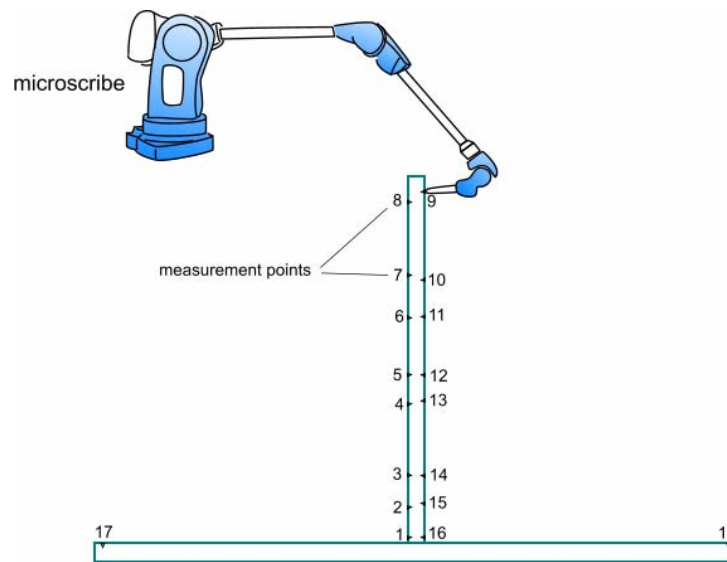


Figure 9: Flatbar (Fc) microscribe measurement points

4.2 Data, Plots and Photos of the Single Frame Tests

Appendix A contains the data and photographs for the single frame tests. Figure 10 shows one of the plots for the flat bar. In this case there are multiple points at which deflection is reported (along the web, below the load). Figure 9 shows the location of the 18 points. The plot shows that all the points along the web deflected in a very similar way, emphasizing that web stayed upright (see also Figure 11).

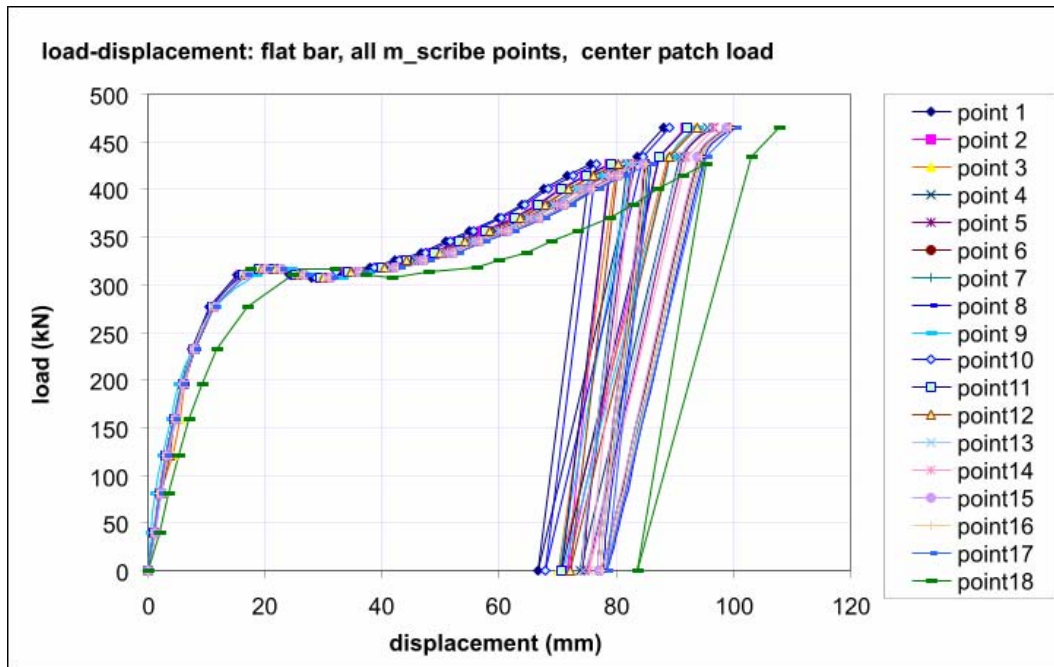


Figure 10: Load-Displacement plot for single frame flatbar test (Fc)



Figure 11: Comparison of T50c and Fc tests.

4.3 Discussion of the Single Frame Tests

The single frame tests were generally quite successful, though several challenges and difficulties arose during the experiments. Many of the lessons learned seem obvious in hindsight, but were not so initially. In terms of experimental lessons learned, the main ones are;

- The strength and stiffness of the support structure was initially underestimated. It proved to be very difficult to employ the ‘strong floor’ in the Memorial structures lab to help resist the forces. A fully self-reacting frame was required. Although costly, support frames should be as large and rigid as possible.
- A photographic technique for measuring 3D deformations was tried. This did not work well for several reasons. The technique worked best with bright but flat lighting (ie no shadows). This proved to be very difficult to achieve and caused such excessive delays in testing that the procedure was abandoned. While such techniques are appealing, much more preparation would be required.
- Application of a uniform pressure proved to be quite difficult and was eventually abandoned in favor of applying a known displacement (with a small square steel block). An air-filled steel pillow may have worked, but was not used due to risk of explosive failure at the very high loads planned. A gel-filled rubber pillow and a coarse steel powder-filled pillow were both tried without success. The extremely high loads required for plastic deformation of the frames caused the pillows to burse. Some much stronger pillow material would be needed.
- While the small steel blocks used to apply the loads worked quite well (simulating a very small high pressure patch, almost a point load), there were drawbacks. At very high loads the loading block would punch through the steel plate. This artificial failure prevented finding the true ultimate strength of the frame. Eventually the frames would be expected to fail by some form of rupture, but not by the punching failure seen in the tests.

The single frame tests illustrated several important aspects of plastic response. Several key insights about plastic frame strength include;

- While the elastic section modulus may be useful as a measure of initial elastic strength, it does not reflect the plastic behavior and capacity. Even the plastic section modulus may be inappropriate. As frames response plastically, they shear and fold. The change in shape negates the ‘plane sections remain plane’ assumption that underpins most beam analysis. The key to plastic capacity in a frame is the resistance to local plastic folding and any other important local mechanisms. These properties are not reflected in ‘modulus’ values.
- Plastic ultimate strength is not an easy concept to define. The plastic behavior may include many aspects, some of which are more desirable than others. There is no single measure that can be used to compare frames. Such measures would be quite useful, and will likely be developed as plastic design become more common.
- The initial post-yield behavior is indistinguishable from elastic behavior. Some frames have considerably more of this post-yield near-elastic behavior than others. In such frames yielding serves to strengthen the frame with no observable effects. The strengthening is created by three separate effects. The first effect is the creating of residual plastic stress pattern that helps support the load (a kind of press-stressing). The second effect is local

strain hardening in the extreme fibers (strengthening those fibers). The third effect, which only occurs with quite large and observable deformations, is the geometric strengthening (equivalent to membrane strength). These behaviors give the possibility of significant cost/benefit improvements, if properly utilized.

5 Large Grillage Tests

5.1 Description of Large Grillage Experiments

The last stage in the program has been the testing of two large grillages. The grillages are supported in a support frame as illustrated in Figure 12. Each test grillage is 6.8m (22.8ft) long and 2.46m (7.9ft) wide (Figure 13). The ends of the 2m frames are supported by a cross stringer with the frames extending through the stringer to a clamped (bolted) support at the extreme ends. The stringers are held by brackets bolted into the main support frame. The load is applied from below as described earlier. It is important to note that all testing should be considered as the testing of one frame. Even in the grillage cases, the load is applied to a single frame. The grillage is there to give the correct boundary conditions for the test frame.

The large grillages were tested with multiple applications of load, rather than one (see Figure 13 and Figure 14). After the first load was applied and removed, the hydraulic ram was moved and the structure was tested again. This gave an indication of the capacity of the frames after damage at nearby locations, and has proven to be very interesting. This is discussed further in section 5.2.

It is very interesting to see how much more capacity a frame has when part of a grillage. This increased capacity, and increased forces applied, resulted in the large grillages failing finally by punching shear in the 10mm shell plate. The load reached 1470kN, applied through a 102x102mm load patch.

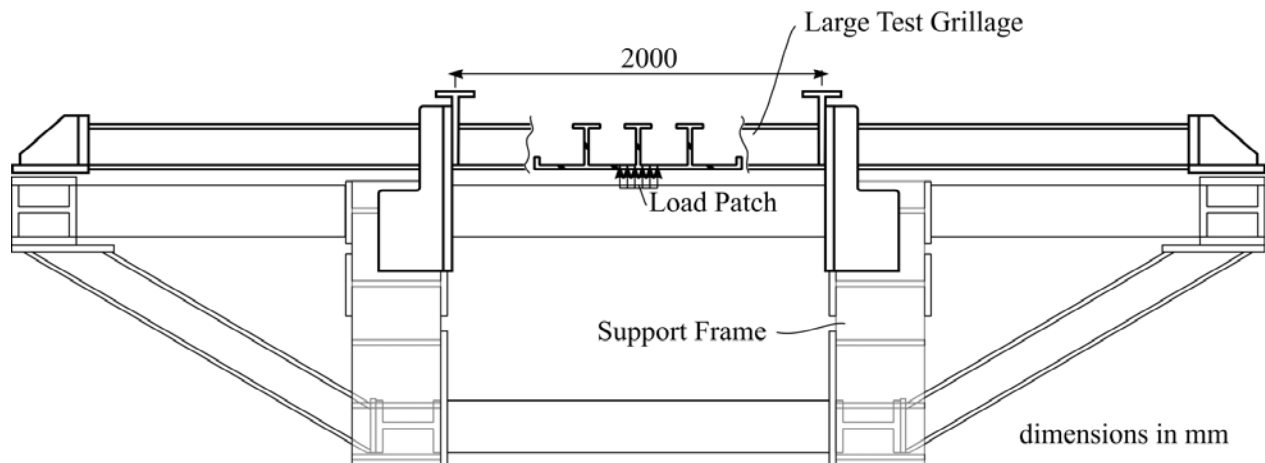


Figure 12: Large Grillage Test Setup

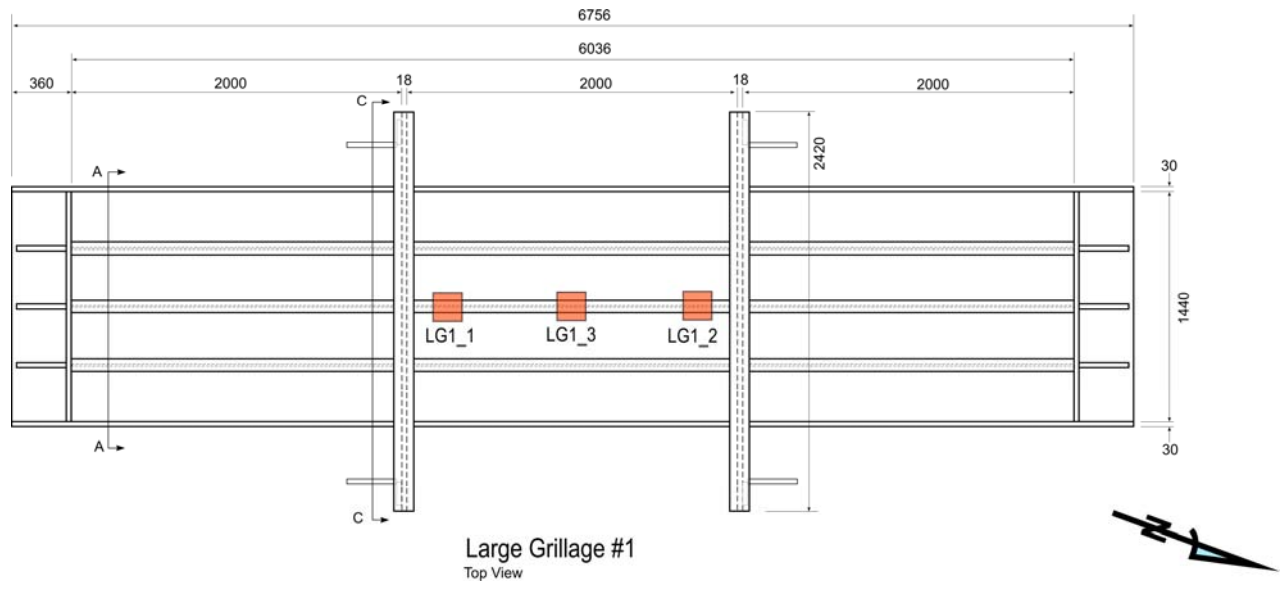


Figure 13: Large Grillage Test 1 Setup

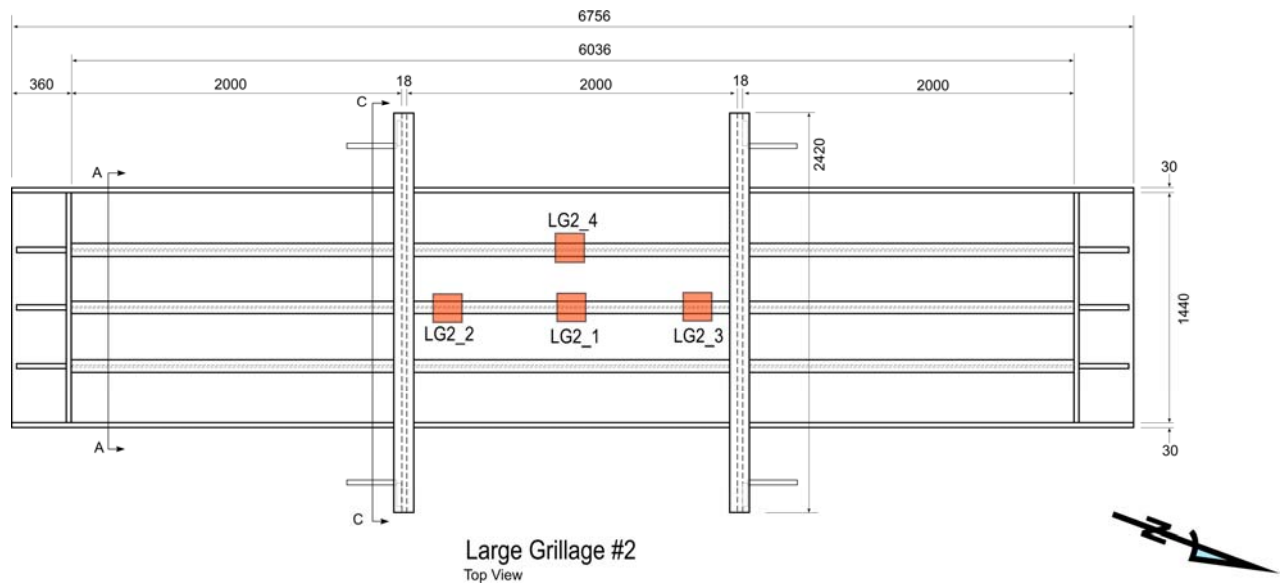


Figure 14: Large Grillage Test 2 Setup.



Figure 15: Large Grillage Test Arrangement

Table 2: Large Grillage Tests Conducted

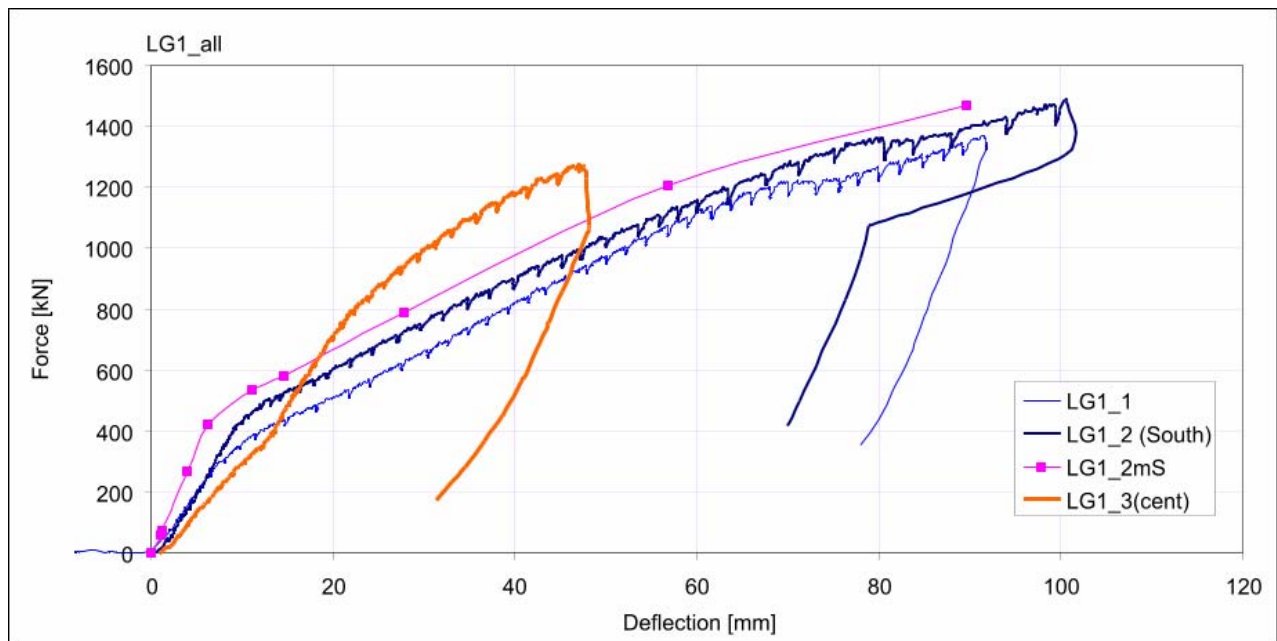
Test Name	Load Position	Test Date	Frame Description*
LG1_1	North End	10/26/2006	200x8,75x10 T
LG1_2	South End	11/23/2006	200x8,75x10 T
LG1_3	Center	11/30/2006	200x8,75x10 T
LG2_1	Center	4/20/2007	200x8,75x10 T
LG2_2	South End	5/23/2007	200x8,75x10 T
LG2_3	North End	6/7/2007	200x8,75x10 T
LG2_4	West Center	7/11/2007	200x8,75x10 T

*dimensions in mm.

5.2 Load-Deflection Results for the Large Grillage

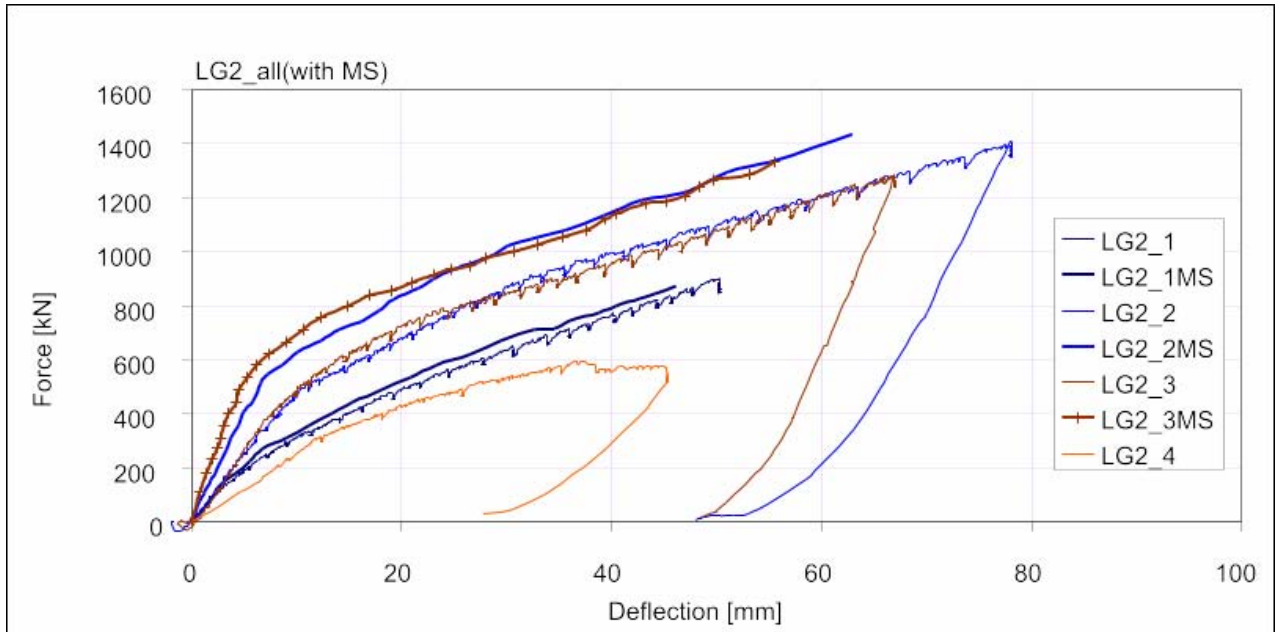
The load-deflection results for the seven large grillage tests are shown in Figure 16 and Figure 17. In all cases the plastic capacity is substantially above the elastic capacity and the initial plastic capacity.

Note also that the second and third load application (LG1_2 and :G1_3 in Figure 16) show greater capacity than the first load (LG1_1). Clearly the deformation is not weakening the structure. This raises the question of the consequences of local plastic damage. Such ‘damage’ may not be very serious, because it does not weaken the structure.



mS refers to the microscribe measurements. See Table 2 for test description and Figure 13 for load locations.

Figure 16. Load-Deflection for Large Grillage 1 (additional plots in Appendix C)



MS refers to the microscribe measurements. See Table 2 for test description and Figure 14 for load locations.

Figure 17. Load-Deflection for Large Grillage 2 (additional plots in Appendix C)

5.3 Photographs of the Large Grillage Tests

There were an extensive number of photographs and video tapes taken of the tests. Shown below is a sample of some of the many individual photos of the tests (Figures 17- 35).



Figure 18: LG1_2 test prior to load

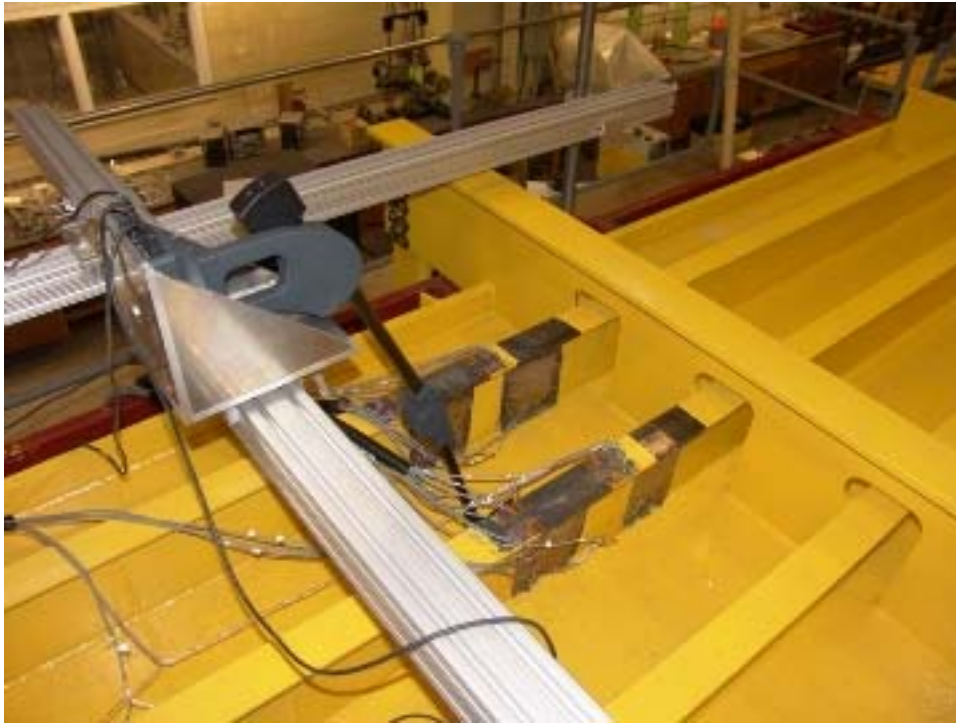


Figure 19: LG1_1 prior to test.



Figure 20: LG1_1 test overview.



Figure 21: LG1_1 test: MicroScribe measurements at 271kips (1205kN)



Figure 22: LG1_1 test: web deformation at 281kips (1250 kN)



Figure 23: LG1_1 test web deformation at 291kips (1294 kN)



Figure 24: LG1_1 View of ram on plate



Figure 25: LG1_1 view of ram after test (note imprint)



Figure 26: LG1_2 test: MicroScribe measurements at 330 kips (1468 kN)



Figure 27: LG1_2 test: web deformation at 330kips (1468 kN)



Figure 28: LG1_2 test: close-up of web deformation at 330kips (1468 kN)



Figure 29: LG1_2: ram after test (note imbedded platen and small tear)



Figure 30: LG1_2 test, web distortion



Figure 31: LG1_3 at 198 kips (note: load is at center, with prior shear damage at end)



Figure 32: LG2_2 side view



Figure 33: LG2_2 at 202kips



Figure 34: LG2_2: End after prior center load.



Figure 35: Large Grillage end clamp arrangement.



Figure 36: Large Grillage test overview.

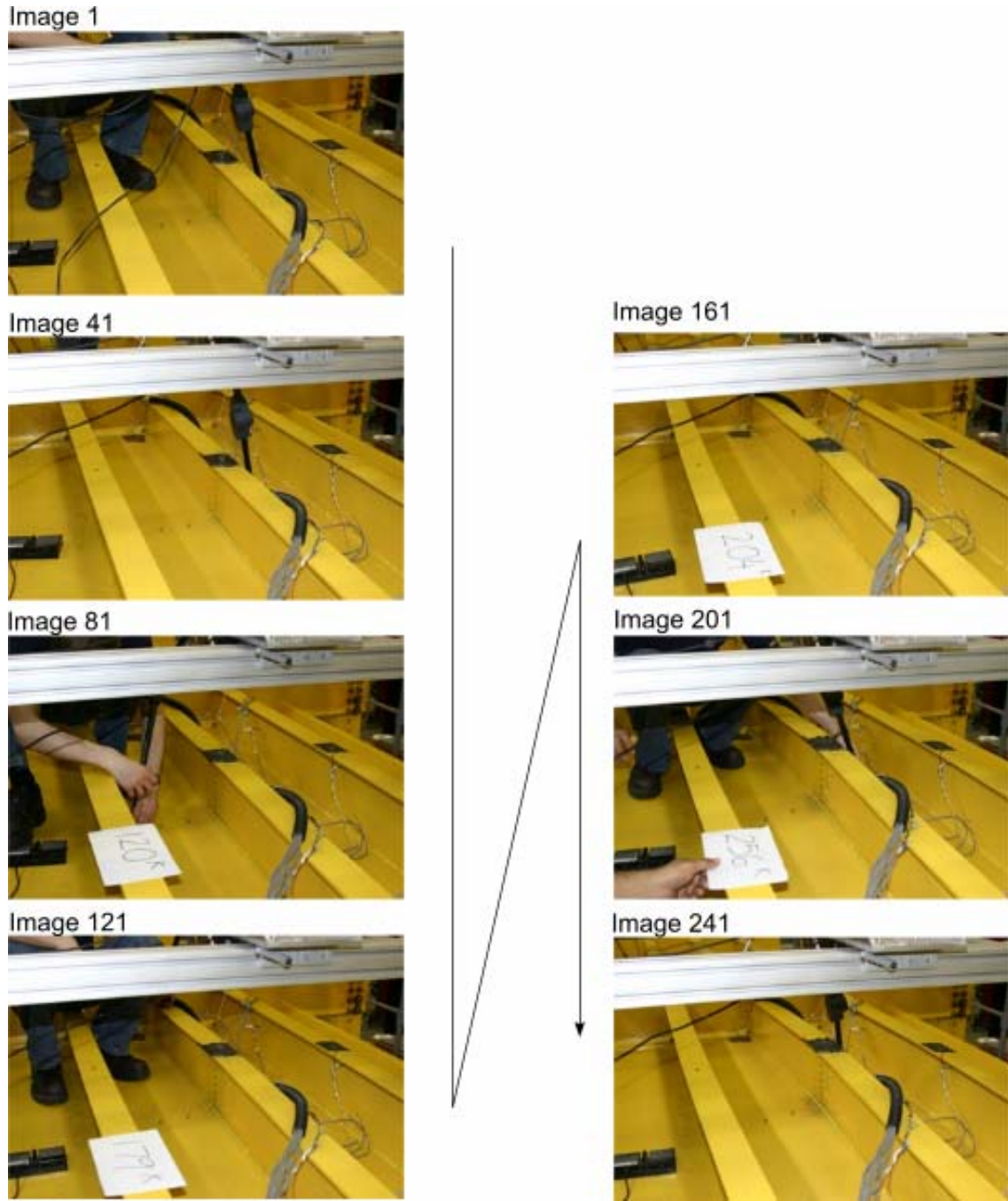


Figure 37: LG2_1 - Partial Image Sequence

5.4 Discussion of Large Grillage Tests

The large grillage tests tended to reinforce some of the conclusions derived from the single frame tests. As well, several new issues were highlighted by the tests. In terms of experimental lessons learned, the main ones are;

- The grillage testing arrangement worked much better than the single frame setup. This was probably due to the general size of the support structure and the considerable distance from the load point to the reactions. The loaded frames failed within the grillage and so there were no boundary condition issues. This was the primary reason for conducting the large grillage tests.
- One of the grillages had a weld very near the point of load. This weld failed prior to large plastic deformations. This was unintended, and was somewhat unfortunate. However, it did emphasize that fracture is a major concern and should be properly studied.

The large grillage tests also resulted in some additional insights into plastic behavior;

- The large grillage tests typically required much higher load levels than did the single frame tests. This emphasizes that neighboring frames have a significant supporting effect. This effect is especially significant with point loads and large deformations. Figure 11 shows two single frames. Figure 16 illustrates the large grillage behavior. Both the initial and post yield capacity for the grillage is considerably higher than that for the single frame.
- When large plastic strains occurred, fingering patterns formed in the yellow paint. Figure 27 and Figure 31 illustrate some typical patterns. These patterns occurred in various forms in practically all tests. It is suspected that these patterns are reflecting strains in the underlying steel, though this has not been proven. These patterns seem to indicate that the steel is deforming by shear slip in the form of ‘fingering’ rather than by a smooth strain pattern. Some of the fingers were very small (mm spacing), while some were quite large (2-3 cm spacing, and nearly 1m long). The importance of this is still unknown. It would appear that such fingering would potentially have serious effect on coating and may interact with fatigue or corrosion processes. The peak strains in the fingers would be very large (eg likely > 100% strain).

6 Material Test Data

Figure 38 shows one of the stress-strain curves taken from a sample of the steel in the webs of the single frames. The steel grade was 300W, a weldable construction steel commonly available in Canada. The measured yield strengths were in the range of 340MPa to 425MPa. Some of the shell plating was made from 250W, and had measured strength as low as 280MPa. Typically the steel exhibited the usual yield plateau, with a subsequent strain hardening region. The (linear-equivalent) post-yield modulus was taking to be about 1.2 GPa.

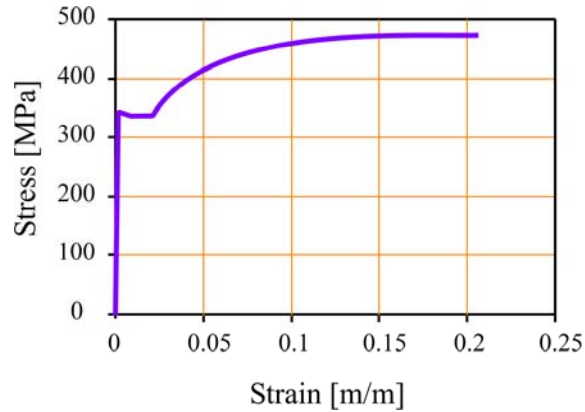


Figure 38: One of the stress-strain curves of the steel used in single frame tests.

7 Conclusions

The experimental program was quite challenging to perform. The load and deflection data gathered was quite extensive and is plotted in the Appendices.

The conclusions from the experimental program are as follows;

- Experimental ship structures research is a simple concept, but is very challenging to execute. A primary challenge is the creation of an adequately stiff and strong support frame. A second challenge is sensor technology, which is rapidly developing. Measurement of accurate 3D deformation patterns, with a resolution sufficient for extraction of strain, is a goal for future research.
- While general plastic response is possible to simulate with non-linear finite element models, there are certain phenomena that are not easily replicated numerically. Strain localization and shear fingering are certainly one aspect that is very difficult to model numerically. The implications of this are still uncertain.
- Post yield response is initially linear and is practically indistinguishable from elastic response. The magnitude of this type of behavior depends on the section shape. This pseudo-elastic behavior is quite small for symmetric I beams (~10% additional capacity beyond yield) but is quite large for flat bar stiffeners in ships (~85% additional capacity beyond yield). This effect presents a significant design opportunity for laterally loaded frames.
- The full range of post-yield behavior can be very large, with potentially several different features. At present there is no clear way to compare designs from a plastic perspective.

8 Recommendations

Continued development of plastic design criteria will require a number of developments. The following recommendations will help improve the state-of-the-art;

- Plastic design, as presently employed, involved assessment of single responses. A more general criterion that combines the multiple responses would be useful in establishing plastic design.
- The initial post-yield region is a linear continuation of the elastic response. It should be possible to make use of this strength, with considerable cost-benefit improvements.
- The issue of plastic strain fingering deserves additional investigation, both experimentally and numerically. The effect of these strains on fatigue, corrosion and coatings all deserves study.
- Three additional types of experiments would add to the understanding of plastic response to lateral loads. One issue is the axial stress in the frames. The reported tests had no initial axial stress. Axial tension arose in the frames as a result of the load and deformation. It is likely that compressive background stresses would significantly reduce the plastic capacity of the frames.
- A second issue is that of moving loads. In most collision cases (ice , rocks, ships) the load would be moving along or across the frames as it deformed the frames inward. This type of multi-directional loads would require a more elaborate setup to apply.
- The third issue is the question of ultimate tearing capacity of the grillage. This is a critical safety question and would require quite specialized equipment. The key issue is the loading platen, which must simulate the contact process more accurately (whether ice, rock of ships). Some form of high capacity load pillow is a possibility. A better choice would be to use the actual material (ice, rock, steel) to apply the loads. This would be challenging to set up, but would be the most convincing from a scientific and practical perspective.

9 References

1. Pavic, M., Daley, C., Hussein, A., Hermanski, “Ship Frame Research Program-A Numerical Study of the Capacity of Single Frames Subject to Ice Load” OERC Report 2004-02, IOT Report TR-2004-04, Prepared for Transport Canada, March 2004
2. Daley, C., Hermanski, G. “Ship Frame/Grillage Research Program-Investigation of Finite Element Analysis Boundary Conditions”, OERC Report 2005-02, March 2004
3. ANSYS 6.0, Finite Element Program by SAS IP, Inc, 2001
4. IACS UR (Draft) I2 “Structural Requirements for Polar Class Ships”, 30 July, 2003
5. Daley, C., “Review of the Tripping Requirements” Prepared for IACS Ad-hoc Group on Polar Class Ships and Transport Canada, Aug. 2003
6. Kendrick, A., and Daley, C.G., “Background Notes to Derivation and use of Formulations For Framing Design - IACS Unified Requirements for Polar Ships” Prepared for IACS Ad-hoc Group on Polar Class Ships and Transport Canada, January 2000
7. Daley, C.G., (2002), “Derivation of Plastic Framing Requirements for Polar Ships”, Journal of Marine Structures, Elsevier, 15(6) pp 543-559
8. Daley, C.G., (2002), “Application of Plastic Framing Requirements for Polar Ships”, Journal of Marine Structures, Elsevier, 15(6) pp 533-542

Appendix A – Single Frame Experimental Data Tables and Plots

List of Single Frame Experimental data included:

Test Name	Load Position	Test Date	Frame Description*	Page
Fc	Center	6/6/2005	200x10 F1	A-2
L75c	Center	10/7/2004	200x8,75x10 L	A-5
T50c	Center	6/16/2005	200x8,50x10 T	A-7
Fe	End	7/28/2004	200x10 F1	A-9
T50e	End	7/16/2004	200x8,50x10 T	A-35
T75e	End	5/19/2004	200x8,75x10 T	A-36

Data from Test: Fc

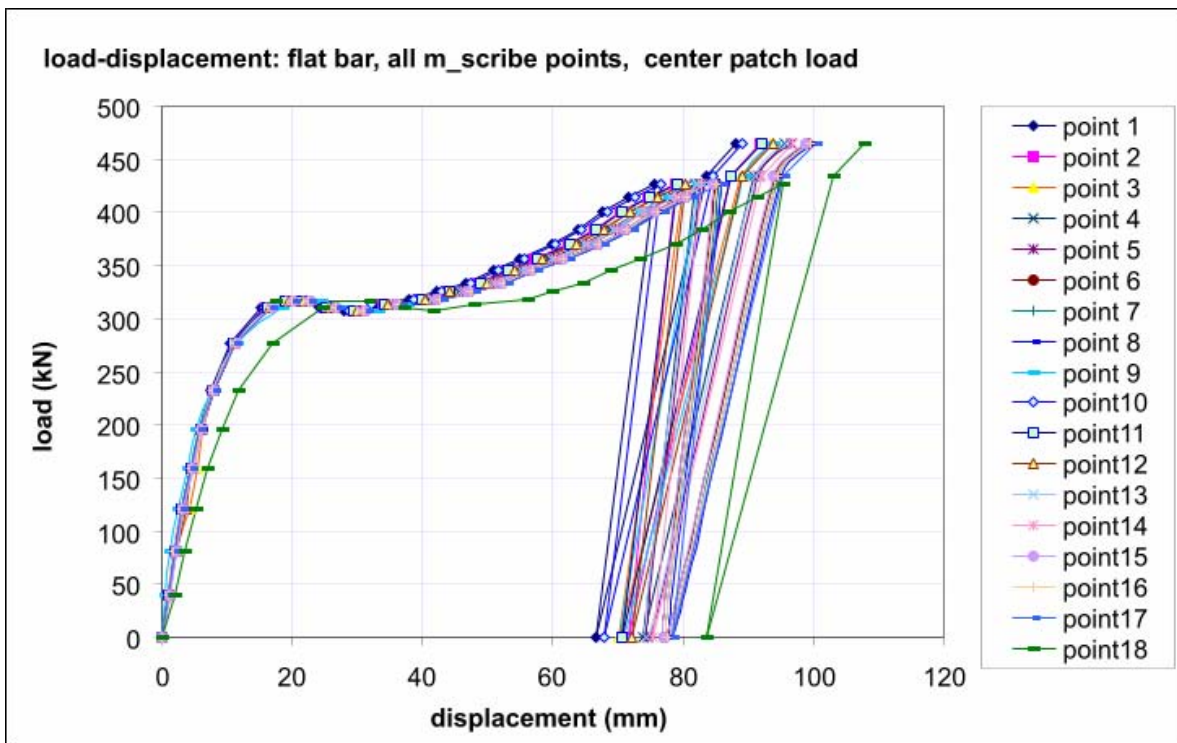
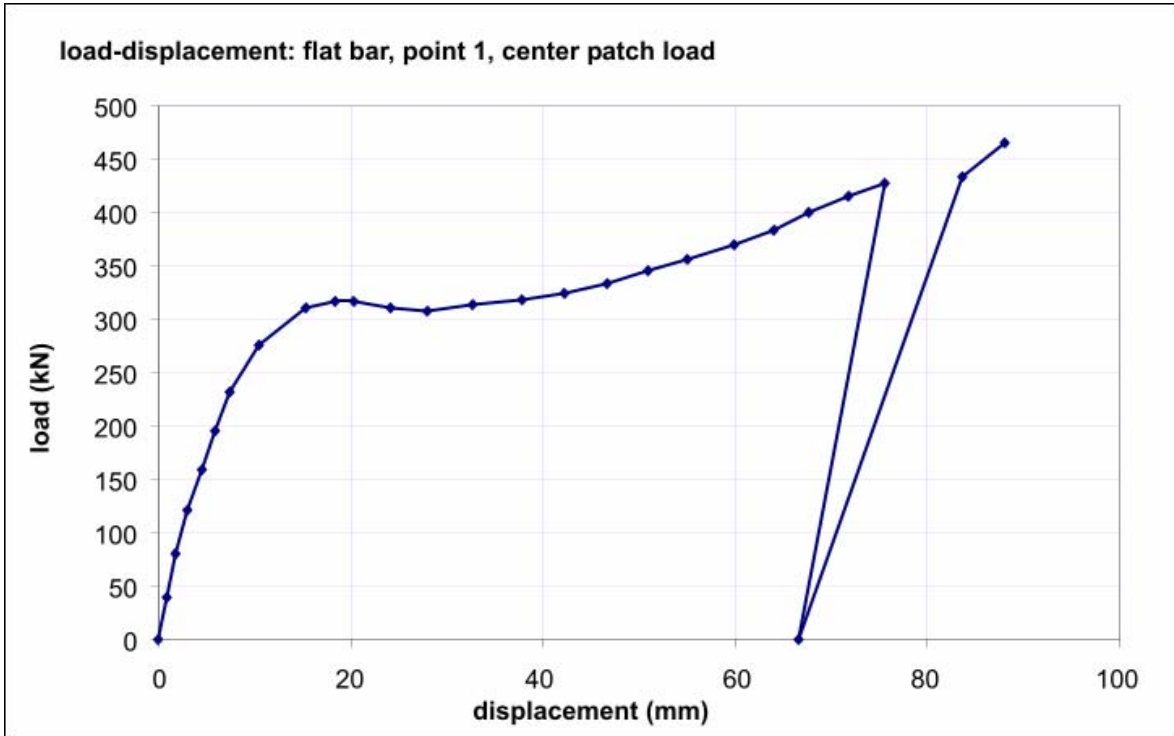
6-Jun-05

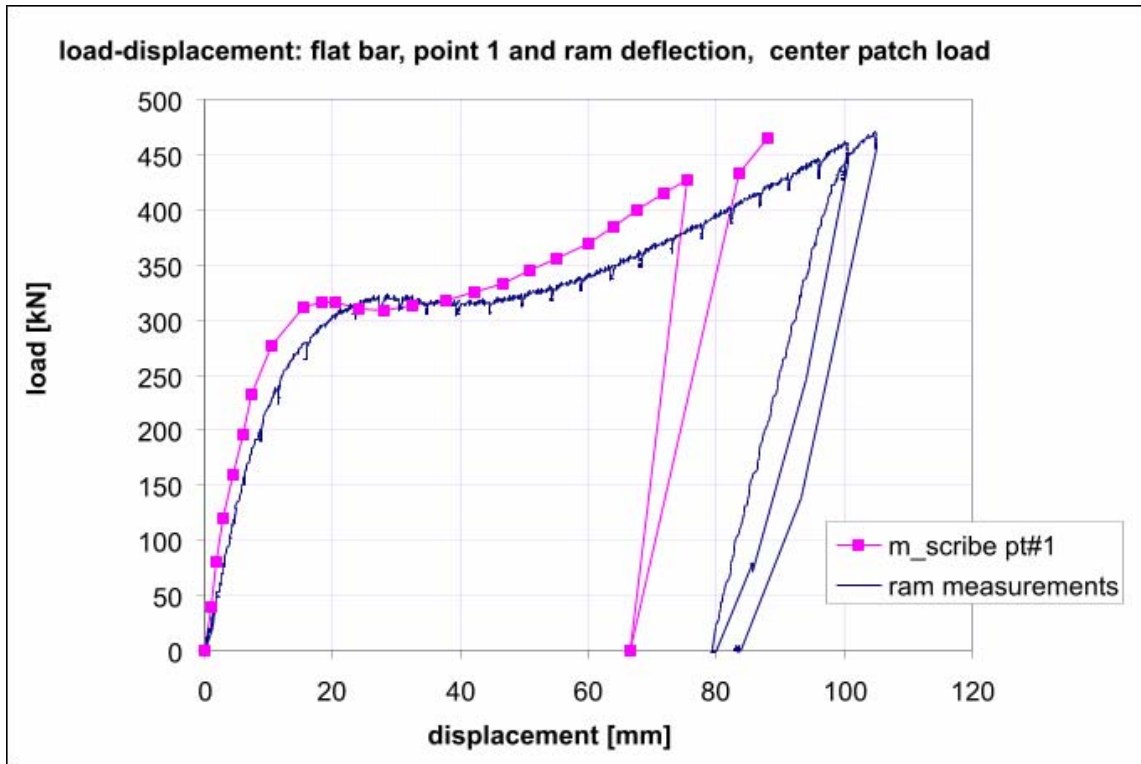
FLAT BAR TEST / CENTER PATCH LOAD

LOAD-dx DISPLACEMENT OF POINTS ABOVE CENTER PATCH LOAD, MICROSCRIBE MEASUREMENT

load			microscribe point deflections dz								
load (kN)	step	kips	1	2	3	4	5	6	7	8	9
			mm	mm	mm	mm	mm	mm	mm	mm	mm
0.0	1	0.0	0.00	0	0	0	0	0	0	0	0
39.3	2	8.8	0.97	1.17	1.06	1.06	0.99	1.04	0.92	0.95	0.46
80.4	3	18.1	1.85	2.00	2.09	2.12	1.92	2.07	1.92	2.07	1.32
120.5	4	27.1	2.98	3.17	4.36	3.04	3.22	3.22	3.01	3.14	2.61
158.9	5	35.8	4.55	4.64	5.61	4.53	4.56	4.77	4.45	4.59	4.03
195.4	6	44.0	5.91	5.96	6.13	5.88	6.14	5.99	5.75	6.09	5.36
232	7	52.2	7.45	7.89	7.90	7.89	7.95	7.96	7.80	7.94	7.66
276	8	62.1	10.56	10.94	11.14	11.11	11.20	11.32	11.15	11.25	11.57
311	9	70.0	15.34	15.98	16.28	16.42	16.50	16.82	16.79	17.02	18.57
316	10	71.1	18.40	19.04	18.71	19.49	19.71	20.12	20.01	20.12	21.66
316	11	71.1	20.42	21.12	21.60	21.90	22.17	22.76	22.43	22.65	24.44
310	12	69.8	24.11	24.96	25.42	25.91	26.17	26.78	26.58	26.95	28.78
308	13	69.3	28.00	29.62	29.13	30.09	30.44	31.11	31.08	31.43	33.09
313	14	70.4	32.61	33.90	34.54	35.22	35.55	36.38	36.32	36.64	37.76
318	15	71.6	37.85	39.53	40.21	40.94	41.43	42.26	42.50	42.90	41.89
325	16	73.1	42.27	44.01	44.76	45.73	46.23	47.26	47.48	47.73	47.05
333	17	74.9	46.60	48.46	49.44	50.47	50.84	52.06	52.22	52.70	51.66
345	18	77.6	50.86	52.95	53.78	54.86	55.38	56.71	56.93	57.46	56.16
356	19	80.1	54.98	57.18	58.25	59.38	60.08	61.40	61.72	62.21	60.61
370	20	83.3	59.88	62.31	63.16	64.67	65.38	66.95	67.24	67.72	65.28
384	21	86.4	63.96	66.48	67.34	68.83	69.60	71.11	71.53	72.12	69.80
400	22	90.0	67.68	70.45	71.80	73.21	74.06	75.71	76.04	76.67	73.66
415	23	93.4	71.68	74.58	75.83	77.57	78.31	80.27	80.58	81.19	77.88
427	24	96.1	75.48	78.86	80.14	81.81	82.66	84.70	85.22	85.72	82.29
0	25	0.0	66.60	71.71	70.19	73.72	74.51	77.01	77.50	78.12	70.58
433.8	26	97.6	83.65	87.32	88.74	90.82	91.63	94.11	94.66	95.02	89.41
465	27	104.6	87.97	91.77	93.35	95.45	96.52	99.08	99.48	100.14	93.76

load			microscribe point deflections dz								
load (kN)	step	kips	10	11	12	13	14	15	16	17	18
			mm	mm	mm	mm	mm	mm	mm	mm	mm
0.0	1	0.0	0	0	0	0	0	0	0	0	0
39.3	2	8.8	1.00	1.02	1.06	1.30	1.20	1.28	0.88	0.93	1.90
80.4	3	18.1	2.08	2.00	2.16	2.23	2.06	2.20	1.85	2.00	3.50
120.5	4	27.1	3.26	2.99	3.62	3.32	3.32	3.25	3.06	2.94	5.13
158.9	5	35.8	4.54	4.38	4.57	4.87	4.66	4.70	4.45	4.42	7.00
195.4	6	44.0	5.87	5.94	6.10	6.17	6.14	6.07	5.88	5.77	9.14
232	7	52.2	7.74	7.71	8.00	8.04	7.83	7.92	7.69	7.86	11.81
276	8	62.1	10.76	11.04	11.15	11.35	11.28	11.50	11.15	11.25	17.00
311	9	70.0	15.74	16.14	16.35	16.81	16.81	17.05	16.70	16.84	24.81
316	10	71.1	18.60	18.96	19.50	19.83	19.81	20.22	20.02	20.15	17.36
316	11	71.1	20.94	21.37	21.80	22.15	22.34	22.71	22.41	22.80	32.04
310	12	69.8	24.49	25.22	25.69	26.08	26.25	26.69	26.57	26.99	37.11
308	13	69.3	28.57	29.42	29.82	30.44	30.73	31.24	31.04	31.36	41.65
313	14	70.4	32.19	34.09	34.78	35.61	35.67	36.26	36.36	36.67	47.87
318	15	71.6	38.66	39.83	40.53	41.39	41.65	42.28	42.55	43.03	56.24
325	16	73.1	43.00	44.18	44.18	46.01	46.45	47.23	47.34	47.80	59.83
333	17	74.9	47.36	48.91	49.81	50.76	51.23	52.13	52.30	52.82	64.60
345	18	77.6	51.52	53.18	54.17	55.23	55.85	56.75	56.91	57.47	68.92
356	19	80.1	55.73	57.59	58.48	59.96	60.31	61.61	61.67	62.29	73.27
370	20	83.3	60.25	62.61	63.54	64.95	65.47	66.79	67.02	67.62	78.92
384	21	86.4	64.38	66.59	67.86	69.36	69.84	71.19	71.46	72.17	82.89
400	22	90.0	68.44	70.61	71.87	73.46	74.21	75.62	75.97	76.72	87.11
415	23	93.4	72.51	74.84	76.04	78.03	78.78	80.35	80.57	81.35	91.27
427	24	96.1	76.49	79.10	80.23	82.14	82.80	84.70	85.06	85.88	95.39
0	25	0.0	67.81	70.63	72.16	74.25	75.26	77.07	77.58	78.35	83.67
433.8	26	97.6	84.48	87.34	89.14	91.18	92.06	93.90	94.49	95.42	103.09
465	27	104.6	88.95	91.95	93.73	95.86	96.73	98.91	99.49	100.37	107.76



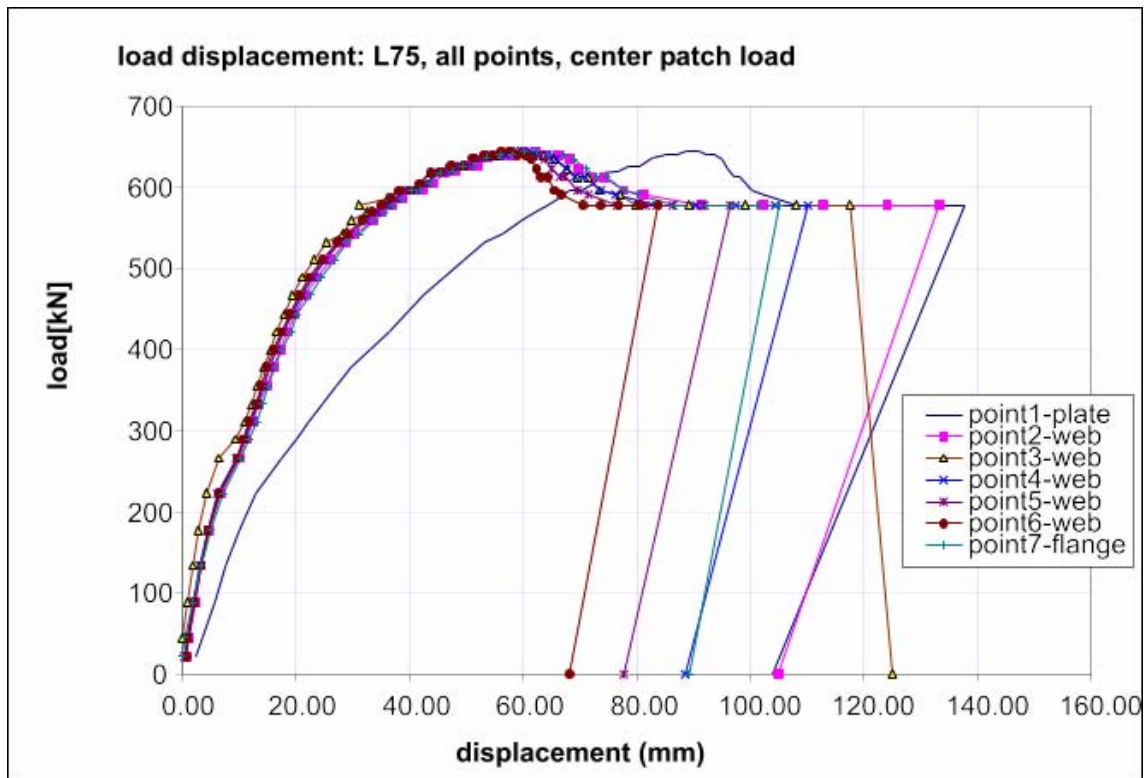
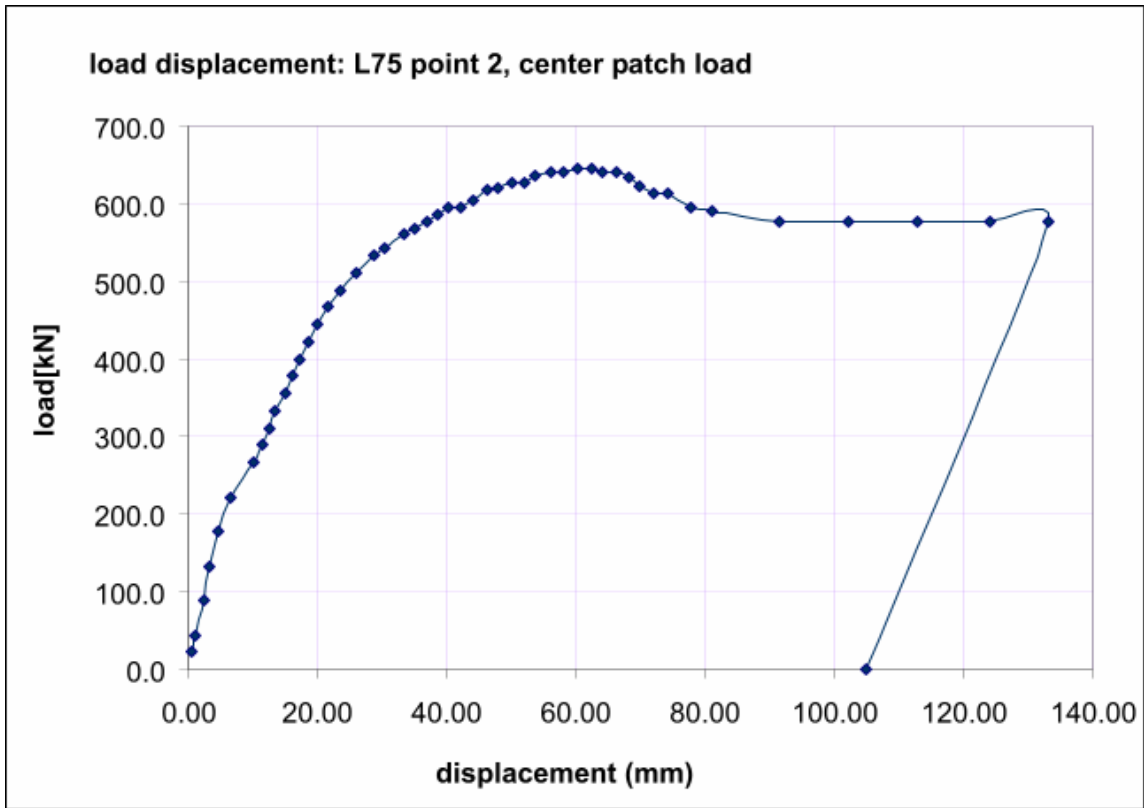


Data from Test: L75c

7-Oct-04 L-75 TEST / CENTER PATCH LOAD

LOAD- DISPLACEMENT OF POINTS ABOVE CENTER PATCH LOAD, MICROSCRIBE MEASUREMENT
 Point 1 - on the plate Points 2-6 - on the web point 7 - on the flange

load			microscribe point deflections dz						
kN	step	kips	1	2	3	4	5	6	7
			mm	mm	mm	mm	mm	mm	mm
22.2	1	5	2.5	0.7	0.0	0.5	0.4	0.7	0.0
44.4	2	10	3.5	1.2	1.0	1.0	1.3	1.0	0.5
88.9	3	20	5.9	2.4	1.9	2.0	2.1	2.2	2.0
133.3	4	30	7.8	3.4	2.9	3.2	3.3	3.4	3.3
177.8	5	40	10.1	4.8	4.3	4.5	4.5	4.6	5.2
222.2	6	50	13.0	6.6	6.4	6.3	6.6	6.4	7.1
266.7	7	60	17.5	10.0	9.5	9.7	9.7	9.7	10.4
288.9	8	65	20.2	11.4	11.1	11.1	10.8	10.8	11.6
311.1	9	70	22.2	12.6	12.1	12.2	12.1	11.8	13.2
333.3	10	75	24.6	13.5	13.2	13.3	13.1	13.1	14.1
355.6	11	80	27.1	15.0	14.3	14.3	14.1	14.0	15.0
377.8	12	85	29.7	16.0	15.5	15.3	15.4	14.9	16.4
400.0	13	90	33.0	17.2	16.6	16.5	16.5	16.1	17.6
422.2	14	95	36.4	18.6	17.9	17.8	17.8	17.6	19.1
444.4	15	100	39.5	19.9	19.4	19.4	19.2	19.0	20.2
466.7	16	105	42.4	21.6	21.1	21.1	20.7	20.5	22.5
488.9	17	110	46.1	23.6	23.3	22.9	22.7	22.4	24.4
511.1	18	115	49.8	26.1	25.4	25.2	24.9	24.6	26.8
533.3	19	120	53.3	28.7	28.3	27.8	27.6	27.3	29.1
542.2	20	122	56.3	30.5	29.8	29.5	29.4	29.0	31.1
560.0	21	126	59.8	33.5	32.7	32.4	32.1	31.6	33.8
568.9	22	128	62.2	35.0	31.3	34.3	34.1	33.4	35.4
577.8	23	130	64.2	36.9	36.3	36.1	35.6	35.0	37.0
586.7	24	132	66.3	38.5	38.3	37.7	37.4	36.6	38.7
595.6	25	134	68.1	40.3	40.0	39.5	39.0	38.2	40.3
595.6	26	134	70.3	42.2	41.8	41.3	40.7	40.3	41.8
604.4	27	136	72.6	44.1	43.7	43.3	42.8	41.7	43.6
617.8	28	139	74.5	46.3	45.6	44.9	44.7	43.6	45.4
620.0	29	139.5	76.6	47.9	47.7	47.0	46.4	45.5	47.5
626.7	30	141	78.6	50.0	49.4	48.7	48.5	47.3	49.3
626.7	31	141	80.7	52.0	51.5	50.6	50.4	49.4	51.3
635.6	32	143	82.9	53.7	53.5	52.9	52.2	51.2	53.5
640.0	33	144	85.0	56.0	55.3	54.9	54.0	53.0	55.8
640.0	34	144	86.7	58.0	57.5	56.9	56.0	54.8	58.0
644.4	35	145	88.9	60.2	59.6	58.6	57.9	56.1	60.3
644.4	36	145	90.9	62.4	61.7	61.0	59.6	57.6	62.4
640.0	37	144	92.3	64.2	63.5	62.4	60.9	59.0	64.6
640.0	38	144	93.7	66.2	65.6	64.3	62.7	60.4	67.2
634.7	39	142.8	95.1	68.1	67.7	65.8	63.8	61.4	68.9
622.2	40	140	95.9	69.9	69.6	67.6	65.1	62.4	71.0
613.3	41	138	97.2	72.0	71.5	69.1	66.4	63.1	72.9
613.3	42	138	98.2	74.1	73.4	70.7	67.5	64.2	74.6
595.6	43	134	100.3	77.7	77.1	73.5	69.7	65.6	77.6
591.1	44	133	102.2	81.0	79.9	76.2	71.5	66.7	80.1
577.8	45	130	108.2	91.5	89.2	83.4	76.5	70.5	86.7
577.8	46	130	115.4	102.3	99.0	90.4	81.6	73.6	92.1
577.8	47	130	122.6	112.9	108.1	97.5	86.4	76.7	96.7
577.8	48	130	131.2	124.1	117.5	104.4	91.8	80.7	101.2
577.8	49	130	137.7	133.1	124.9	110.2	96.3	83.8	105.1
0.0	50	0	103.9	104.8	99.5	88.4	77.6	68.2	89.2

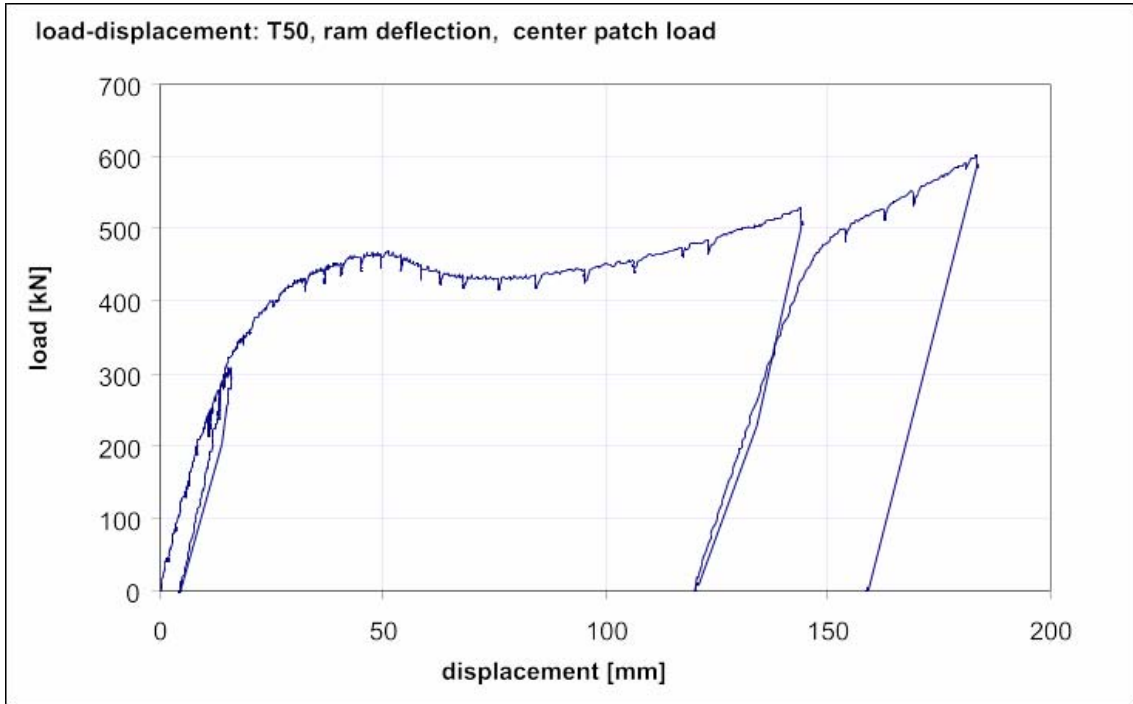


Data from Test: T50c

16-Jun-05 **T50 TEST / CENTER PATCH LOAD**

LOAD-DISPLACEMENT, RAM MEASUREMENT

load			Ram displacement
load (kN)	step	load [kips]	mm
0.0	1	0.0	0.0
43.9	2	9.9	1.6
85.9	3	19.3	3.5
141.6	4	31.9	5.7
184.5	5	41.5	7.6
231.1	6	52.0	11.4
249.3	7	56.1	11.8
300.5	8	67.6	14.9
284.0	9	63.9	15.9
270.3	10	60.8	15.6
266.7	11	60.0	15.6
201.8	12	45.4	14.0
0.0	13	0.0	4.8
0.0	14	0.0	4.8
36.6	15	8.2	5.7
173.5	16	39.0	10.8
237.5	17	53.4	12.7
307.8	18	69.2	14.6
339.7	19	76.4	17.2
360.7	20	81.2	20.0
400.9	21	90.2	25.4
410.0	22	92.3	27.0
430.1	23	96.8	33.0
453.9	24	102.1	40.3
464.8	25	104.6	49.2
446.6	26	100.5	60.0
432.0	27	97.2	70.8
431.1	28	97.0	80.0
442.0	29	99.5	90.2
452.1	30	101.7	100.3
464.8	31	104.6	110.2
478.5	32	107.7	120.3
497.7	33	112.0	130.5
519.6	34	116.9	140.0
528.8	35	119.0	144.1
504.1	36	113.4	144.1
227.4	37	51.2	134.0
6.4	38	1.4	121.0
0.9	39	0.2	120.3
18.3	40	4.1	120.6
176.3	41	39.7	129.2
267.6	42	60.2	134.3
367.1	43	82.6	140.0
454.8	44	102.3	146.4
499.5	45	112.4	153.7
491.3	46	110.5	154.3
526.0	47	118.4	162.6
550.7	48	123.9	169.2
591.8	49	133.1	181.0
585.4	50	131.7	183.5
0.9	51	0.2	159.1



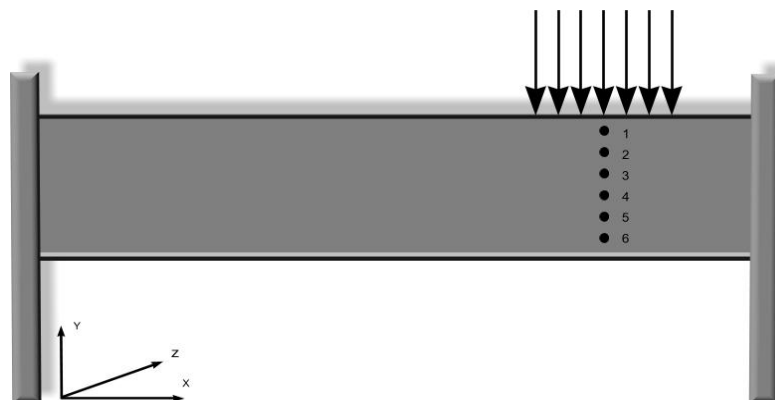
Data from Test: Fe

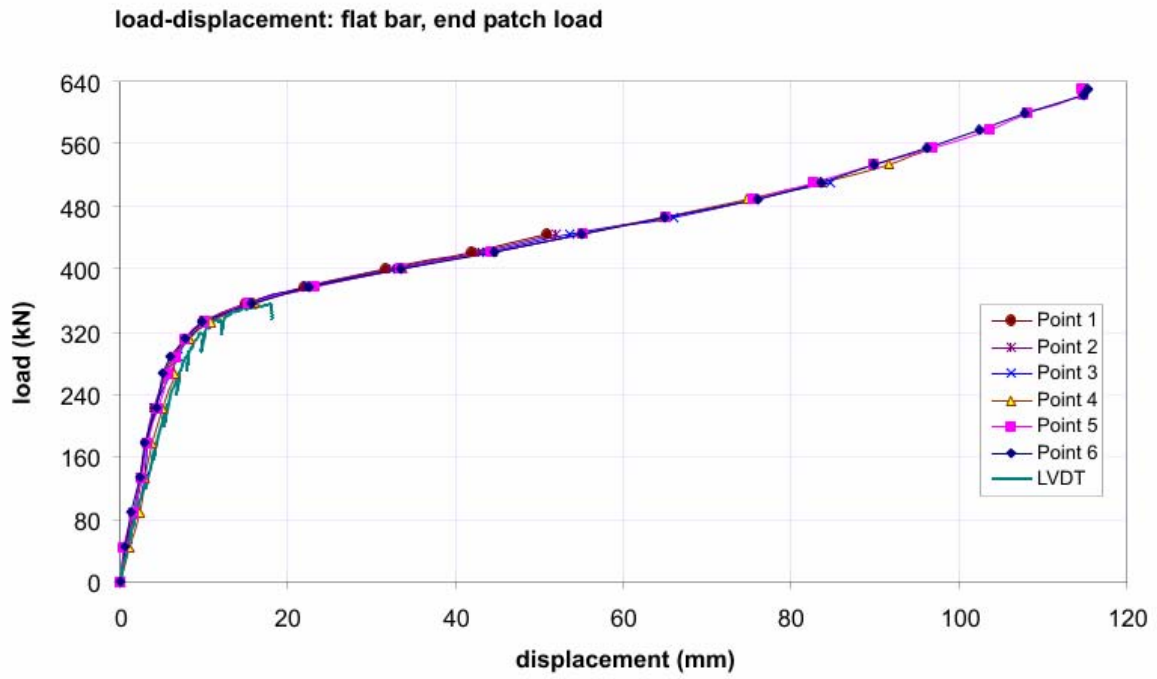
28-Jul-04

FLAT BAR TEST / END LOAD

LOAD-DISPLACEMENT OF POINTS AT END LOAD

load			microscribe point deflections dz					
load (kN)	step	load (kip)	1	2	3	4	5	6
			mm	mm	mm	mm	mm	mm
0	1	0	0	0	0	0	0	0
44.4	2	10	0.7	0.6	1.0	1.1	0.3	0.5
88.9	3	20	1.6	1.7	2.0	2.3	1.7	1.3
133.3	4	30	2.5	2.3	2.9	2.9	2.6	2.4
177.8	5	40	3.1	3.1	3.2	3.8	3.2	2.9
222.2	6	50	4.1	4.0	4.1	5.0	4.4	4.3
266.7	7	60	5.4	5.6	5.9	6.4	5.7	5.1
288.9	8	65	6.4	6.5	6.8	6.4	6.7	6.0
311.1	9	70	7.7	7.9	8.1	8.2	7.8	7.7
333.3	10	75	9.8	10.1	10.6	10.8	10.1	9.7
355.6	11	80	15.0	15.0	15.3	16.1	15.3	15.6
377.8	12	85	21.9	22.1	22.3	23.0	23.1	22.4
400.0	13	90	31.6	32.2	33.0	33.7	33.4	33.3
422.2	14	95	41.9	42.7	43.6	44.5	44.2	44.6
444.4	15	100	50.9	52.0	53.6	55.0	55.1	55.0
466.7	16	105			66.0	64.6	65.0	64.9
488.9	17	110			75.5	74.8	75.5	75.9
511.1	18	115			84.5	83.5	82.6	83.5
533.3	19	120				91.7	89.9	89.9
555.6	20	125				96.7	96.8	96.1
577.8	21	130					103.7	102.4
600.0	22	135					108.1	107.7
622.2	23	140					114.7	114.7
629.4643	24	141					114.7	115.3





The Strain gauge data plots for the flat bar end load test is included in the following pages.



In Charts **ROSSETE_POS_FRONT**, **ROSSETE_POS_BACK** location of rosettes and strain gages on a beam is presented.

In Chart **ROSSETE** is an explanation how to calculate normal strains in x and y direction and shear strain as well. There is also explanation how to calculate principal strains and maximum shear strain. Finally there is a formula how to determine orientation of principal strains.

In Chart **FlatBar_end load** are test data. For each rosette there is an explanation about the position. Strain gages within rosette are labeled as a, b and c and formulae from Chart **ROSSETE** are applied to calculate other strains.

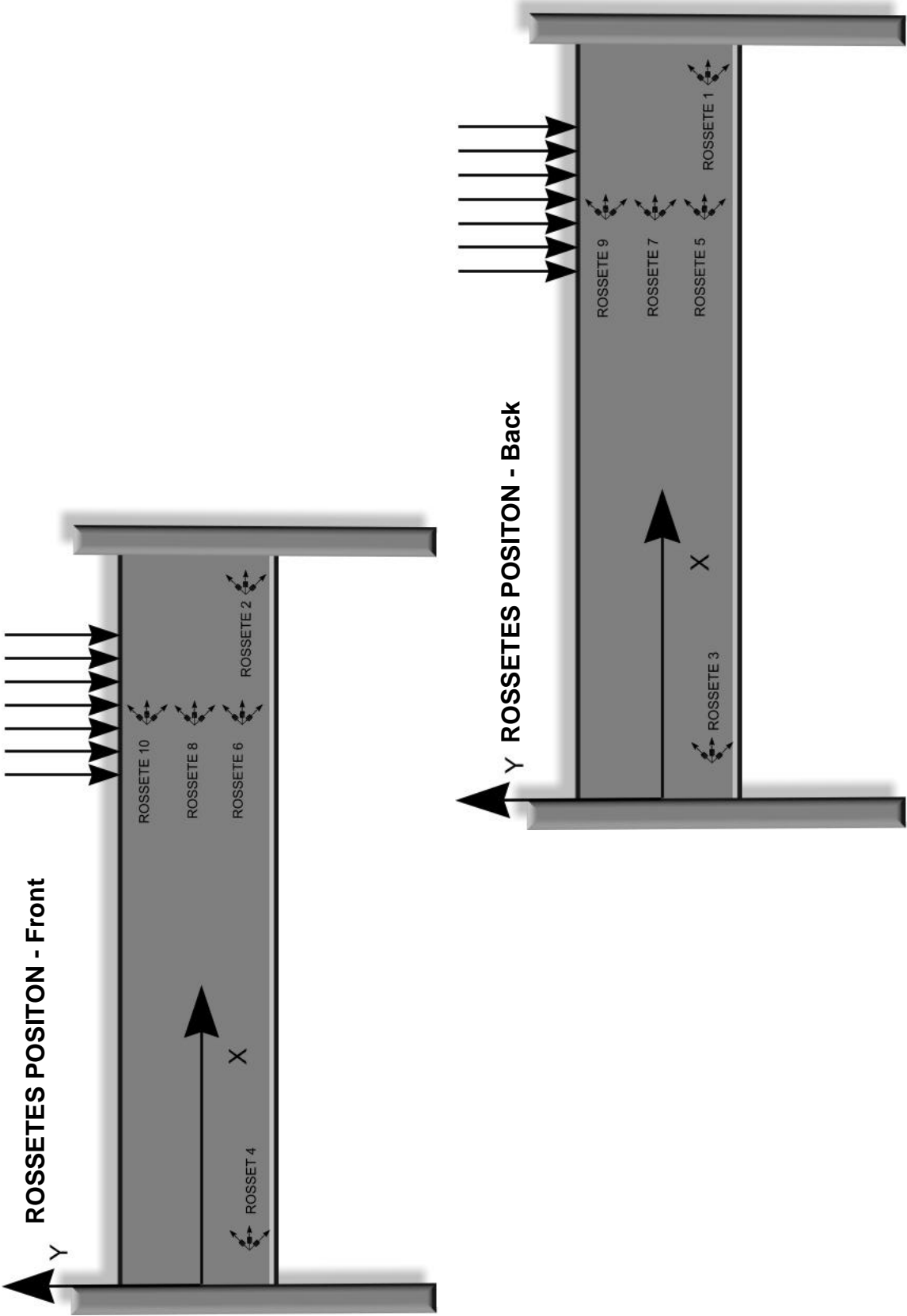
For each rosette there are four charts with measured and calculated data.
For example rosette 1:

Rossete1 - Measured (raw) data are presented. Load in term of normal strains in "a, b and c" direction is plotted.

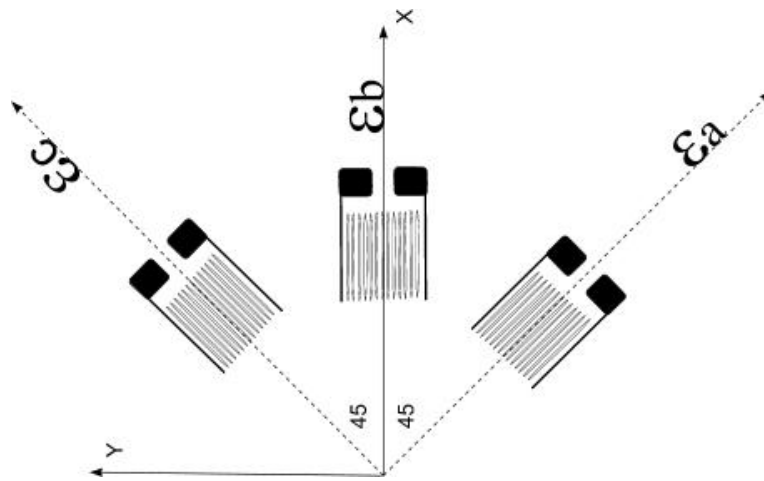
Rossete1_exx_eyy_axy - Load in term of normal strains in x nad y direction and shear strain xy (calculate using formulaes from Chart **ROSSETE**) is plotted.

Princ.strains1_e1_e2_e12 - Load in term of principal strains 1 and 2 and max. shear strain 12 (calculate using formulaes from Chart **ROSSETE**) is plotted.

Theta1 - Load in term of angle which determines position of principle plane 1.



ROSSETE



$$\begin{aligned} \epsilon_{xx} &= \epsilon_x \\ \epsilon_{yy} &= \epsilon_x + \epsilon_y + \epsilon_z \\ \epsilon_{xy} &= \frac{1}{2}(\epsilon_x - \epsilon_y) \end{aligned}$$

Normal strains in x and y direction

$$\epsilon_{xy} = \frac{1}{2}(\epsilon_x - \epsilon_y)$$

Shear strain

$$\epsilon_{1,2} = \frac{\epsilon_{xx} + \epsilon_{yy}}{2} \pm \sqrt{\left(\frac{\epsilon_{xx} - \epsilon_{yy}}{2}\right)^2 + (\epsilon_{xy})^2}$$

Principal strains

$$\tan 2\theta = \frac{2\epsilon_{xy}}{\epsilon_{xx} - \epsilon_{yy}}$$

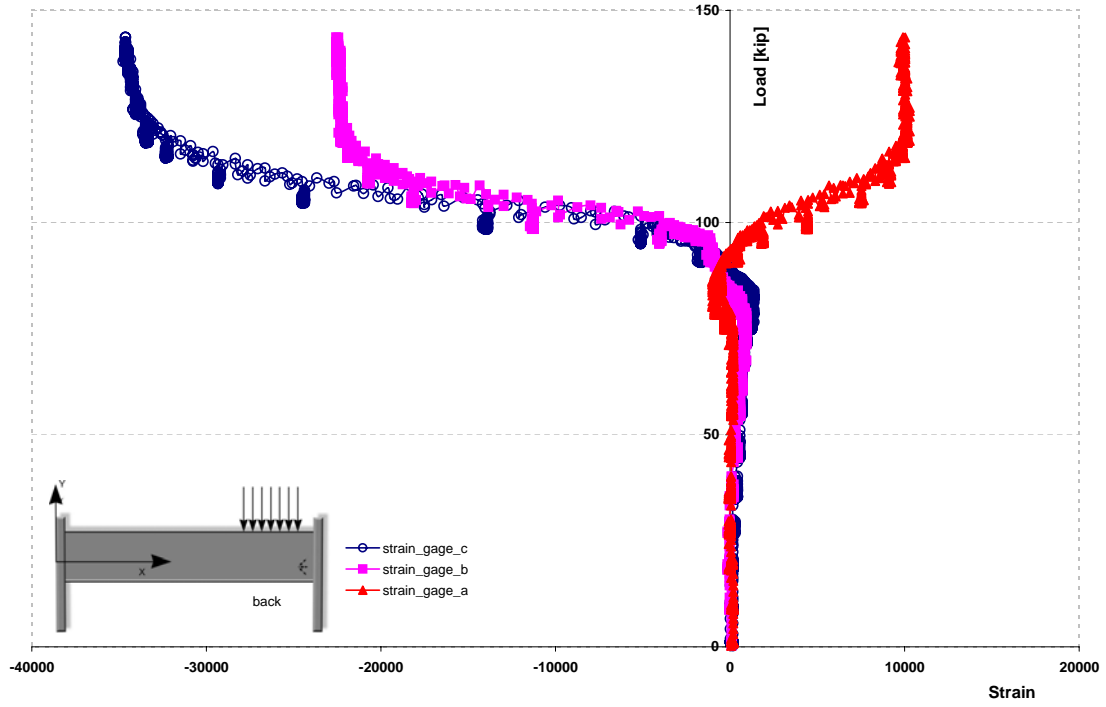
Position of principle strain I

$$\epsilon_{1,2} = \left(\frac{\epsilon_{xx} + \epsilon_{yy}}{2}\right) \pm \sqrt{\left(\frac{\epsilon_{xx} - \epsilon_{yy}}{2}\right)^2 + (\epsilon_{xy})^2}$$

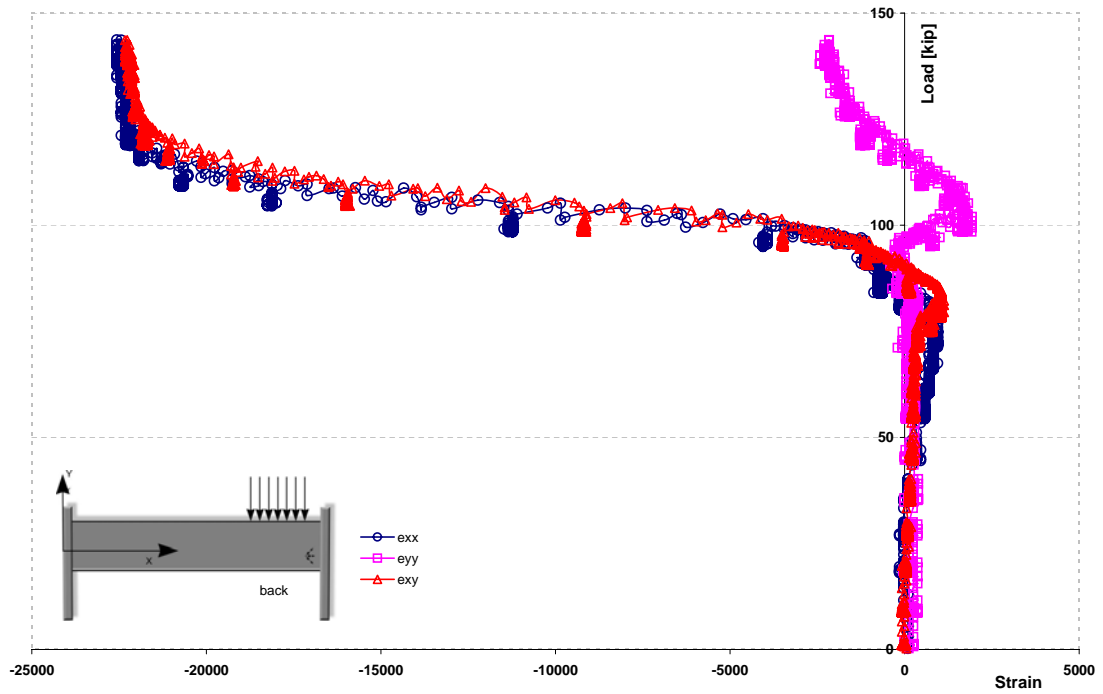
Max. Shear strain

$\theta' = \theta + 45^\circ$ Position of plane with max. shear strain

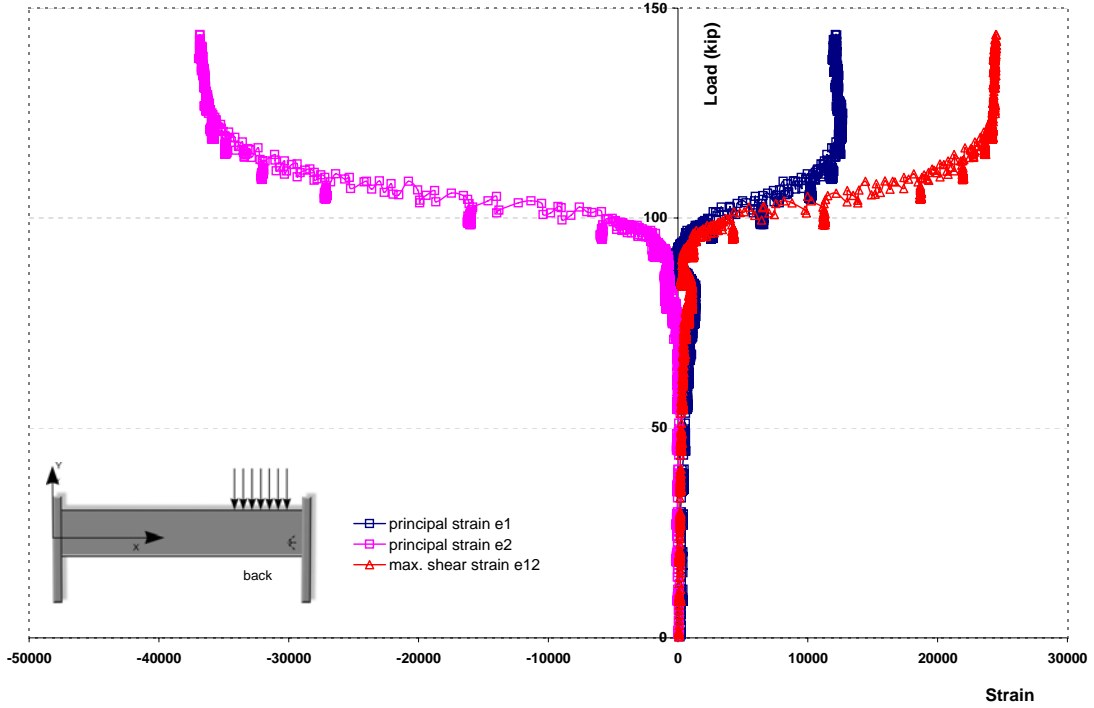
Load-Strain curves for the measuring point 100 mm from the end (beside patch load)



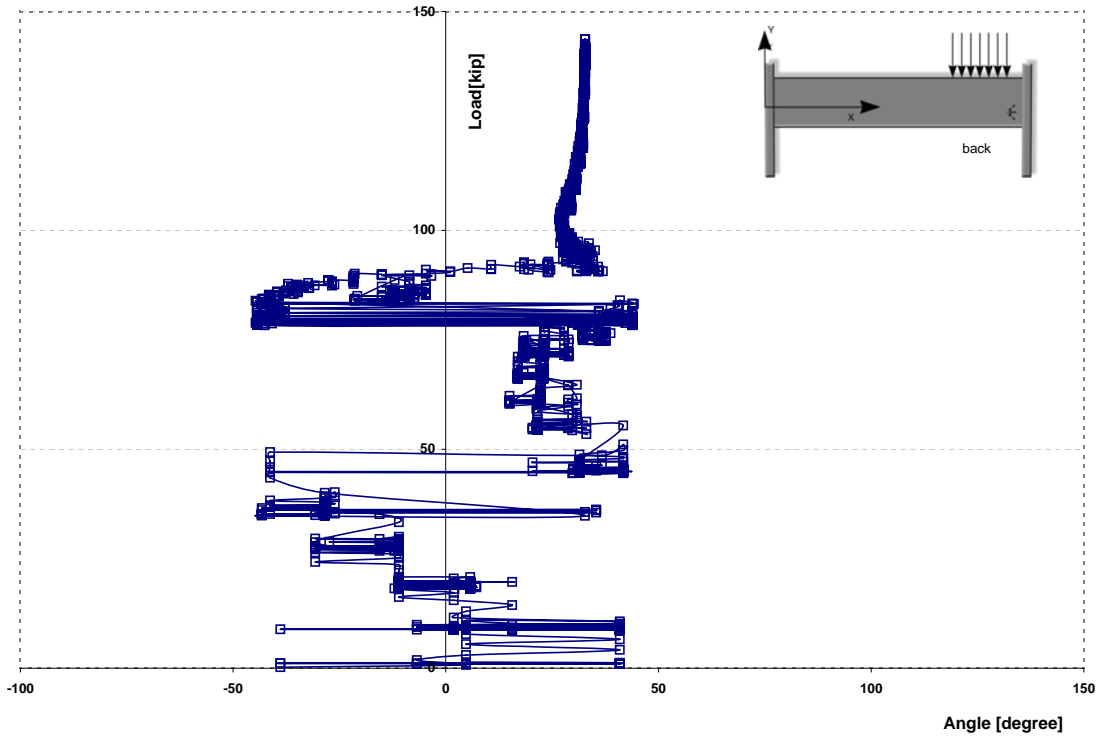
Load-Strain curves for the measuring point 100mm from the end (beside patch load)



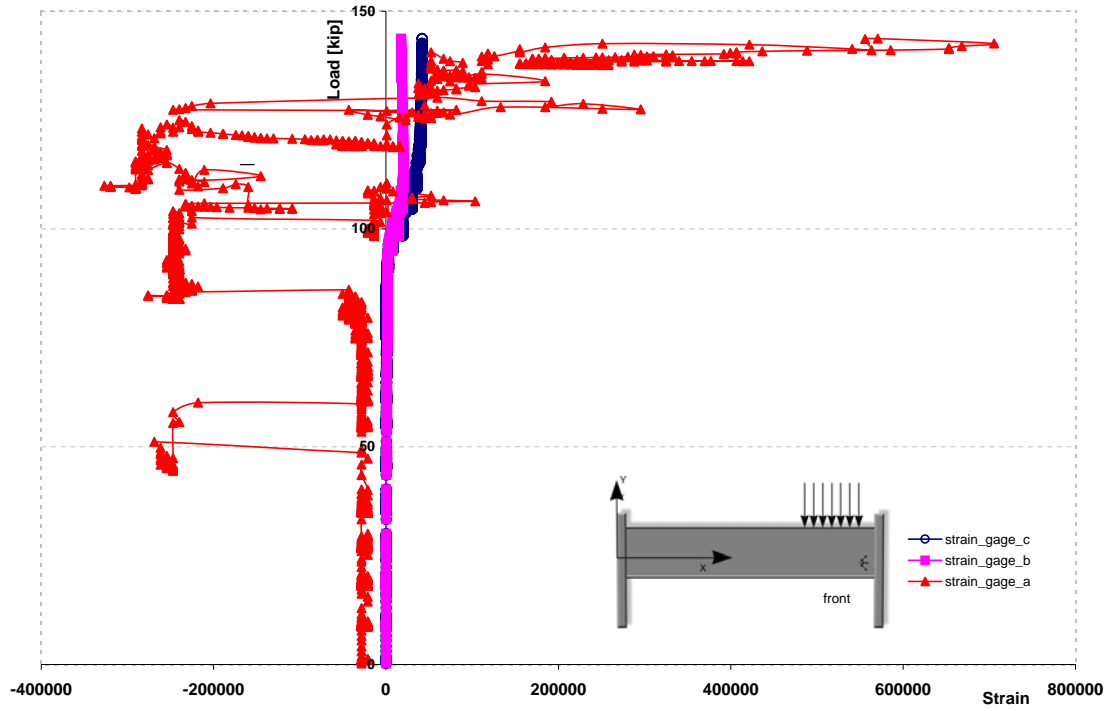
Load-Principal Strain curves for the measuring point 100mm from the end (beside patch load)



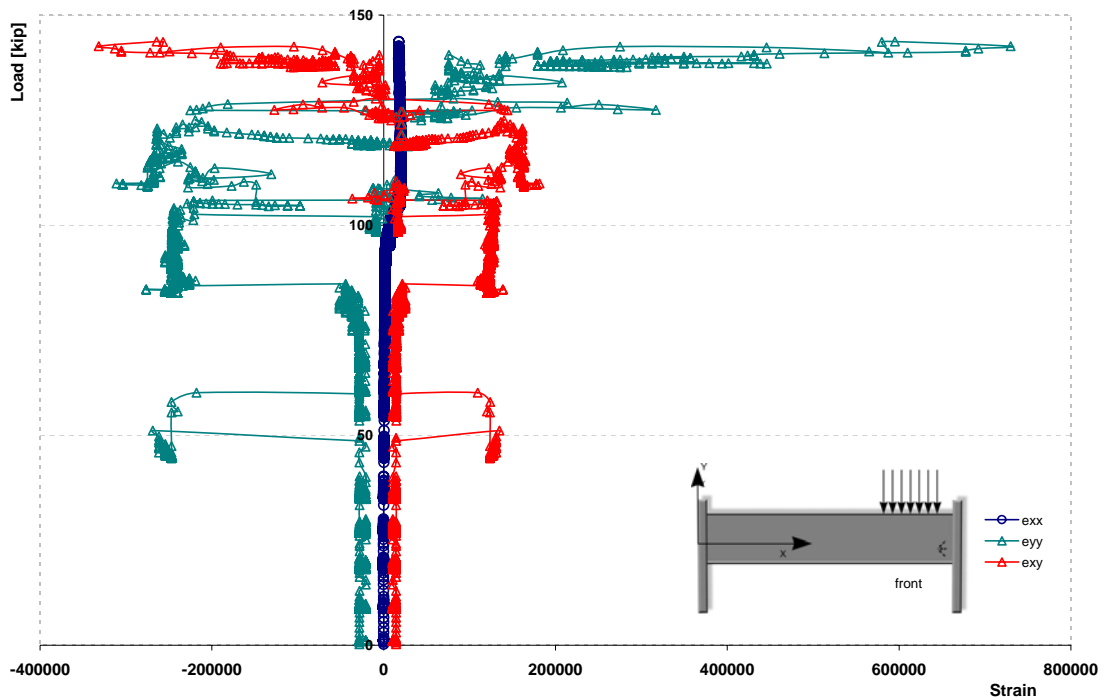
Principal Plain I Orientation



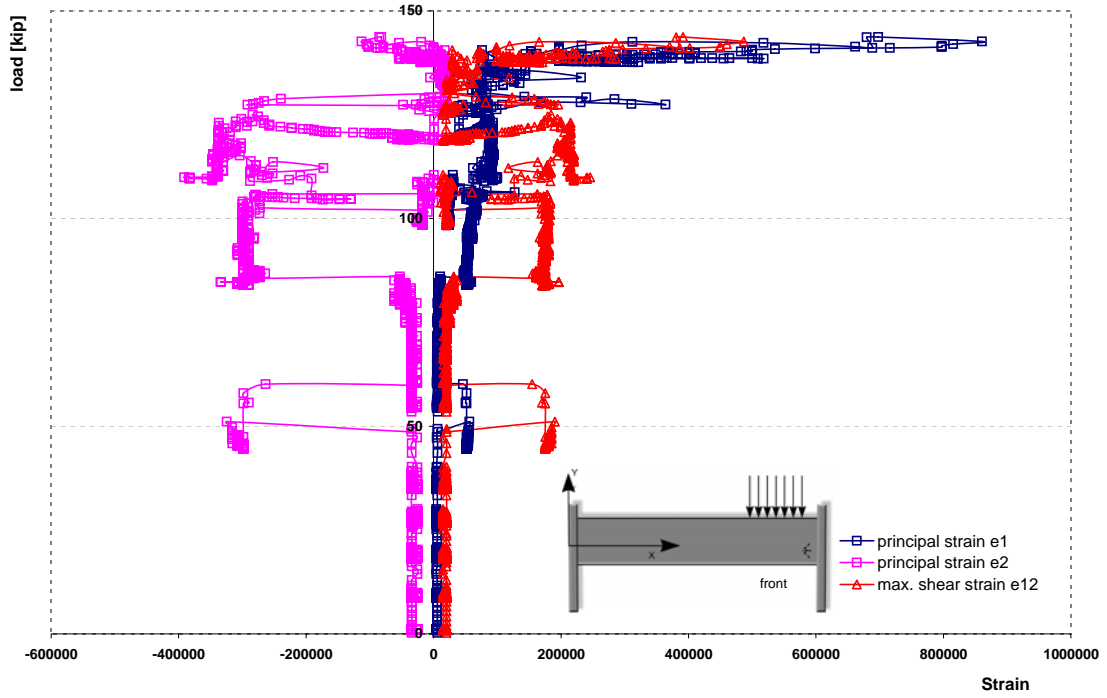
Load-Strain curves for the measuring point 100mm from the end (beside patch load)



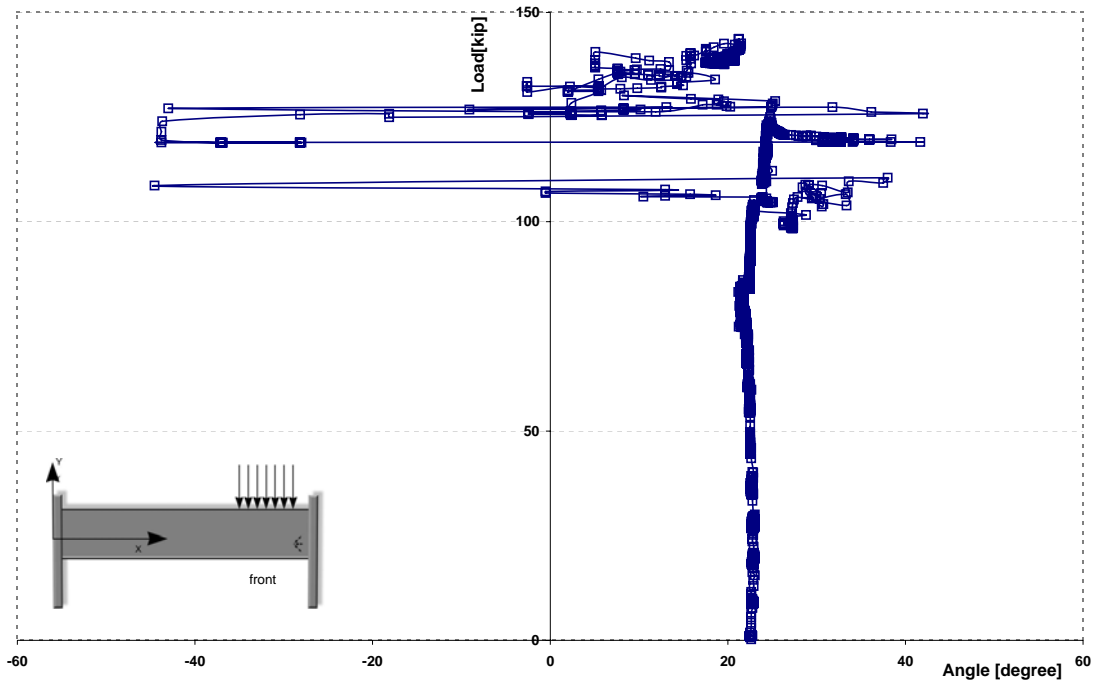
Load-Strain curves for the measuring point 100mm from the end (beside patch load)



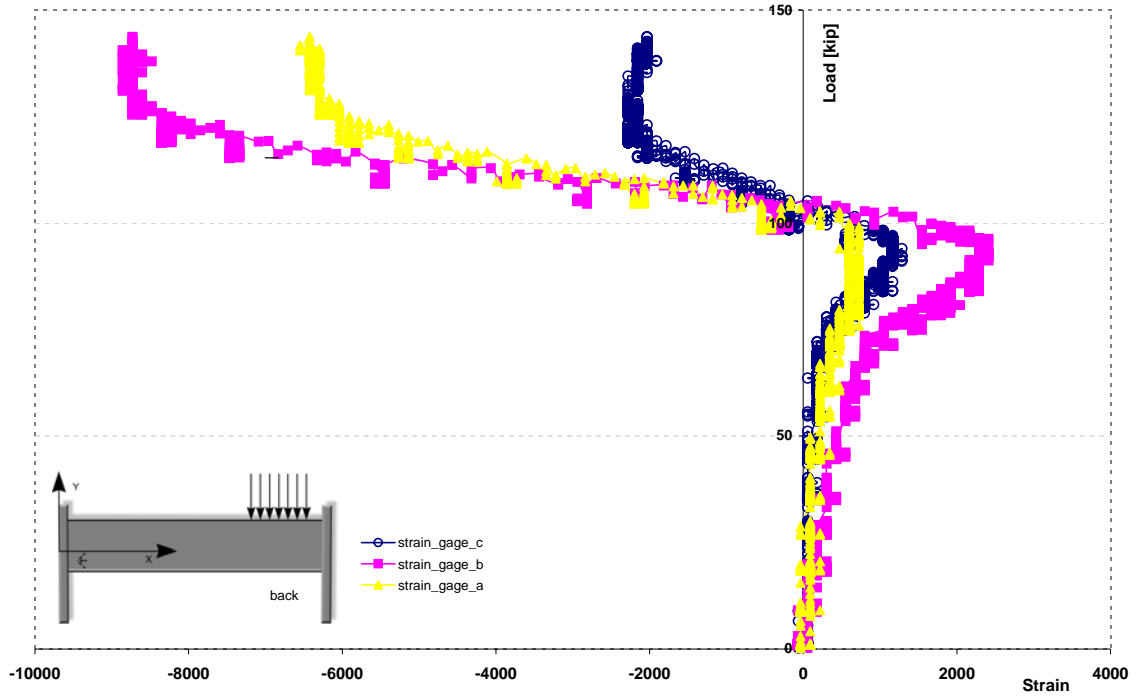
Load-Principal Strain curves for the measuring point 100mm from the end (beside patch load)



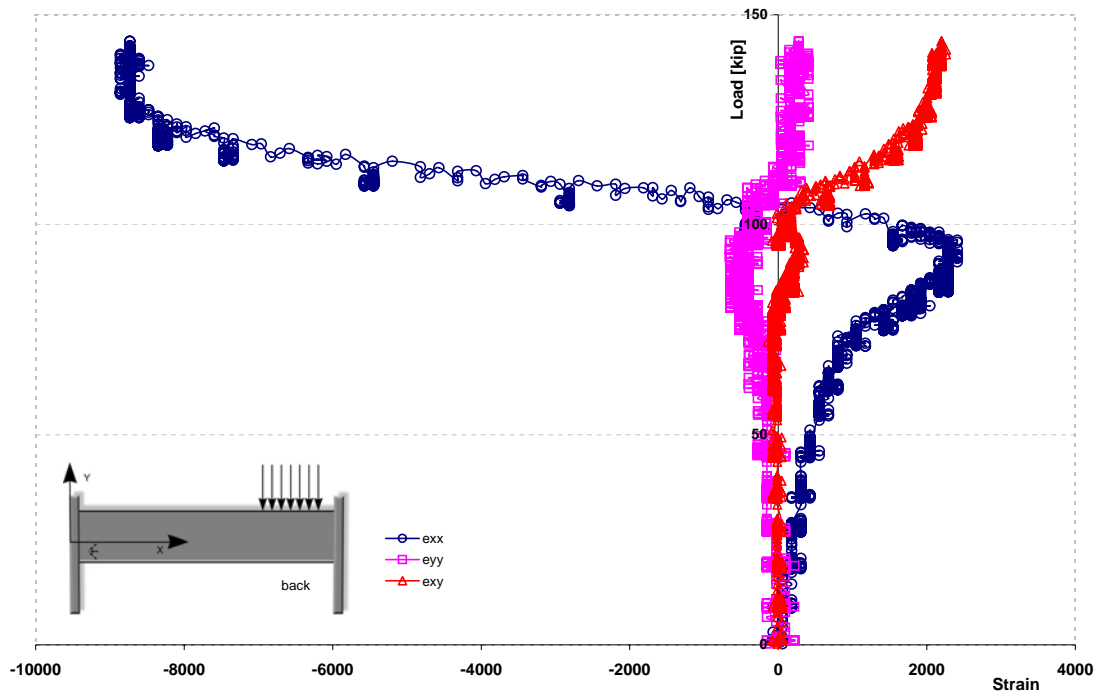
Principal Plain I Orientation



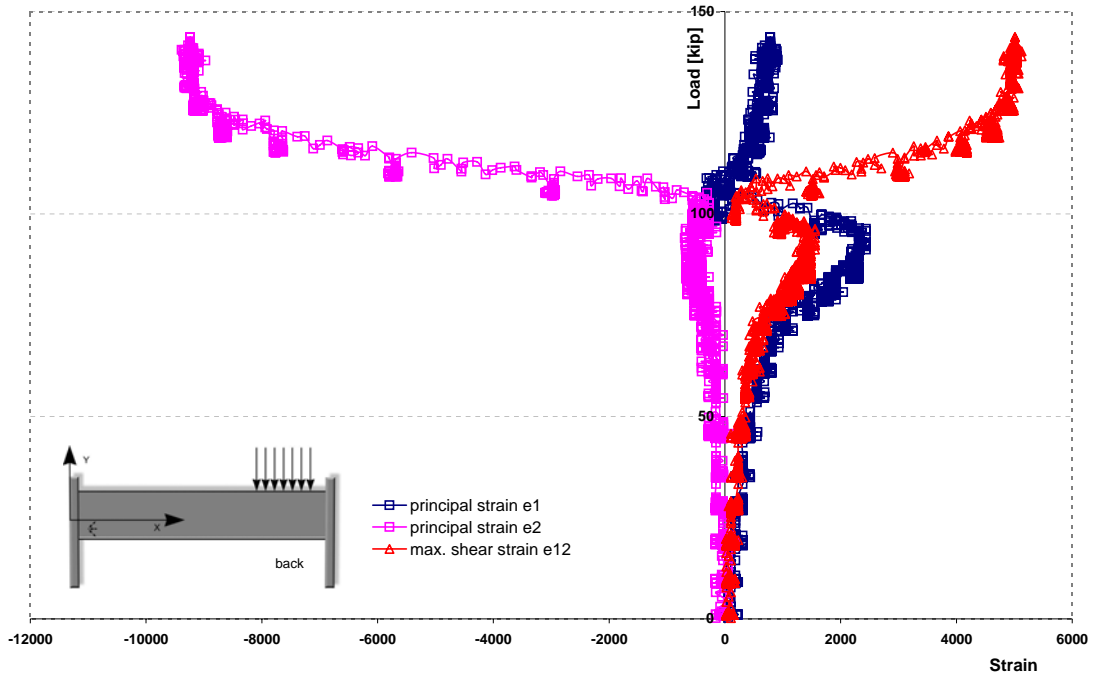
Load-Strain curves for the measuring point 100 mm from the end (opposite from patch load)



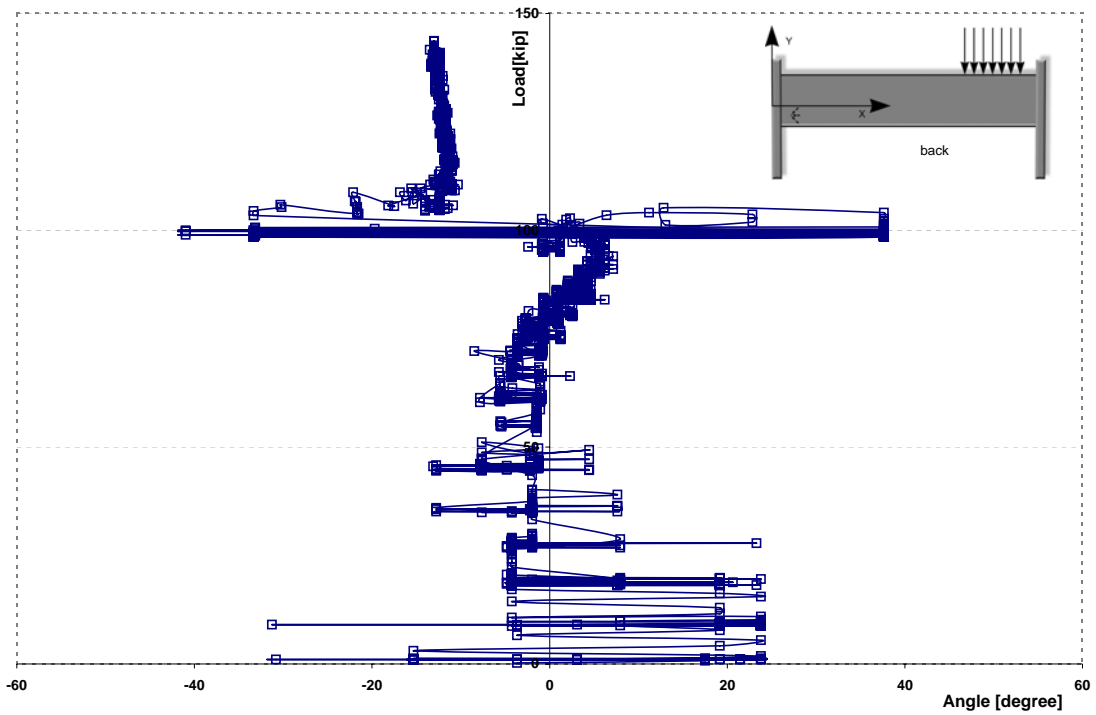
Load-Strain curves for the measuring point 100 mm from the end (opposite from patch load)



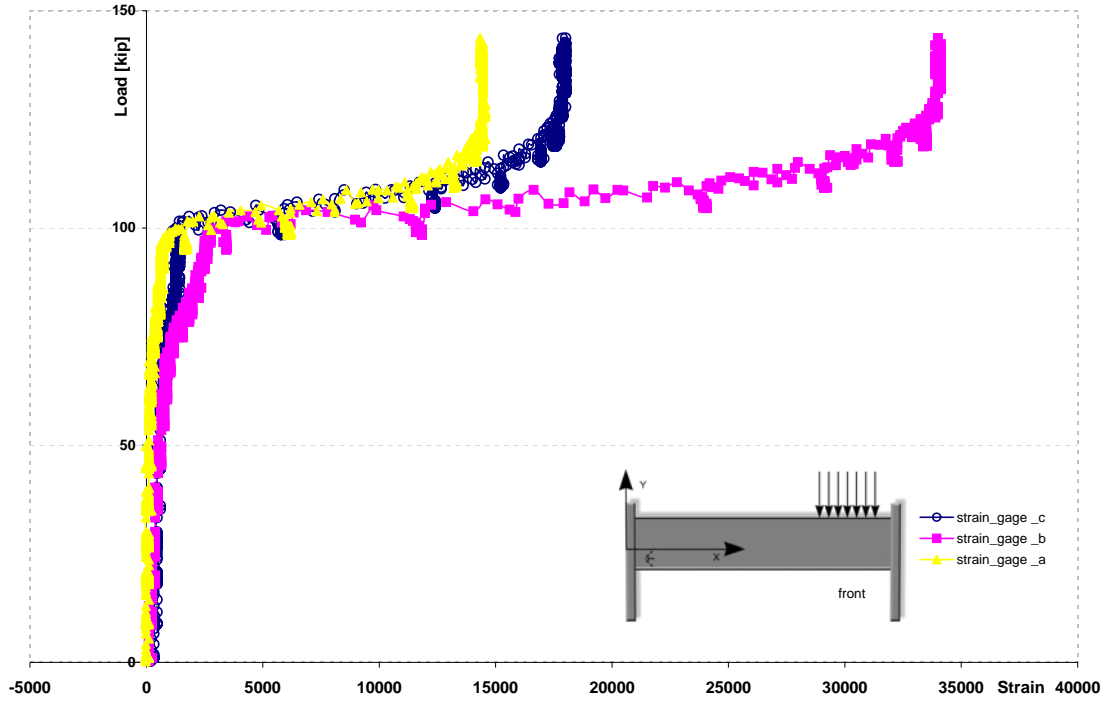
Load-Principal Strain curves for the measuring point 100mm from the end (opposite from patch load)



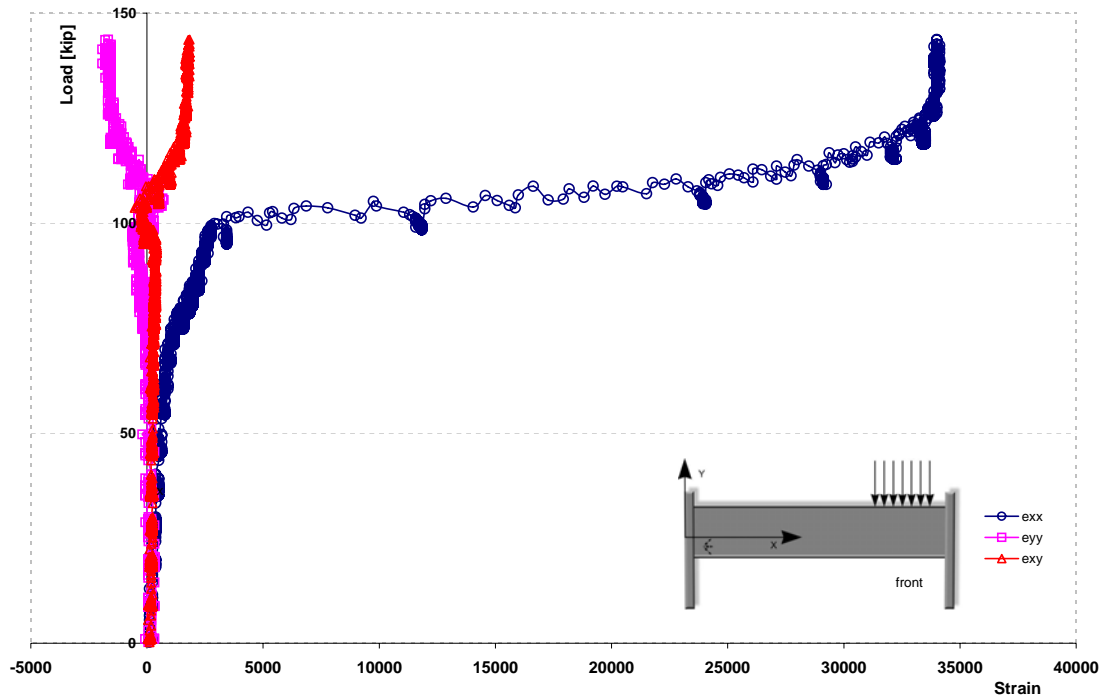
Principal Plain I Orientation



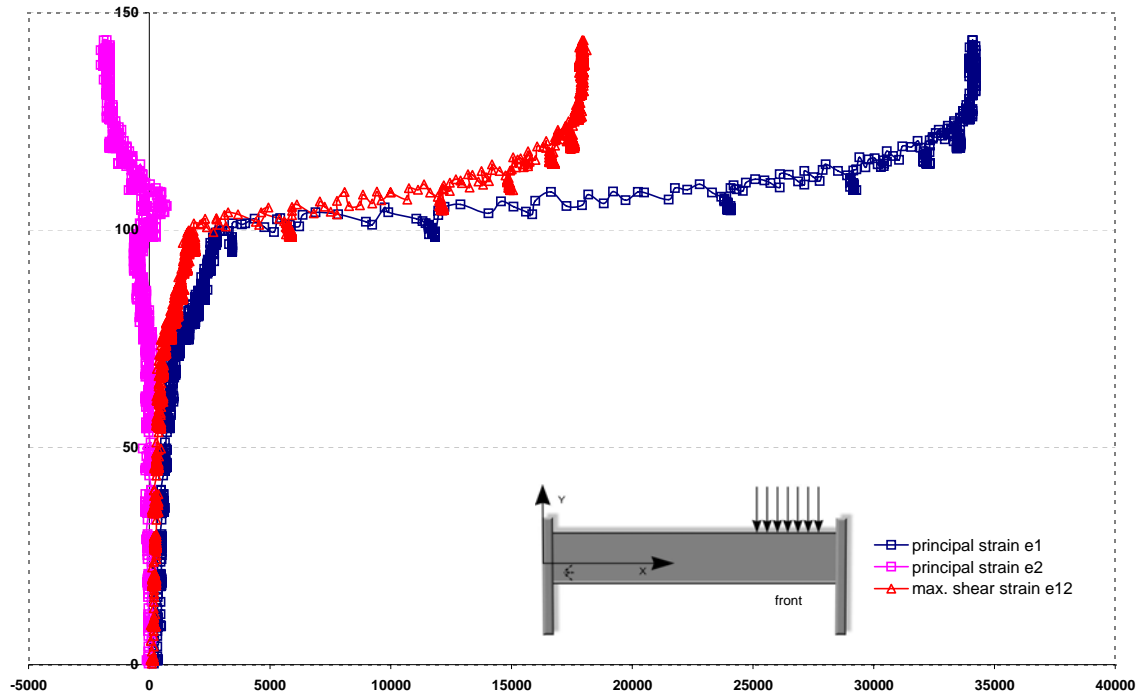
Load-Strain curves for the measuring point 100 mm from the end (opposite from patch load)



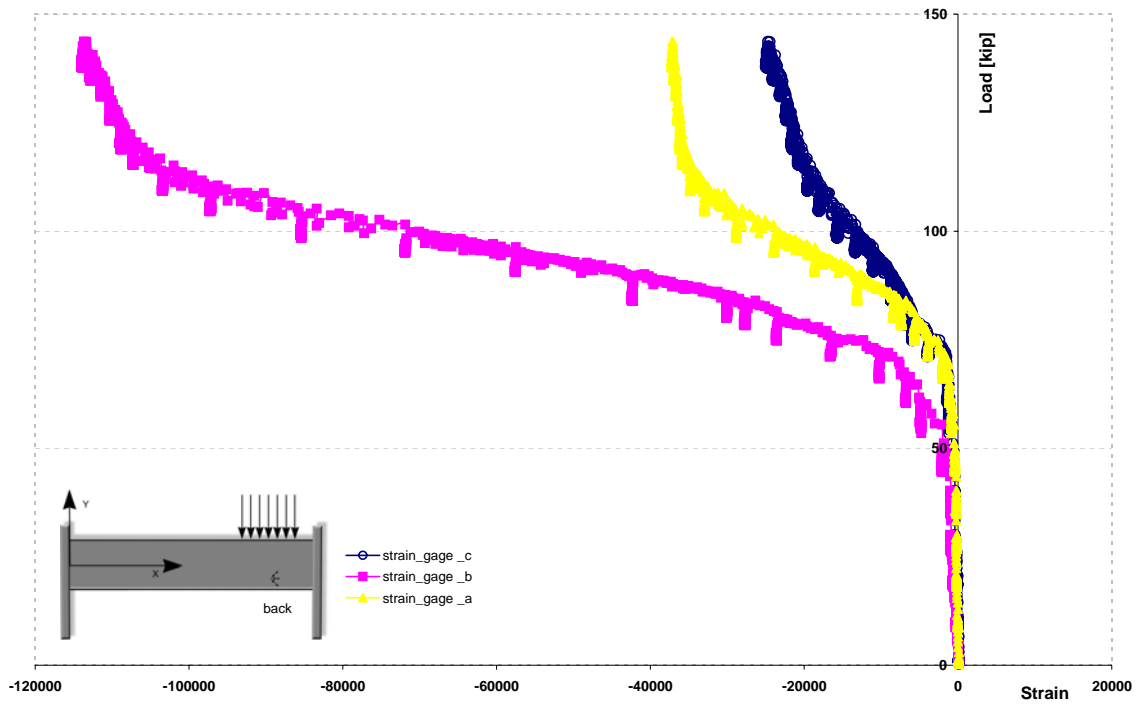
Load-Strain curves for the measuring point 100 mm from the end (opposite from patch load)



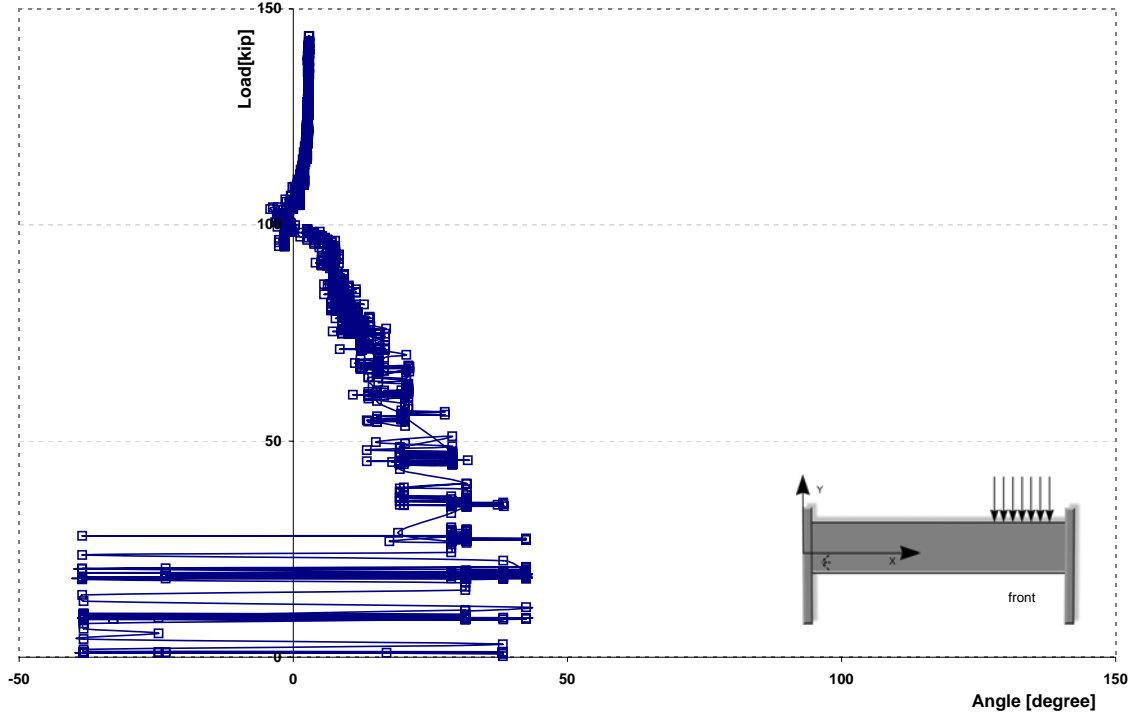
Load-Principal Strain curves for the measuring point 100mm from the end (opposite from patch load)



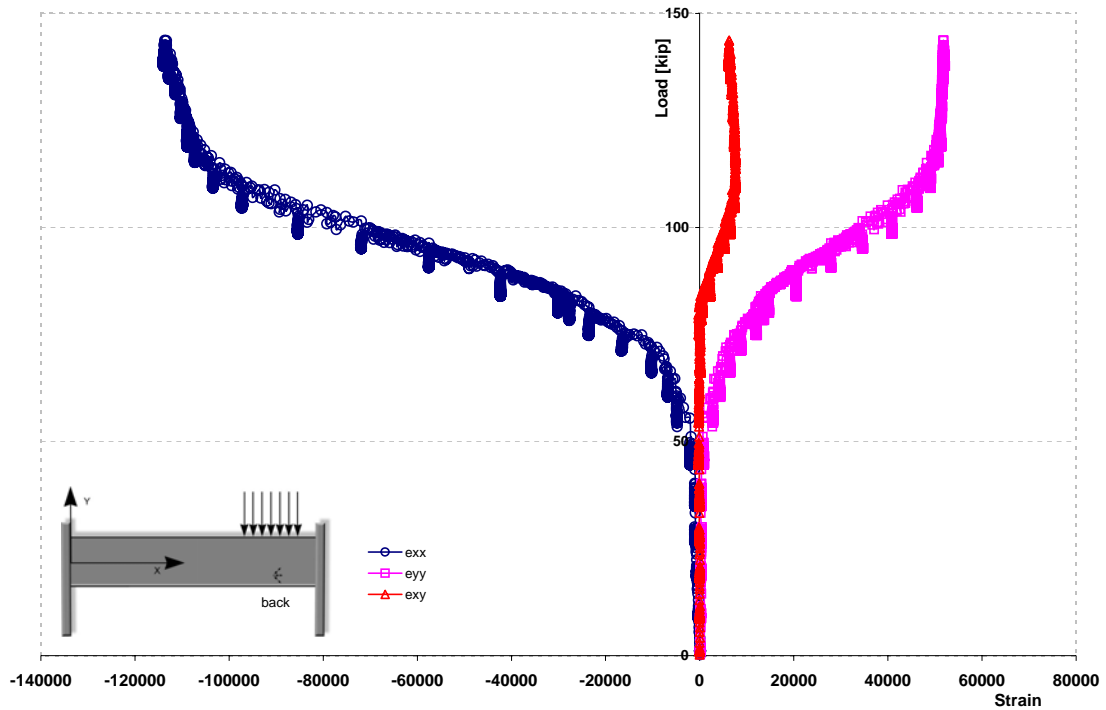
Load-Strain curves for the measuring point 400mm from the end (under the patch load)



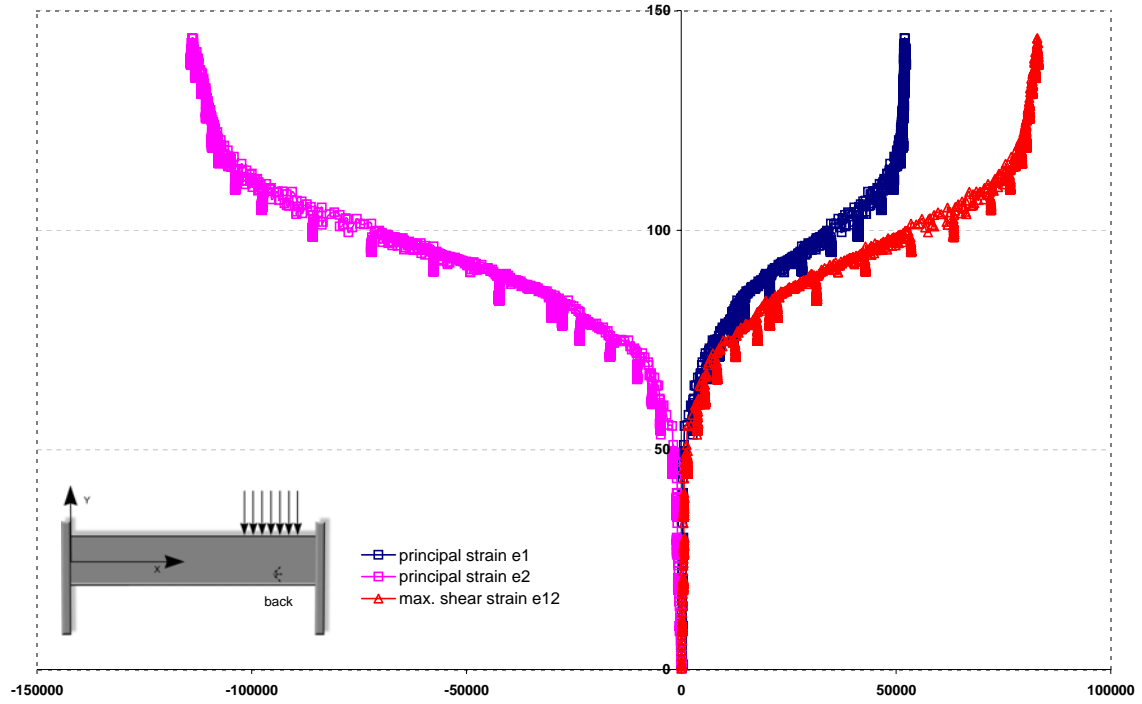
Principal Plain I Orientation



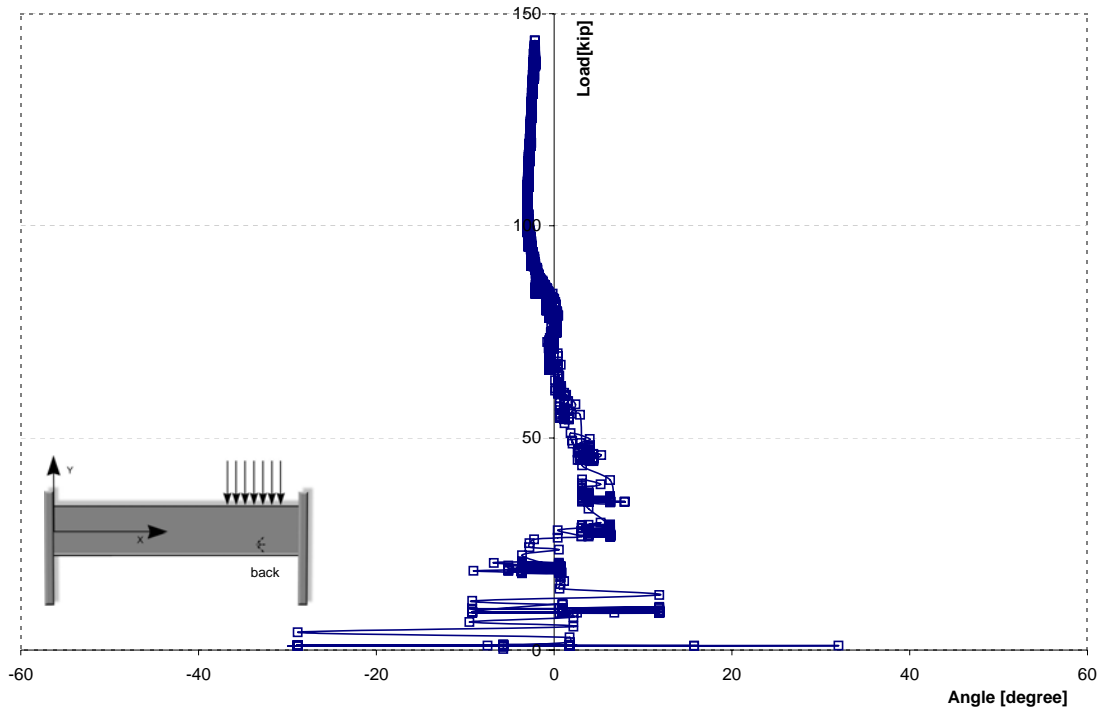
Load-Strain curves for the measuring point 400mm from the end (under the patch load)



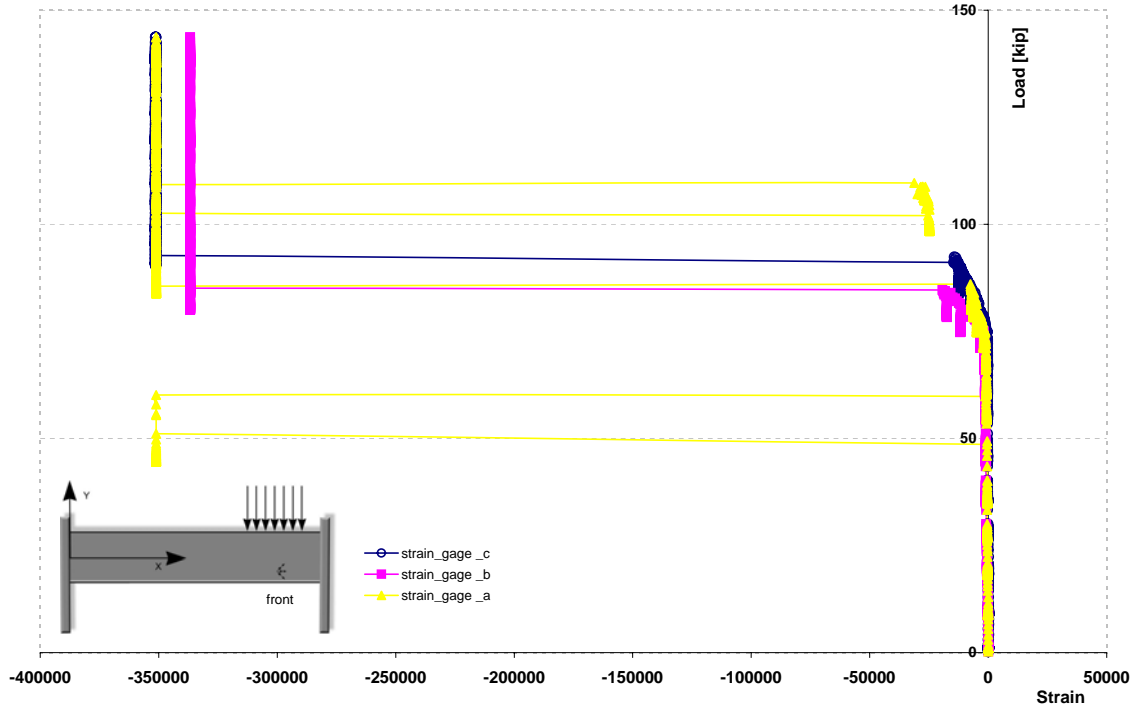
Load-Principal Strain curves for the measuring point 400mm from the end (under the patch load)



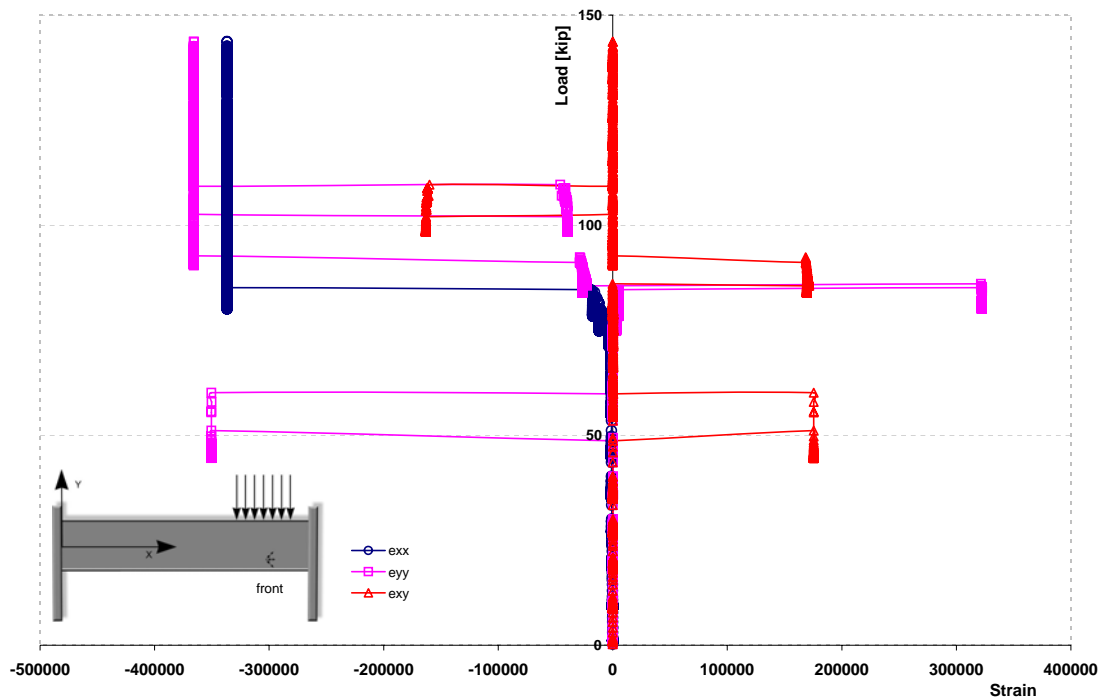
Principal Axes Orientation



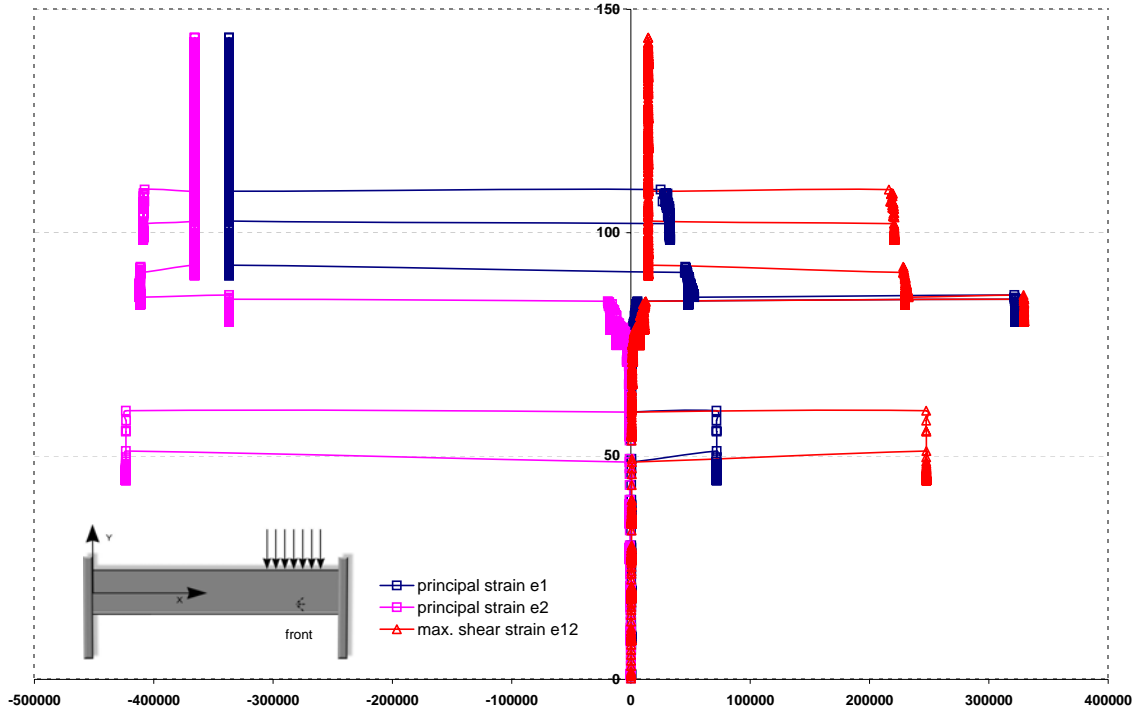
Load-Strain curves for the measuring point 400mm from the end (under the patch load)



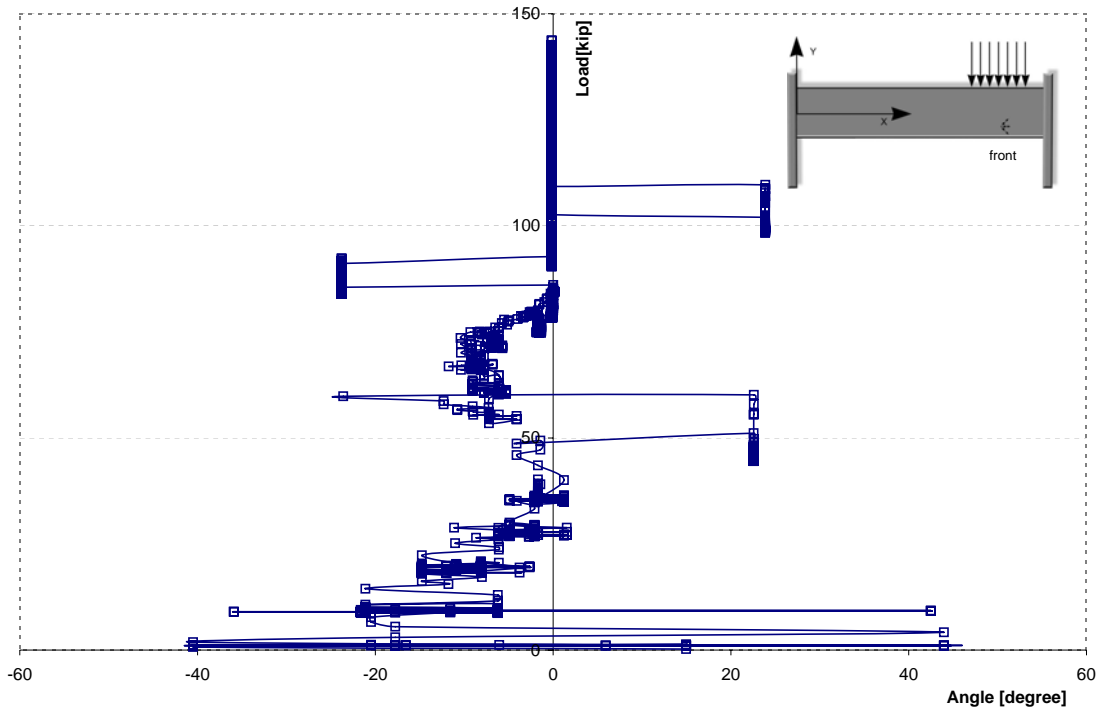
Load-Strain curves for the measuring point 400mm from the end (under the patch load)



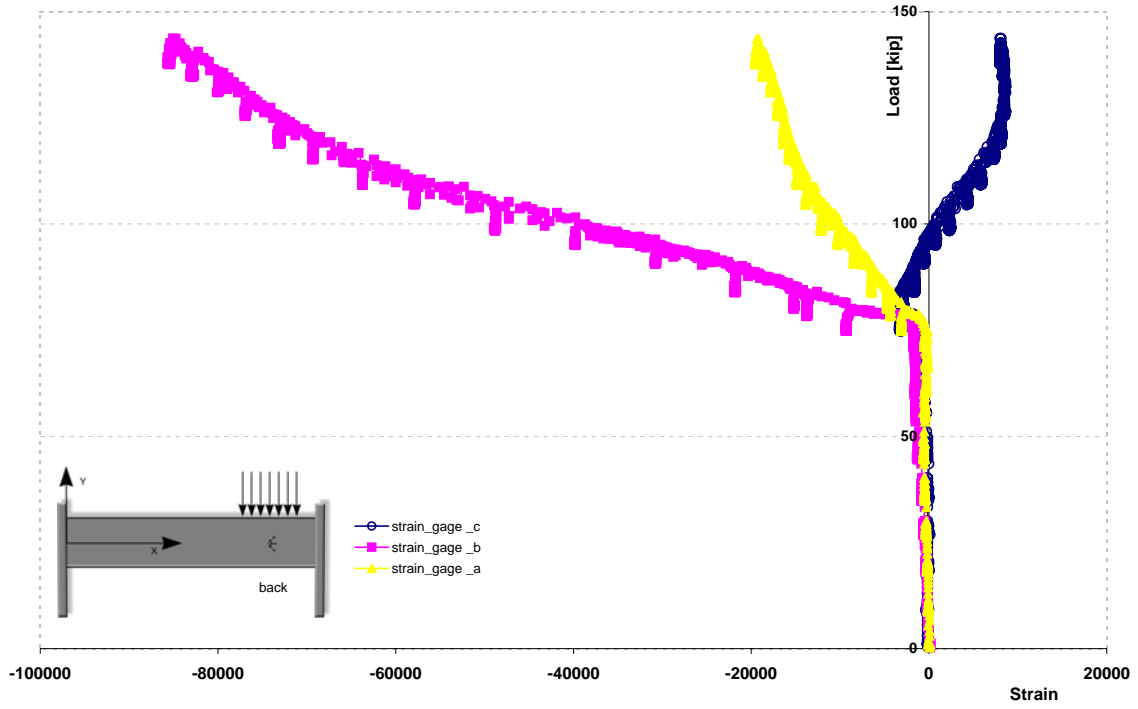
Load-Principal Strain curves for the measuring point 400mm from the end (under the patch load)



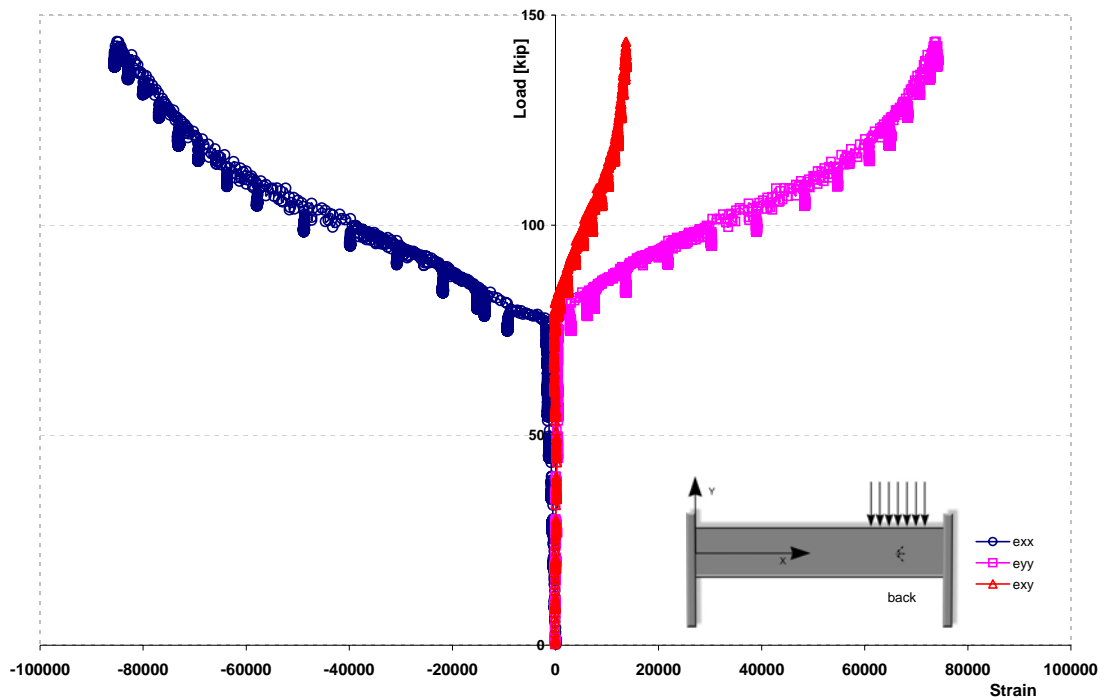
Principal Axes Orientation



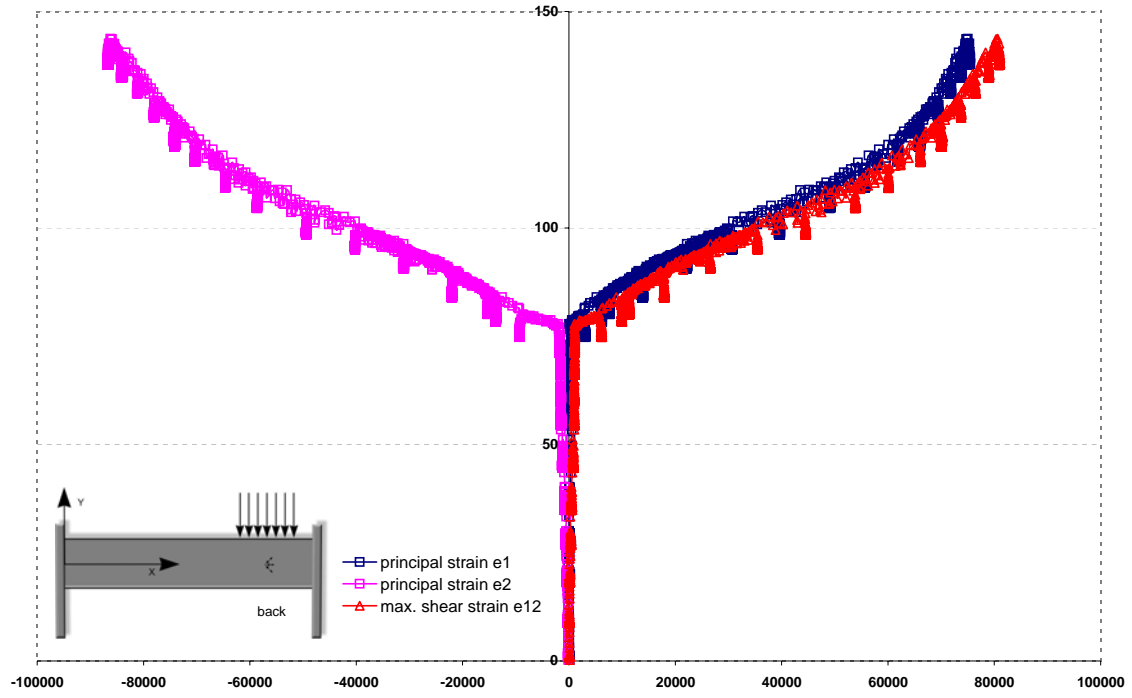
Load-Strain curves for the measuring point 400mm from the end (under the patch load)



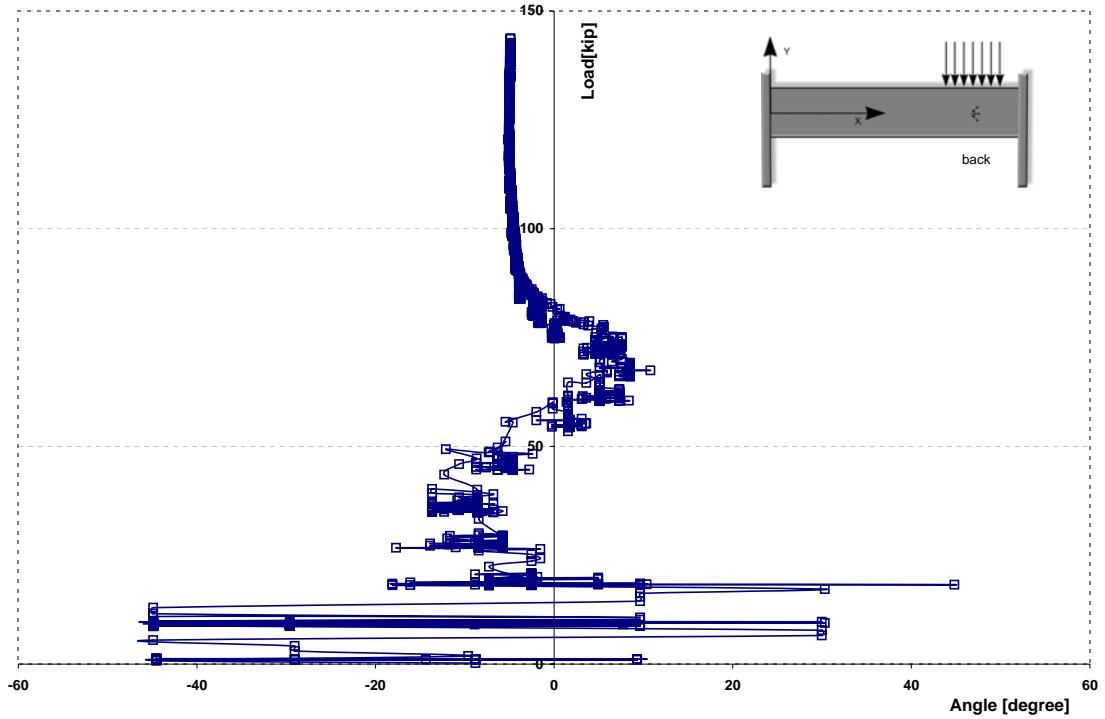
Load-Strain curves for the measuring point 400mm from the end (under the patch load)



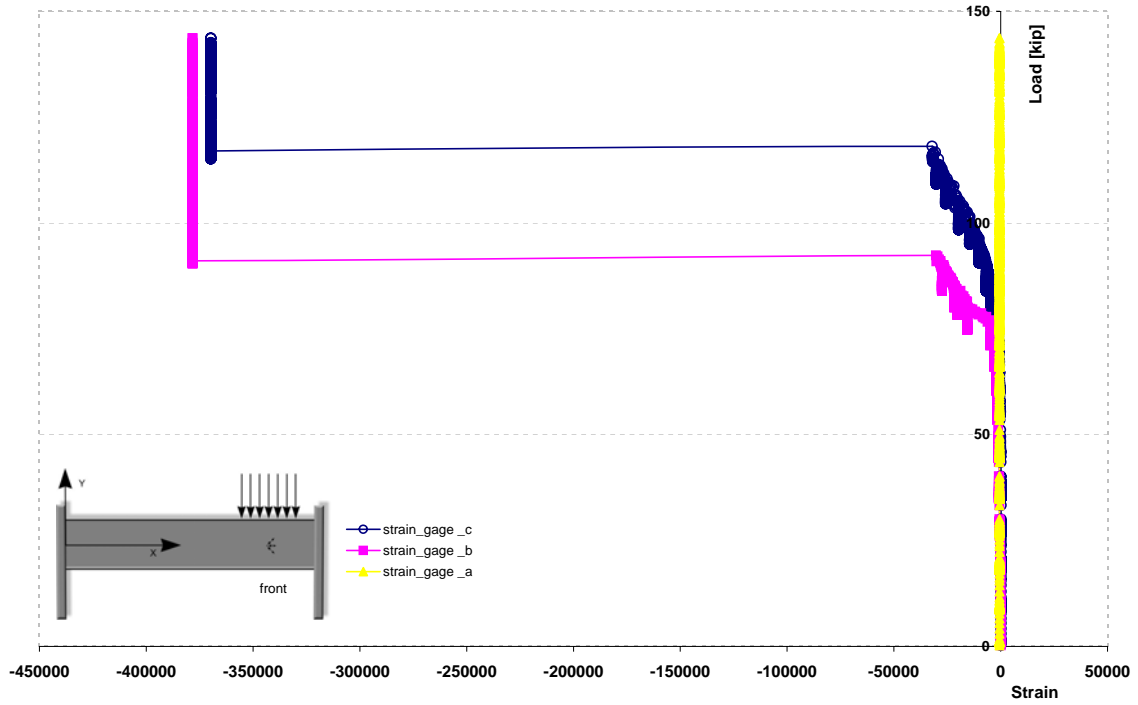
Load-Principal Strain curves for the measuring point 400mm from the end (under the patch load)



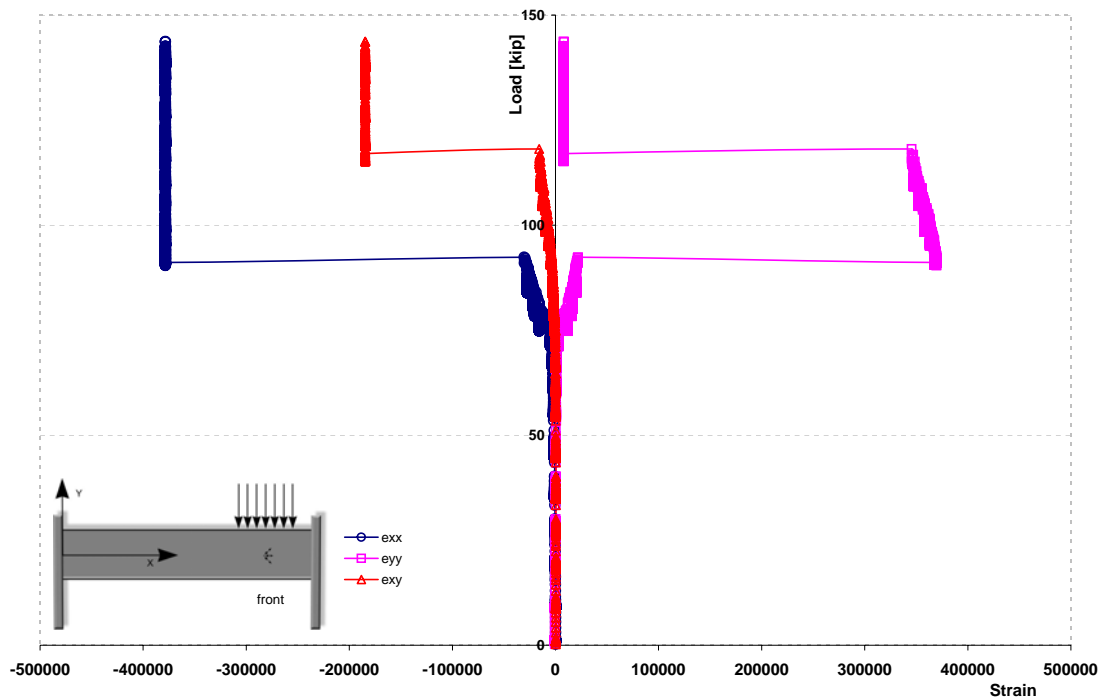
Principal Axes Orientation



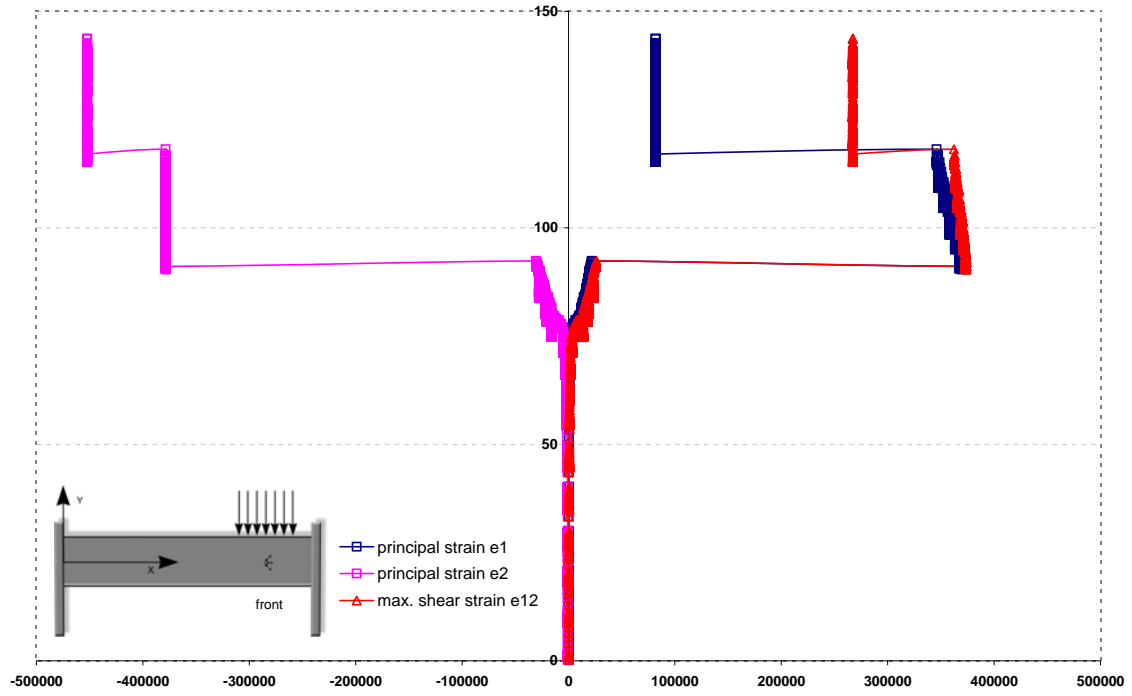
Load-Strain curves for the measuring point 400mm from the end (under the patch load)



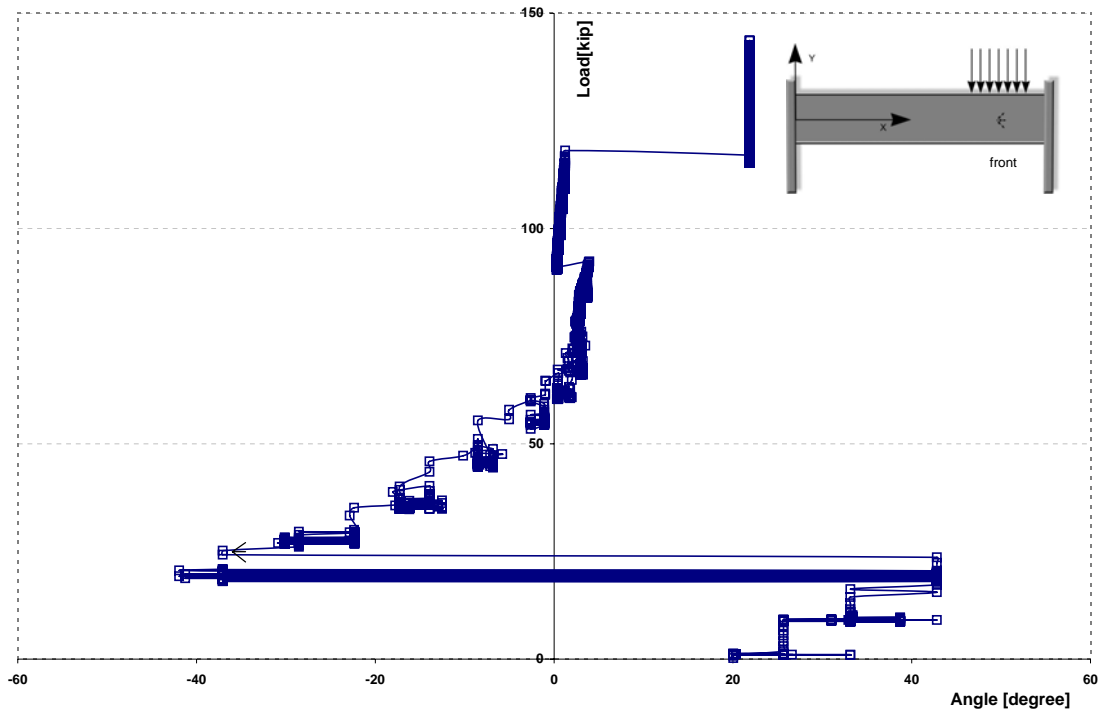
Load-Strain curves for the measuring point 130mm from the end (beside patch load)



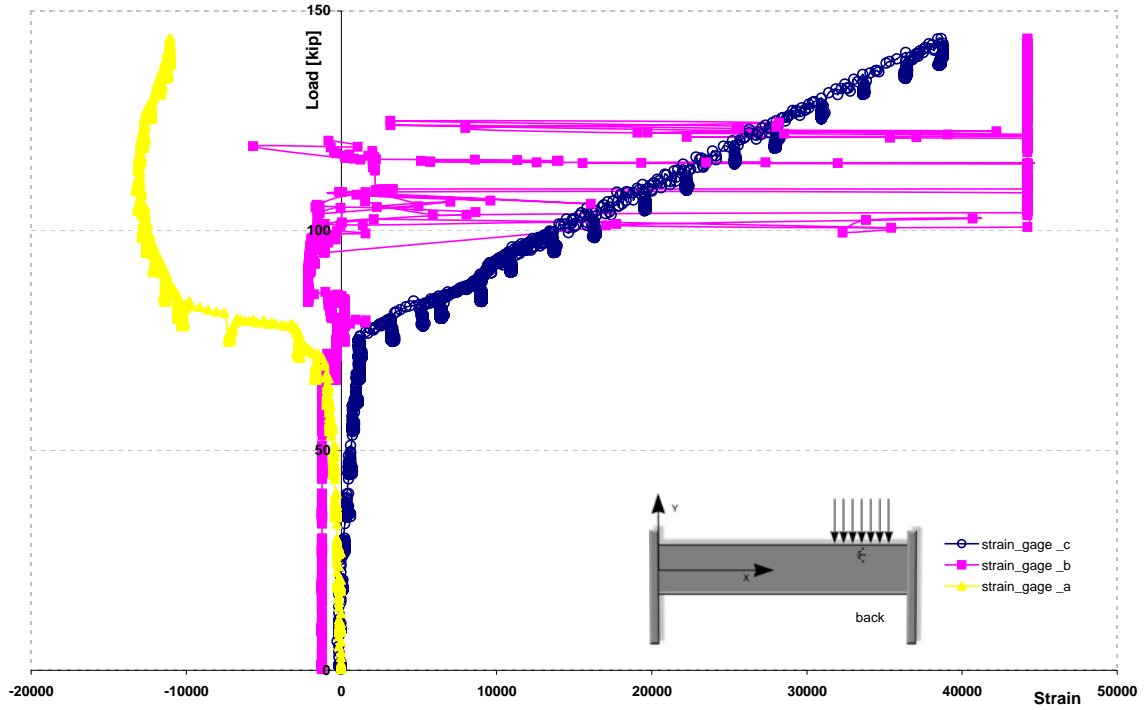
Load-Principal Strain curves for the measuring point 400mm from the end (under the patch load)



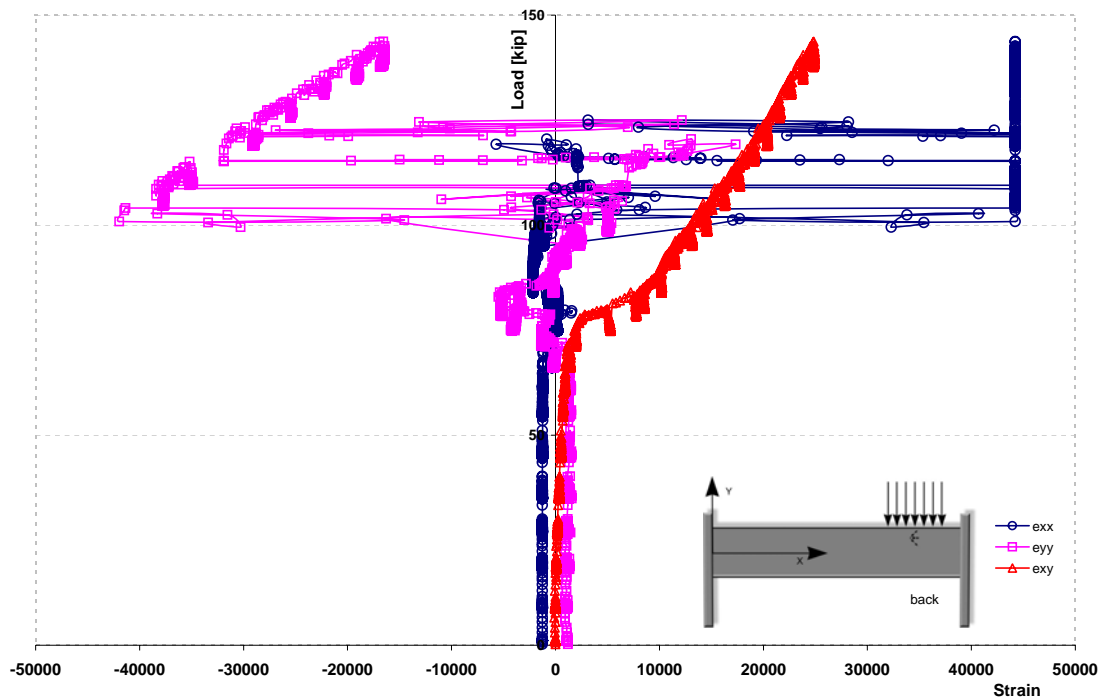
Principal Axes Orientation



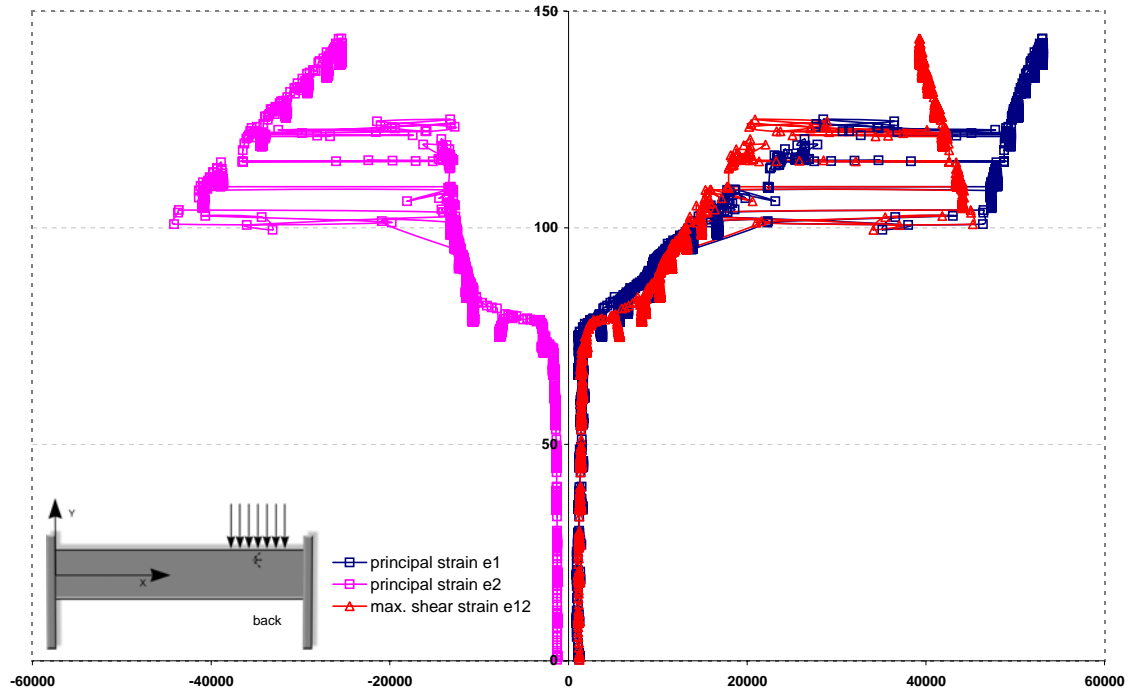
Load-Strain curves for the measuring point 400mm from the end (under the patch load)



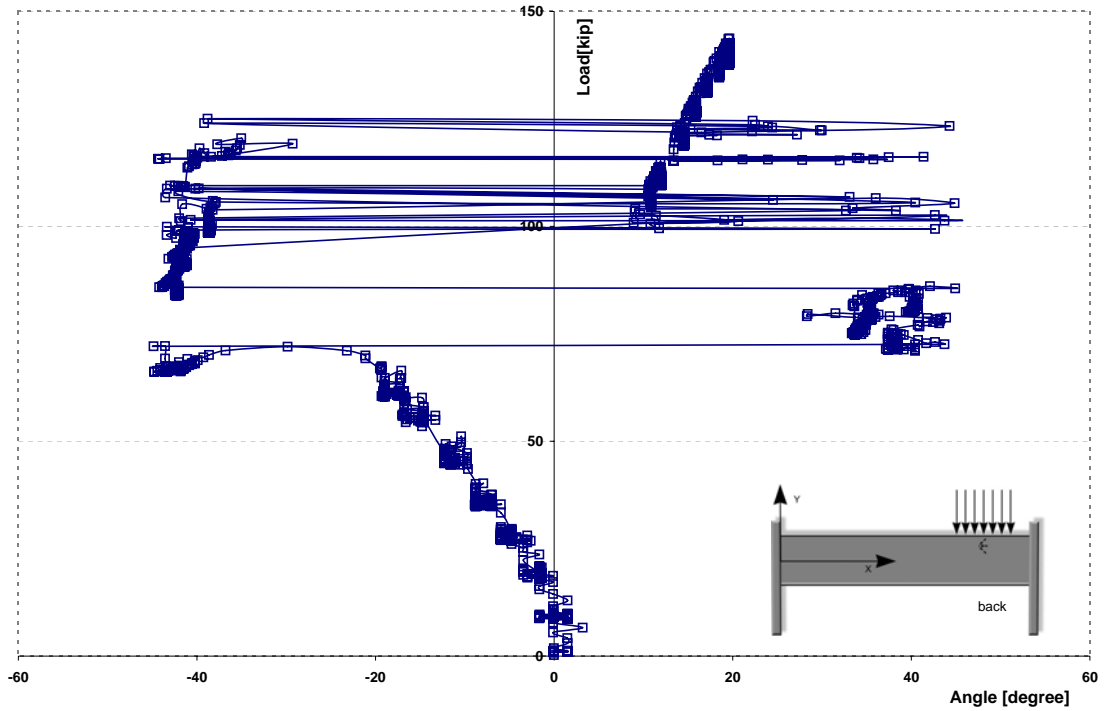
Load-Strain curves for the measuring point 400mm from the end (under the patch load)



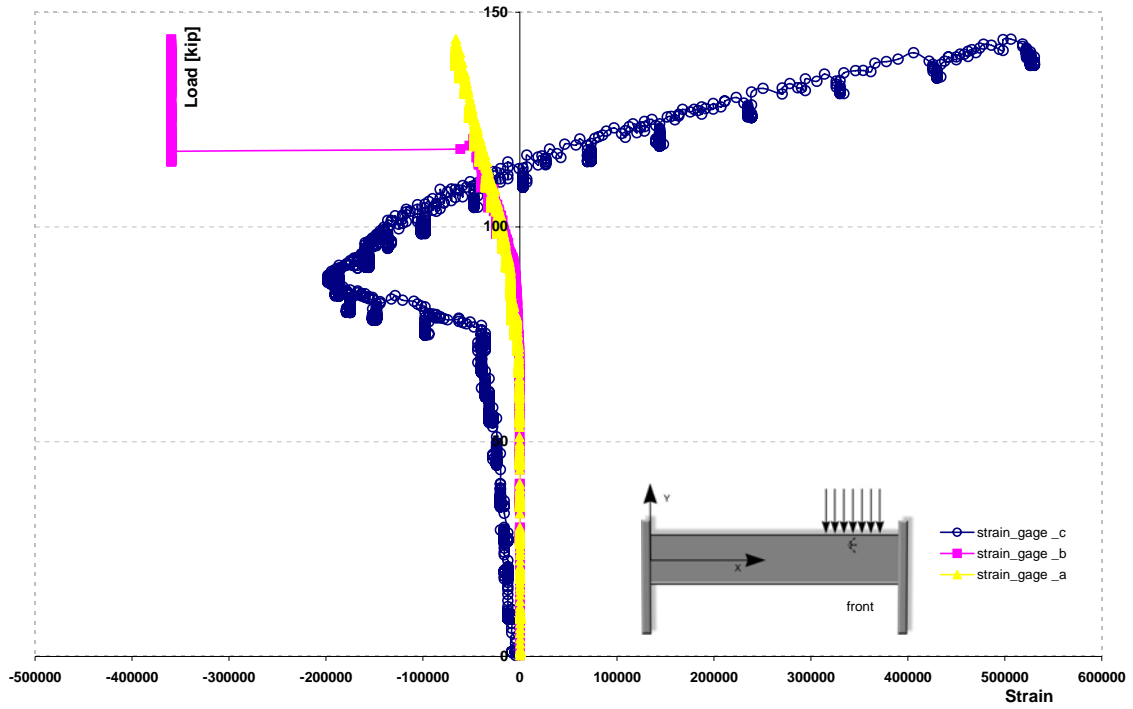
Load-Principal Strain curves for the measuring point 400mm from the end (under the patch load)



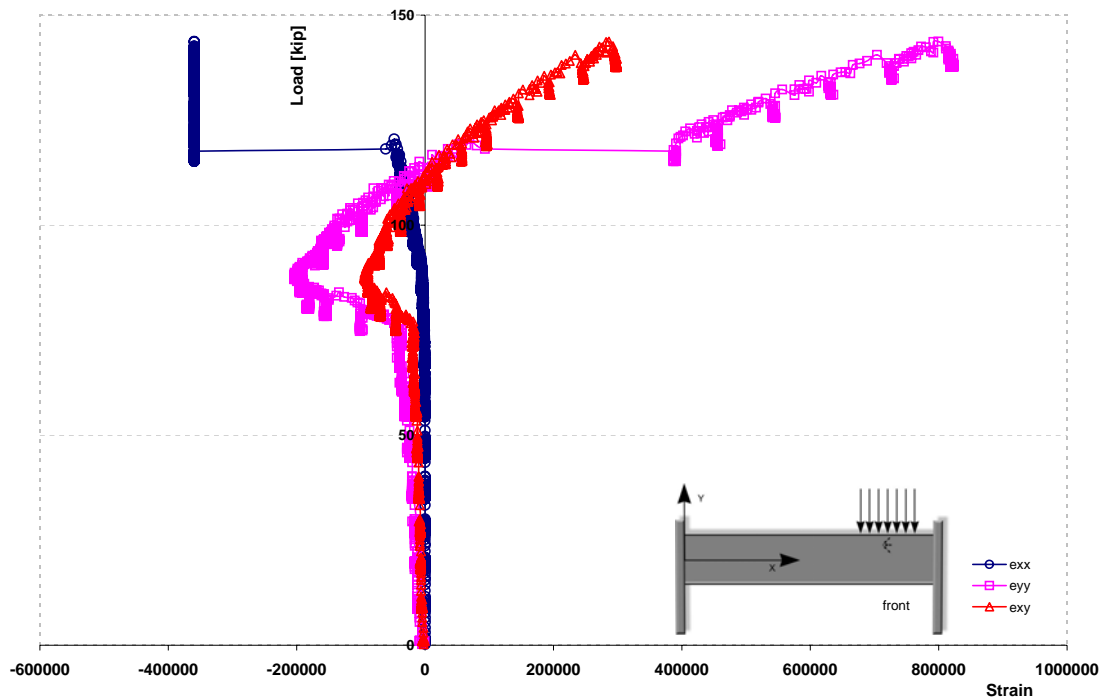
Principal Axes Orientation



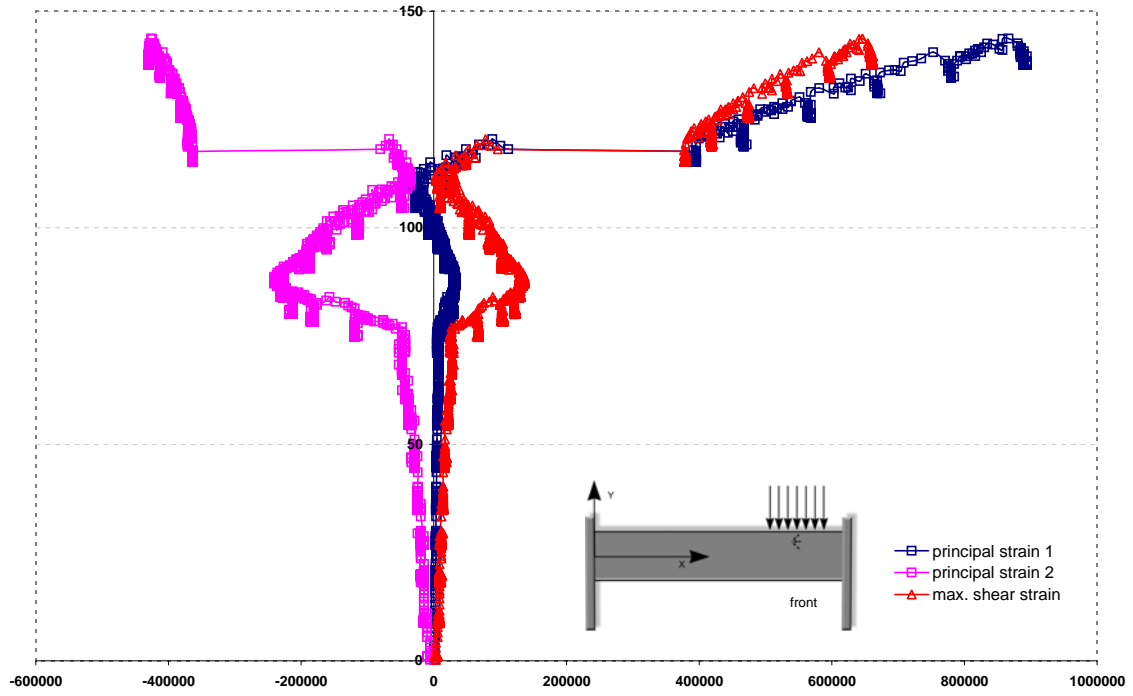
Load-Strain curves for the measuring point 400mm from the end (under the patch load)



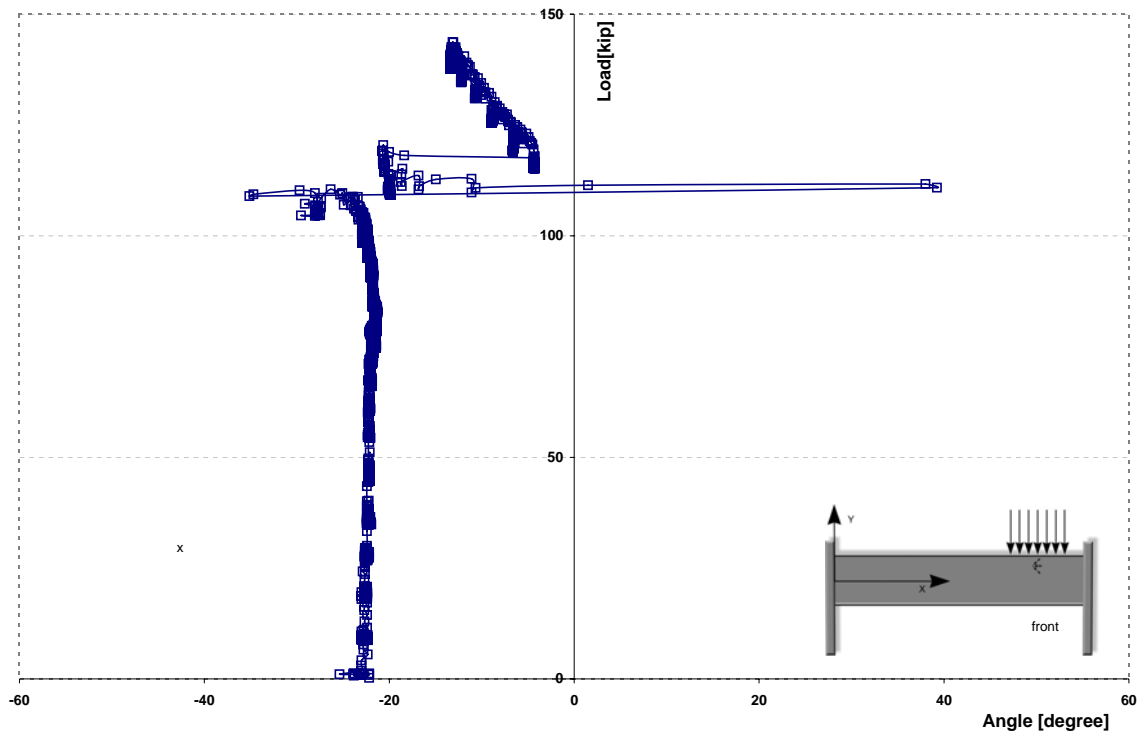
Load-Strain curves for the measuring point 400mm from the end (under the patch load)



Load-Principal Strain curves for the measuring point 400mm from the end (under the patch load)



Principal Axes Orientation



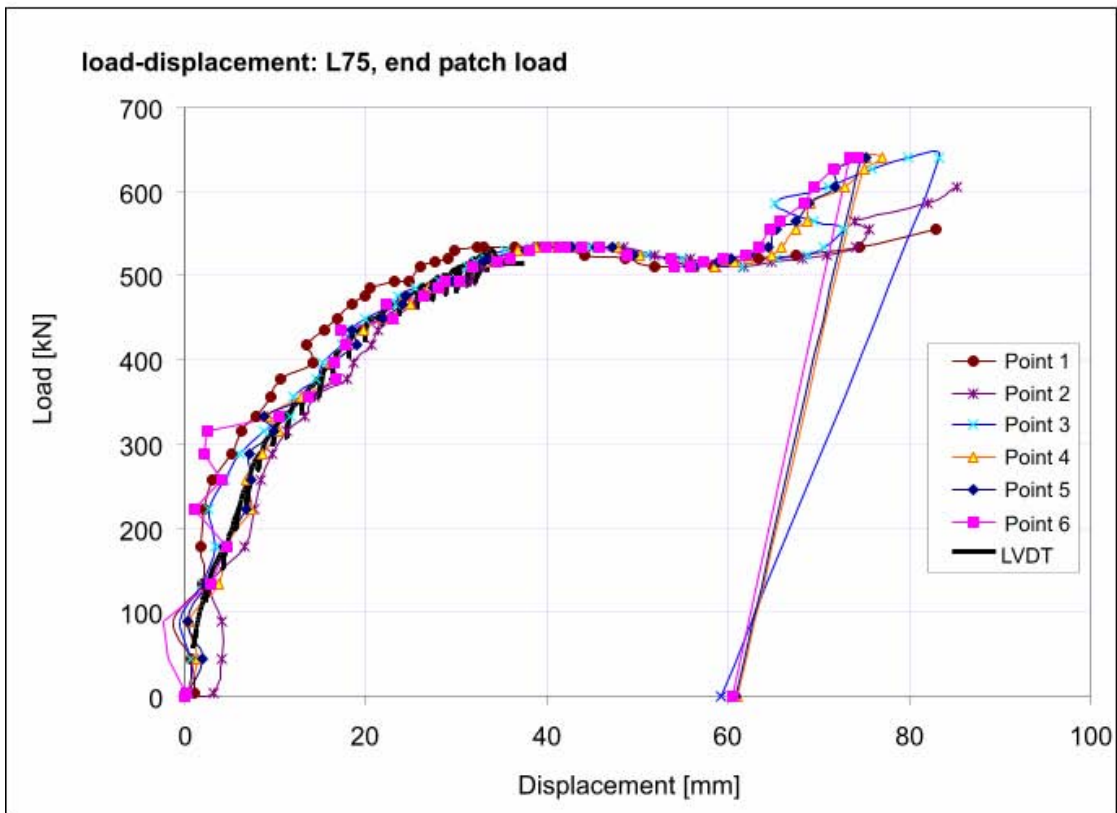
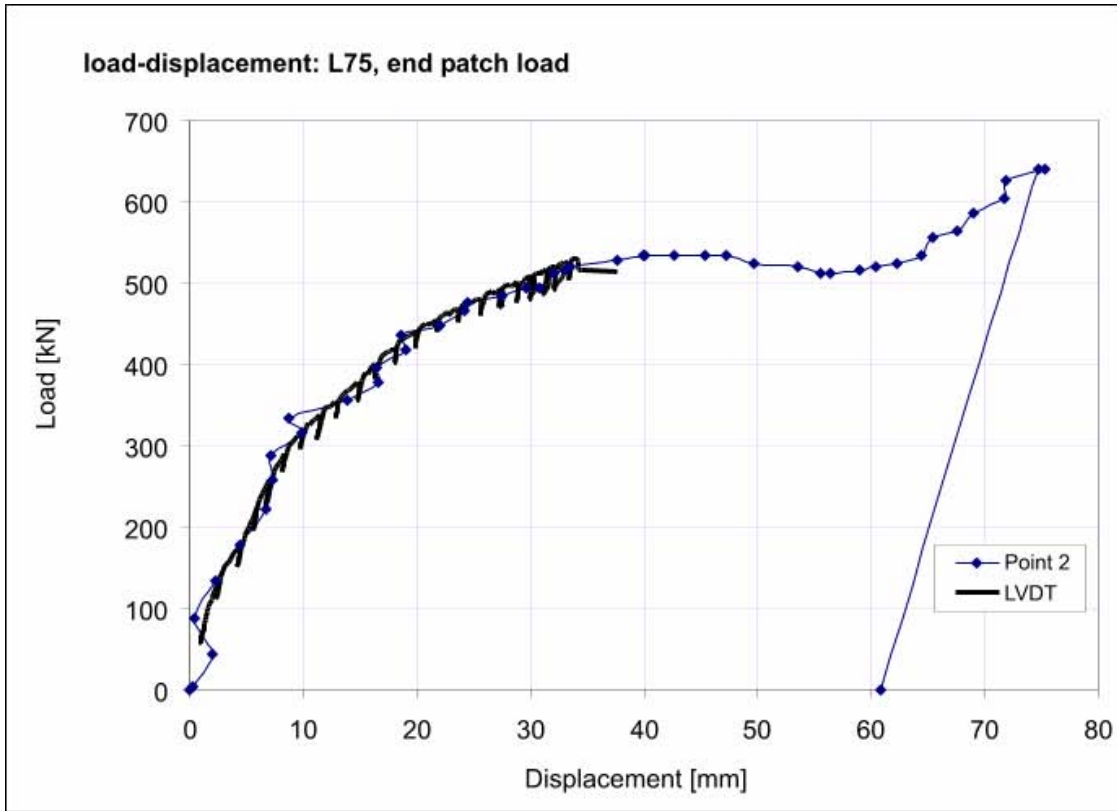
Data from Test: L75e

18-Aug-04

L75 / END LOAD

LOAD-DISPLACEMENT OF POINTS AT END LOAD

load			microscribe point deflections dz					
load (kN)	step	load (kip)	Point 1	Point 2	Point 3	Point 4	Point 5	Point 6
			mm	mm	mm	mm	mm	mm
0.0	1	0	0	0	0	0	0	0
4.4	2	1	0.2	0.3	0.2	0.3	3.3	1.0
44.4	3	10	-1.7	2.0	1.4	0.6	4.1	0.6
88.9	4	20	-2.4	0.4	0.5	-0.6	4.1	-1.3
133.3	5	30	2.8	2.3	3.8	2.0	2.8	2.0
177.8	6	40	4.6	4.4	4.5	3.4	6.7	1.7
222.2	7	50	1.0	6.8	7.3	2.6	7.8	2.1
257.8	8	58	4.2	7.4	6.8	4.5	8.5	3.1
288.9	9	65	2.2	7.2	8.7	6.0	9.8	5.2
315.6	10	71	2.5	9.9	10.5	8.7	11.3	6.3
333.3	11	75	10.3	8.7	9.1	11.7	13.3	7.8
355.6	12	80	13.6	13.8	13.0	12.1	14.3	9.5
377.8	13	85	16.7	16.6	16.5	14.5	18.0	10.6
395.6	14	89	16.5	16.5	16.1	15.3	18.7	14.1
417.8	15	94	17.8	19.0	17.9	17.5	20.6	13.5
435.6	16	98	17.3	18.5	19.8	18.5	21.3	15.4
448.9	17	101	22.9	22.0	21.9	20.0	23.1	16.9
466.7	18	105	22.2	24.1	24.9	23.3	25.3	18.6
475.6	19	107	26.5	24.5	24.3	23.5	26.4	19.9
484.4	20	109	27.9	27.5	26.8	25.6	28.5	20.4
493.3	21	111	28.8	29.7	29.0	28.1	30.3	23.2
493.3	22	111	30.3	30.7	30.6	29.6	31.6	24.7
511.1	23	115	31.9	32.1	31.7	31.2	33.1	26.0
515.6	24	116	34.5	33.1	33.3	32.1	34.7	27.6
520.0	25	117	35.9	33.5	34.0	33.3	36.1	29.0
528.9	26	119	38.0	37.7	36.8	35.4	37.6	29.9
533.3	27	120	41.4	40.1	38.8	38.2	39.2	32.3
533.3	28	120	39.9	40.0	40.6	40.3	40.6	33.0
533.3	29	120	42.0	42.7	42.6	42.9	43.0	36.5
533.3	30	120	43.7	45.4	45.8	44.8	45.1	38.8
533.3	31	120	45.7	47.2	47.8	47.8	48.5	41.1
524.4	32	118	48.8	49.6	50.3	50.9	51.9	44.1
520.0	33	117	53.7	53.6	54.1	54.9	55.9	48.7
511.1	34	115	54.1	55.6	56.1	56.4	58.7	51.9
511.1	35	115	55.9	56.4	58.5	61.6	61.8	58.3
515.6	36	116	57.2	58.9	60.8	61.9	64.9	60.4
520.0	37	117	59.4	60.4	62.4	65.4	68.1	63.4
524.4	38	118	62.0	62.3	64.7	68.8	71.0	67.5
533.3	39	120	63.4	64.4	65.9	70.5	74.1	74.6
555.6	40	125	64.7	65.4	67.4	72.7	75.5	82.9
564.4	41	127	65.6	67.5	68.8	69.5	74.0	
586.7	42	132	68.3	68.9	69.1	65.1	82.1	
604.4	43	136	69.5	71.7	72.9	71.2	85.2	
626.7	44	141	71.7	71.9	75.1	75.9		
640.0	45	144	74.4	75.3	77.0	80.0		
640.0	46	144	73.5	74.7	75.2	83.3		
0.0	47	0	60.5	60.9	61.0	59.2		

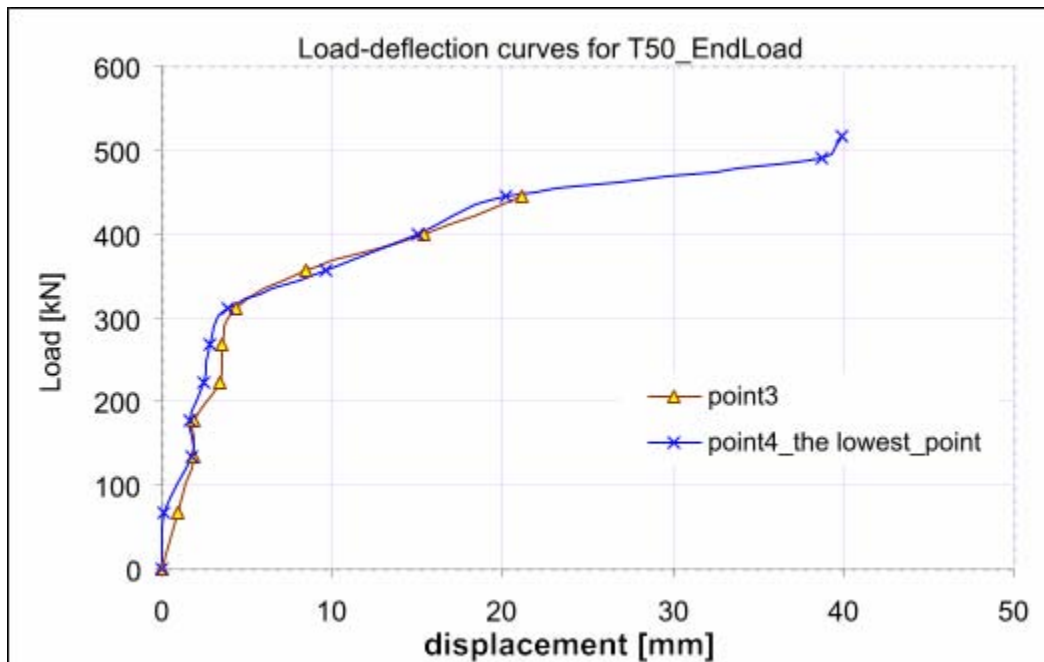


Data from Test: T50e

16-Jul-04

T50 / END LOAD

load			microscribe point deflections dz			
load (kN)	step	load (kip)	Point 1 mm	Point 2 mm	Point 3 mm	Point 4 mm
0	1	0	0	0	0	0
67	2	15	0.287386	-2.838005	0.978332	0.169636
133	3	30	1.682649	1.094168	1.827456	1.740034
178	4	40	2.310469	0.200472	1.897849	1.609882
222	5	50	5.199295	2.745327	3.388068	2.442438
267	6	60		0.410392	3.5165	2.825772
311	7	70		2.033306	4.343485	3.83838
356	8	80		6.390114	8.396435	9.660142
400	9	90		13.4328	15.37958	15.07023
444	10	100		24.41745	21.17356	20.20959
489	11	110				38.68158
516	12	116				39.86465
533	13	120				37.85169
578	14	130				43.94923
622	15	140				43.63576
667	16	150				40.22744

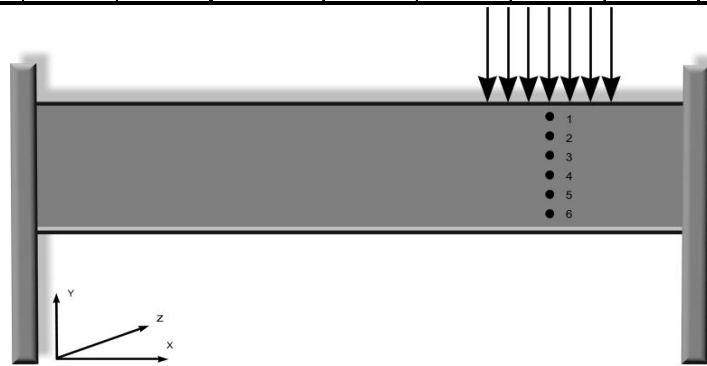


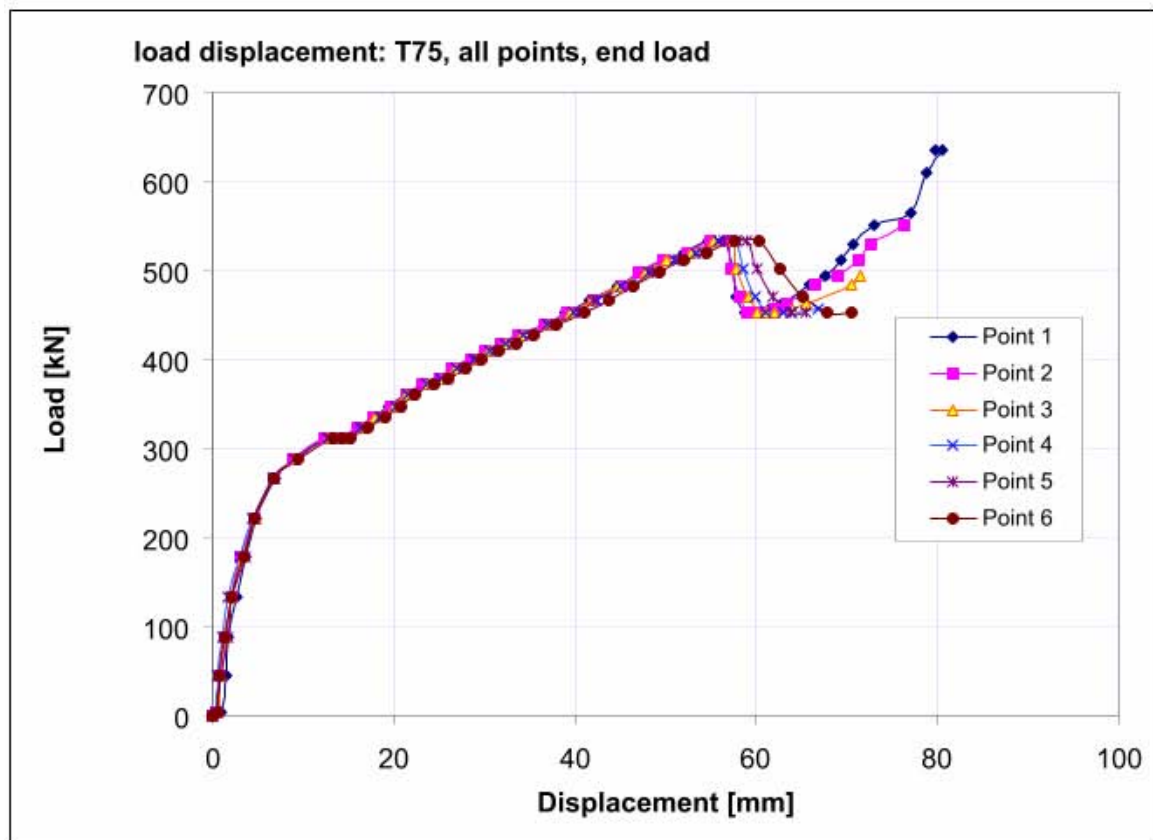
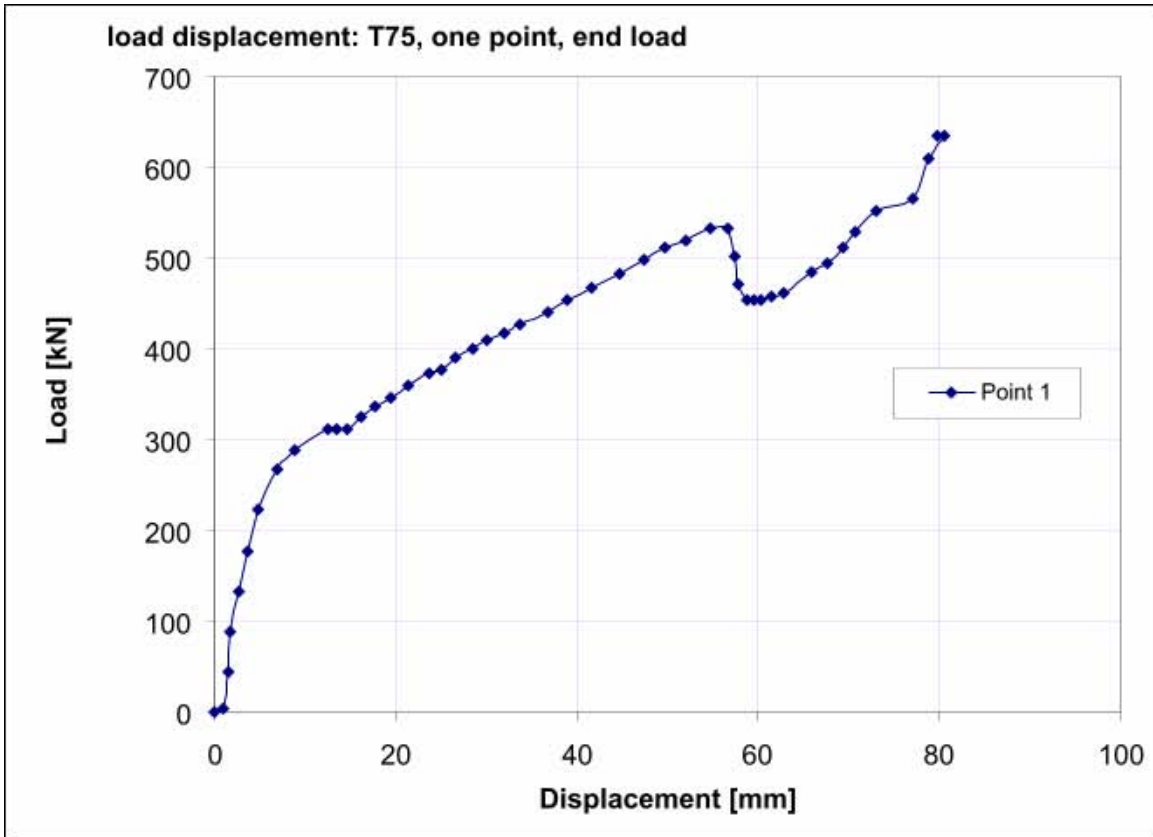
Data from Test: T75e

16-Jul-04

T75 / END LOAD

load			microscribe point deflections dz					
			Point 1	Point 2	Point 3	Point 4	Point 5	Point 6
load (kN)	step	load (kip)	mm	mm	mm	mm	mm	mm
0	1	0	0.0	0.0	0.0	0.0	0.0	0.0
4	2	1	1.0	0.4	0.6	0.4	0.3	0.6
44	3	10	1.5	0.7	1.0	0.7	0.9	0.8
89	4	20	1.7	1.3	1.6	1.2	1.7	1.3
133	5	30	2.7	2.0	2.1	1.6	2.1	2.1
178	6	40	3.6	3.0	3.2	3.2	3.7	3.4
222	7	50	4.9	4.6	4.8	4.5	4.7	4.6
267	8	60	7.0	6.7	6.7	6.7	6.9	6.8
289	9	65	8.9	8.9	9.0	9.0	9.1	9.5
311	10	70	12.5	12.3	12.7	12.7	12.9	13.2
311	11	70	13.6	13.4	13.8	13.9	14.2	14.3
311	12	70	14.7	14.3	14.5	14.8	15.0	15.2
324	13	73	16.2	16.1	16.5	16.5	16.8	17.1
336	14	75.6	17.8	17.7	18.0	18.4	18.6	19.0
347	15	78	19.4	19.7	20.0	20.2	20.7	20.8
360	16	81	21.3	21.4	21.5	21.6	22.2	22.4
373	17	84	23.7	23.1	23.6	23.8	24.3	24.4
378	18	85	25.0	25.0	25.4	25.3	26.0	25.9
390	19	87.8	26.7	26.3	26.8	26.9	27.7	27.9
400	20	90	28.4	28.5	29.0	29.0	29.3	29.6
409	21	92	30.1	30.1	30.5	30.7	31.2	31.7
418	22	94	31.9	31.8	32.4	32.3	33.0	33.5
427	23	96	33.8	33.7	34.1	34.3	35.1	35.4
440	24	99	36.7	36.6	37.0	37.0	37.4	38.0
453	25	102	39.0	39.2	39.6	39.9	40.5	41.0
467	26	105	41.6	42.0	41.9	42.4	42.0	43.7
482	27	108.5	44.7	45.0	44.7	45.0	46.0	46.4
498	28	112	47.4	47.1	47.7	48.1	48.5	49.3
511	29	115	49.7	49.7	50.1	51.0	51.5	52.1
520	30	117	52.0	52.4	52.8	53.3	54.2	54.6
533	31	120	54.8	55.0	55.3	55.8	56.5	57.6
533	32	120	56.6	56.8	57.3	57.8	58.9	60.4
502	33	113	57.4	57.3	57.8	58.7	60.2	62.5
471	34	106	57.8	58.2	59.1	59.9	61.9	65.1
453	35	102	58.8	58.9	60.1	61.0	63.8	67.9
453	36	102	59.6	60.1	61.2	62.9	65.4	70.5
453	37	102	60.4	60.9	62.1	63.9		
458	38	103	61.4	62.1	64.0	66.8		
462	39	104	62.8	63.5	65.5			
484	40	109	65.9	66.5	70.4			
493	41	111	67.6	69.0	71.4			
511	42	115	69.5	71.2				
529	43	119	70.6	72.7				
551	44	124	73.0	76.2				
564	45	127	77.0					
609	46	137	78.8					
636	47	143	80.5					
636	48	143	79.7					





Appendix B – Single Frame Material Test Data Tables and Plots

List of material test data:

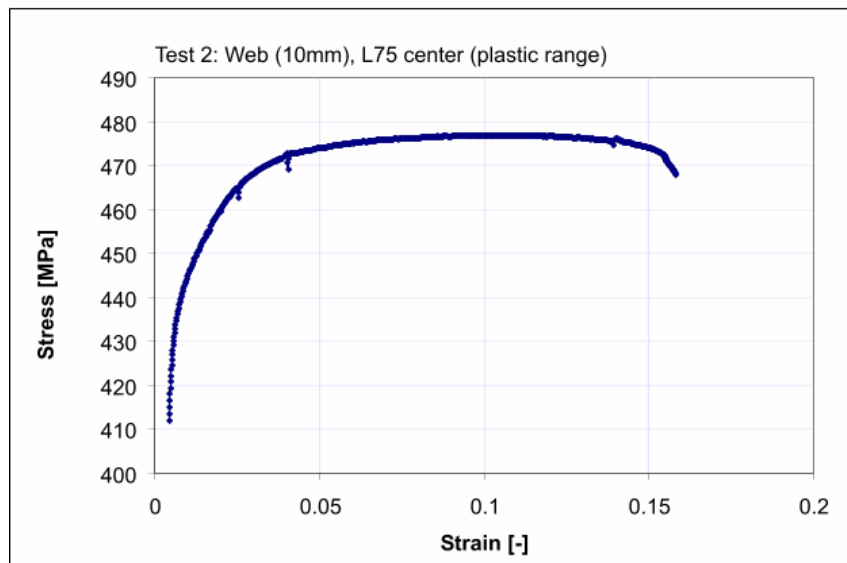
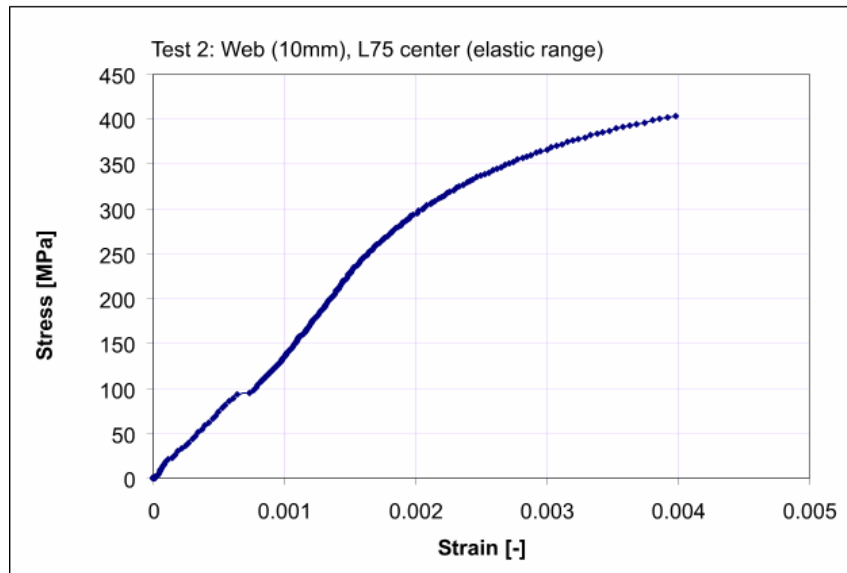
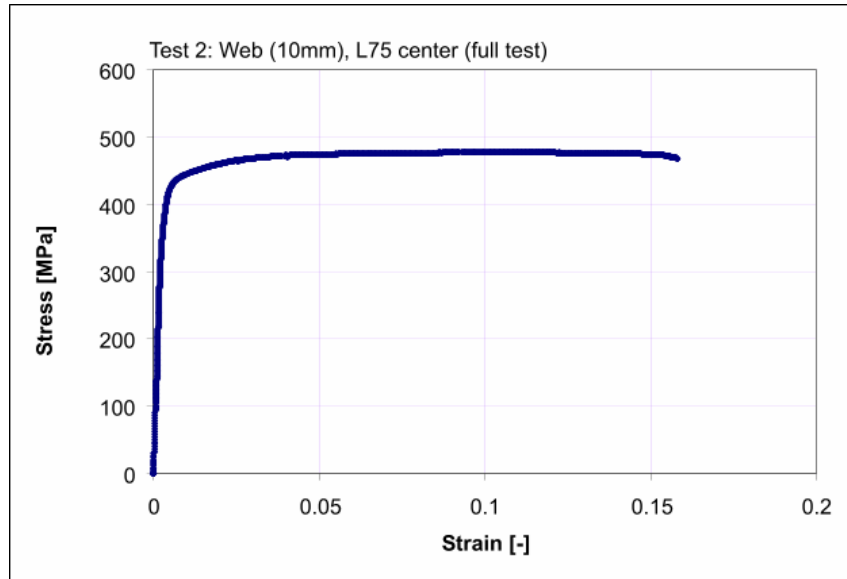
Cross Sectional Heights for 15 Steel Testing Specimens

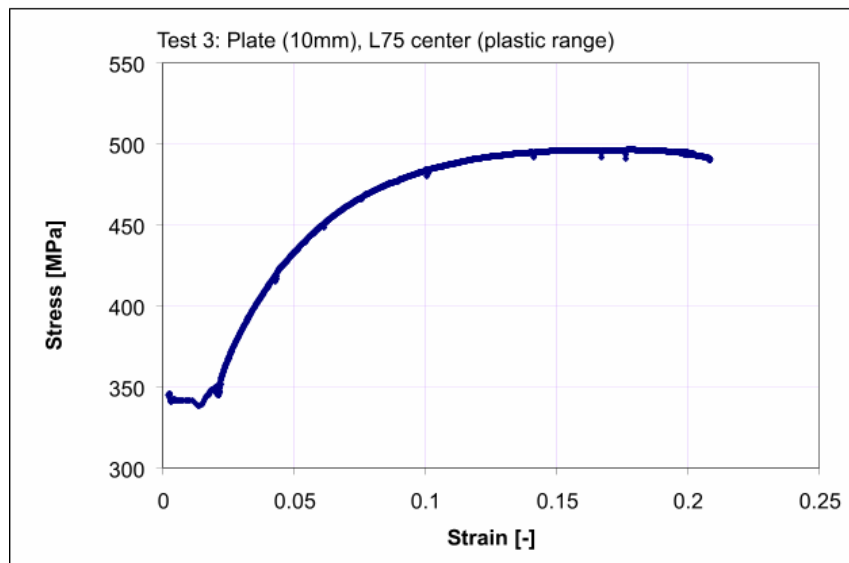
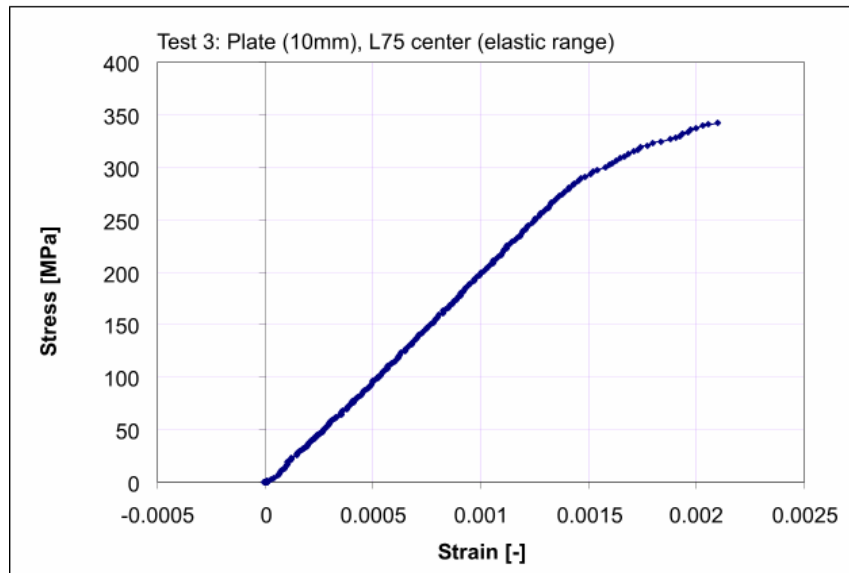
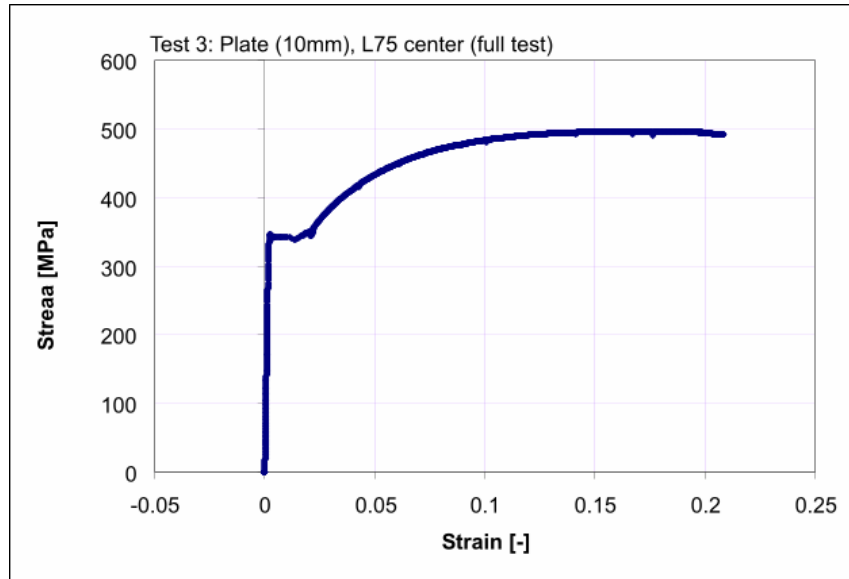
Note: It is assumed that each specimen has the same gauge length and width

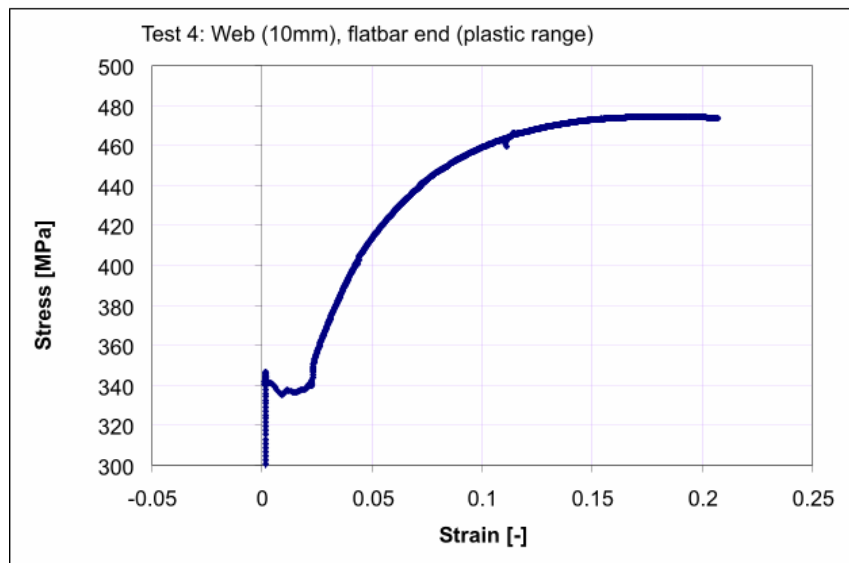
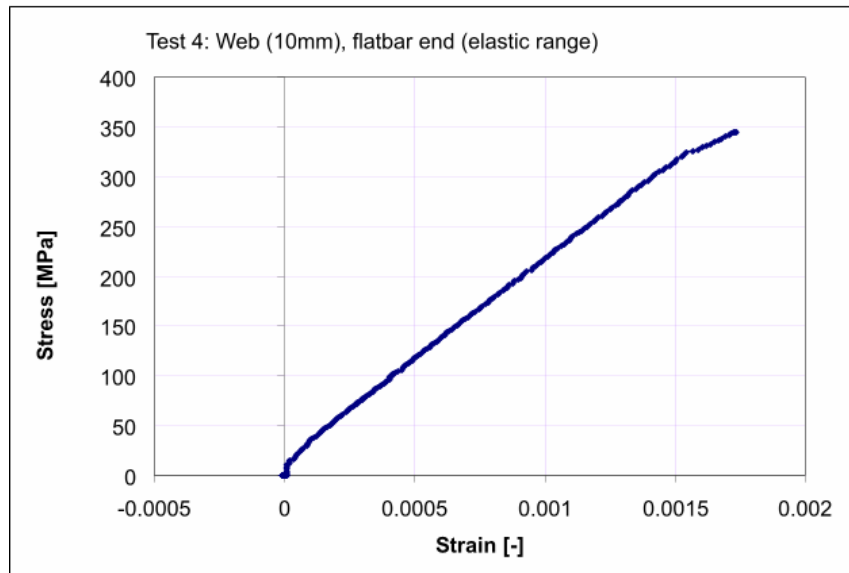
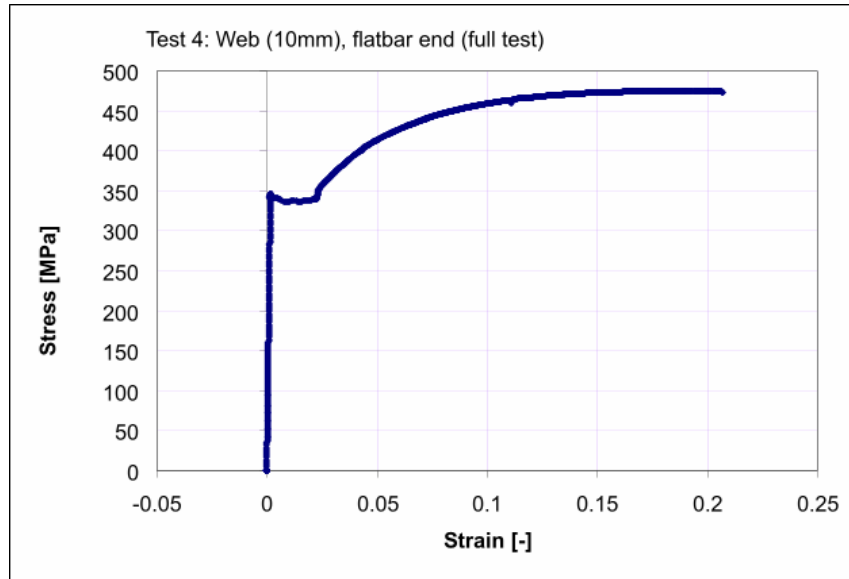
Width	12.7 mm
-------	---------

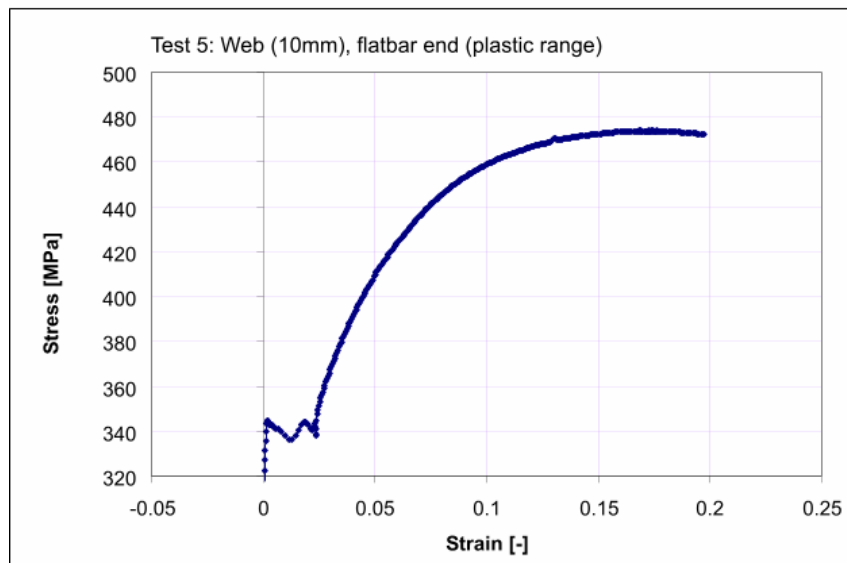
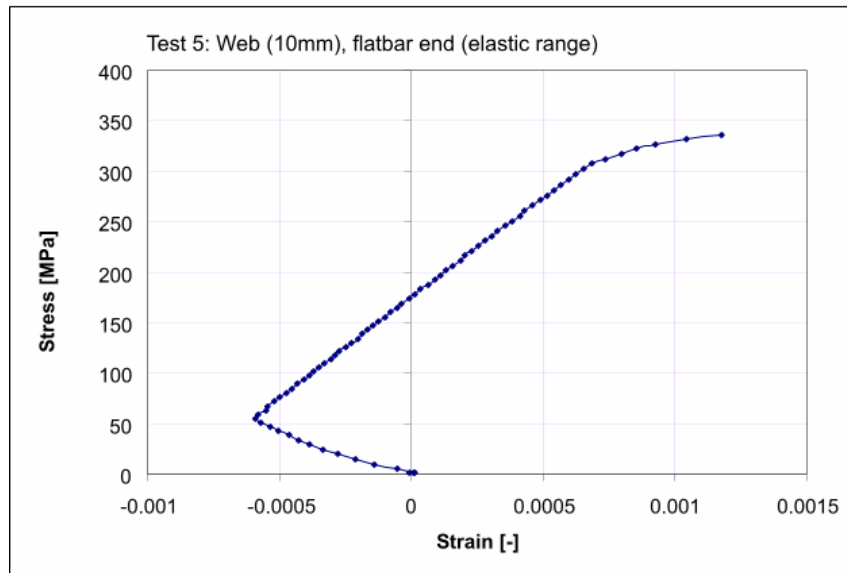
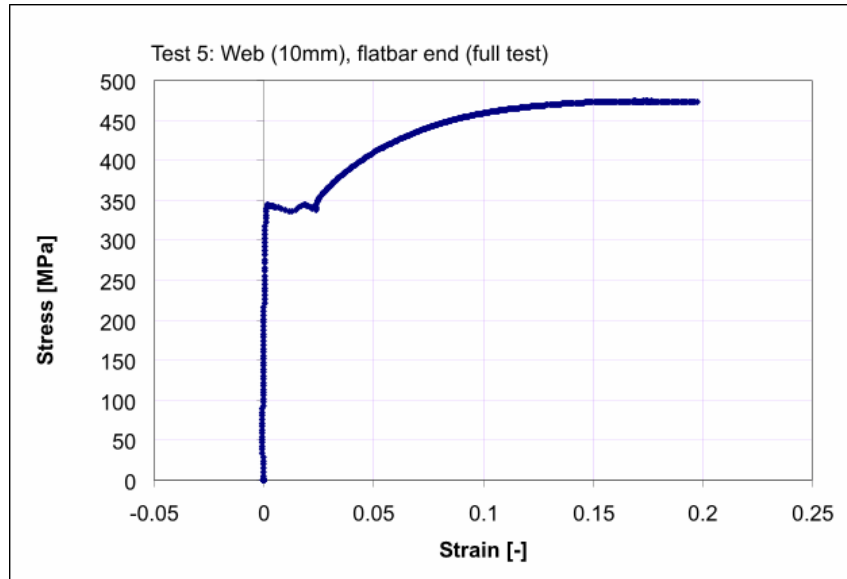
Speciman #	Cross Section 'A' (# Side) (mm)	Cross Section 'B' (mm)	Mid Cross Section (mm)	Average	Area	type	frame	t_steel [mm]	fy_approx	
1	8.702	8.579	8.687	8.66	109.93	web	L_75 cent	10	425	bad test
2	8.639	8.745	8.737	8.71	110.58	web	L_75 cent	10	300	no plateau
3	8.771	8.646	8.709	8.71	110.60	Plate	L_75 cent	10	340	
4	8.917	8.958	8.901	8.93	113.35	web	Flat end	10	340	
5	9.036	9.072	8.956	9.02	114.57	web	Flat end	10	340	
6	8.745	8.750	8.698	8.73	110.88	web	L_75 end	10	385	no plateau
7	8.851	8.663	8.720	8.74	111.06	web	L_75 end	10	405	
8	7.183	7.186	7.182	7.18	91.23	web	T_75 end	8	330	
9	7.230	7.191	7.216	7.21	91.60	web	T_75 end	8	320	
10	7.515	6.586	7.175	7.09	90.07	web	T_75 cent	8	320	
11	8.762	8.772	8.757	8.76	111.30	Plate	Flat end	10	290	
12	8.758	8.723	8.688	8.72	110.78	Plate	Flat end	10	280	
13	9.012	8.937	8.984	8.98	114.02	Plate	T_75 end	10	280	
14	8.697	8.719	8.691	8.70	110.52	Plate	L_75 end	10	360	bad test
15	8.752	8.635	8.698	8.70	110.43	web	L_75 cent	10	350	no plateau

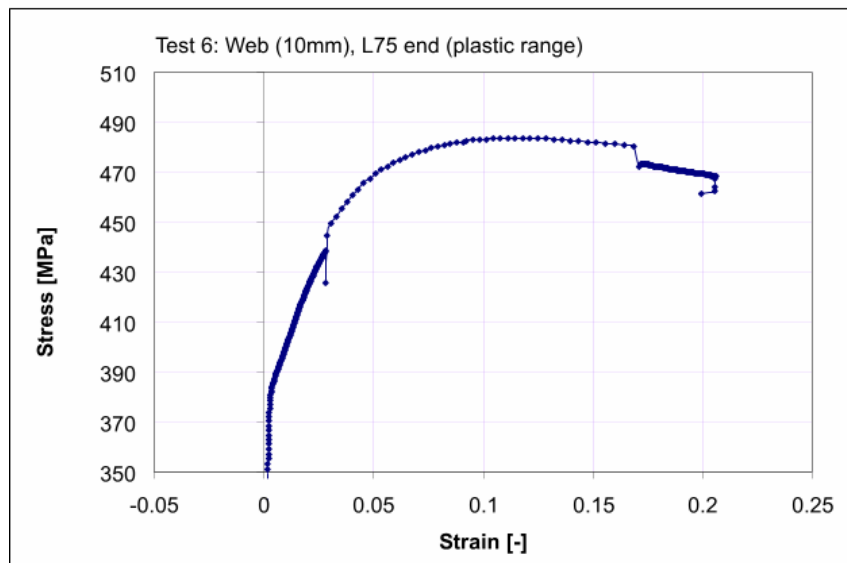
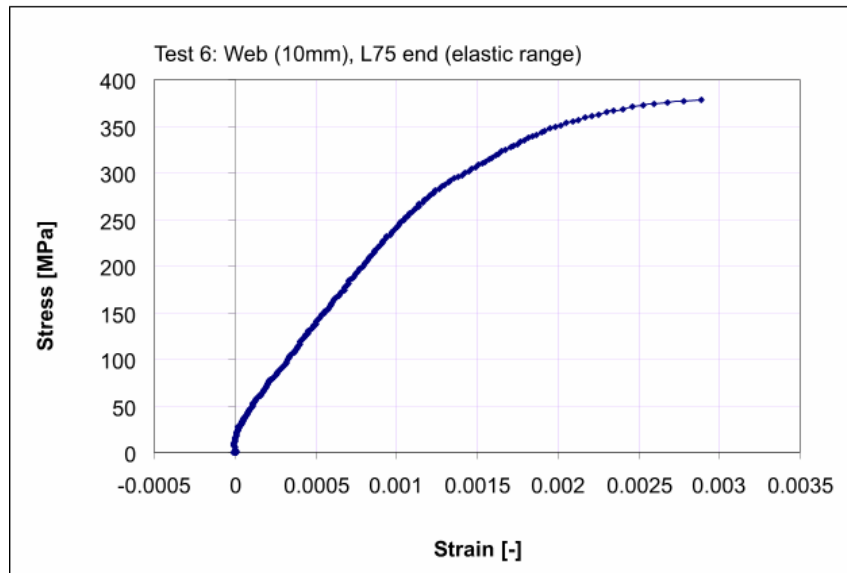
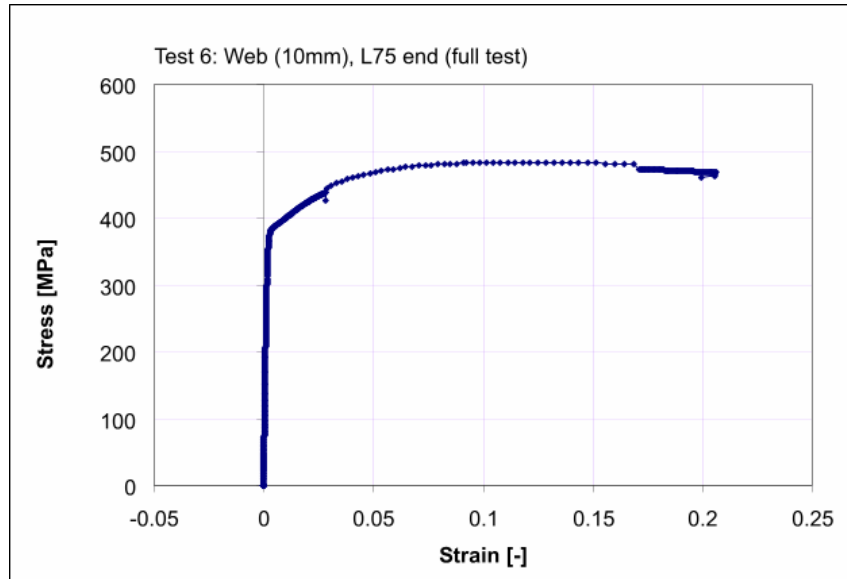
The following pages contain plots of the stress-strain curves from the tensile material tests. Each page contains three plots from one test. The first plot covers the whole stress and strain range. The second covers the initial elastic portion and the third covers the post-yield portion. These allow the reader to see the details better.

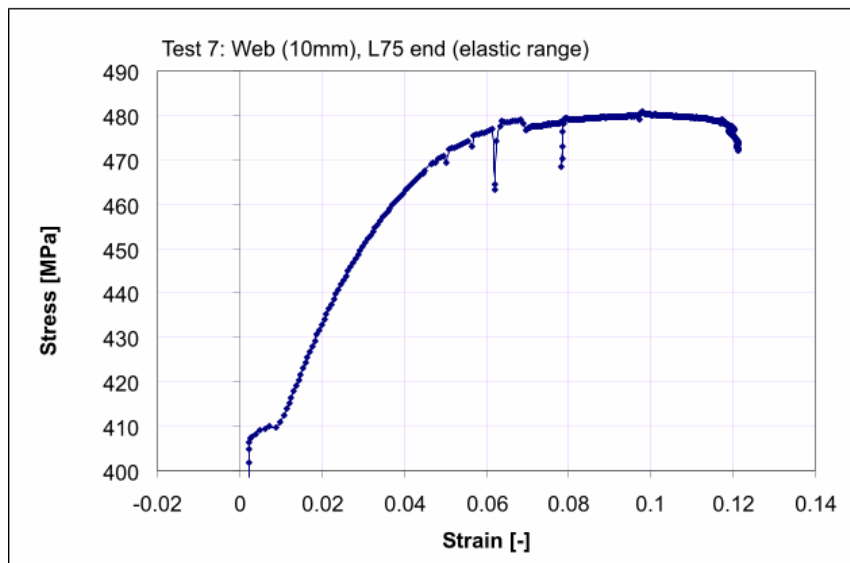
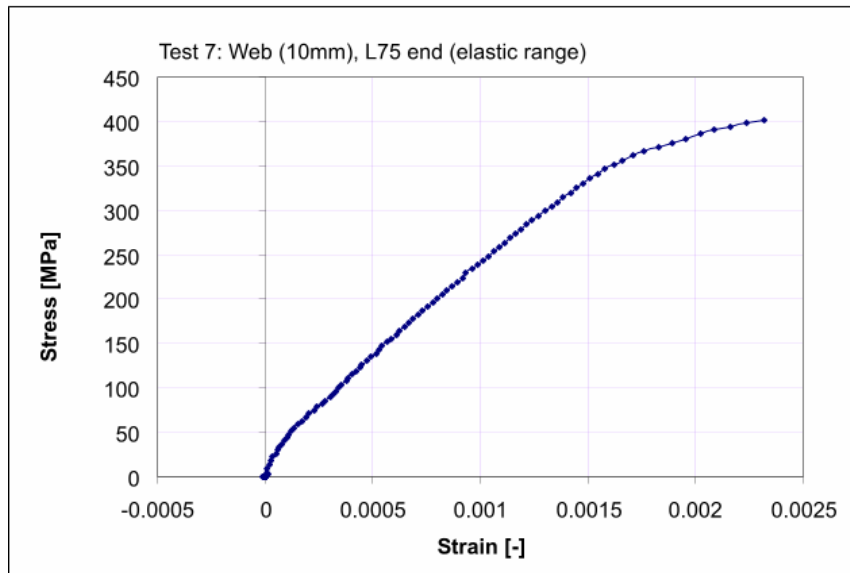
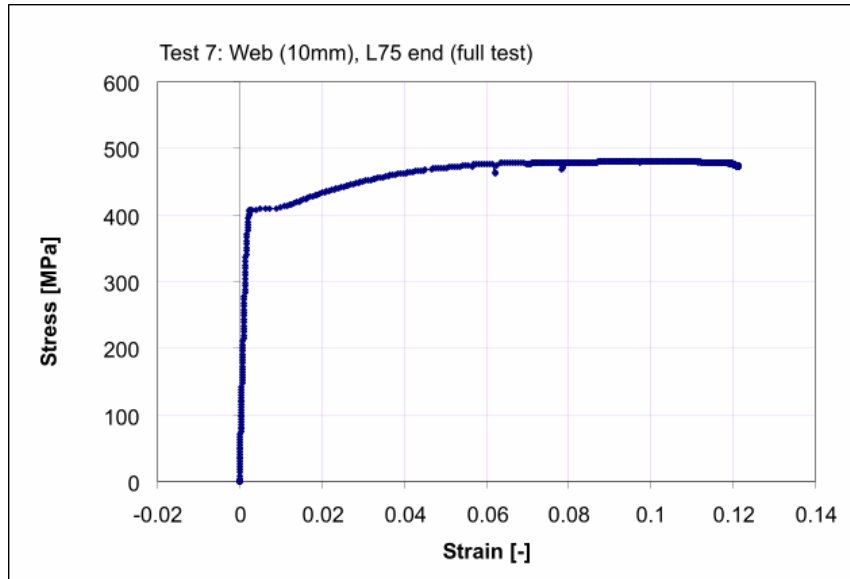


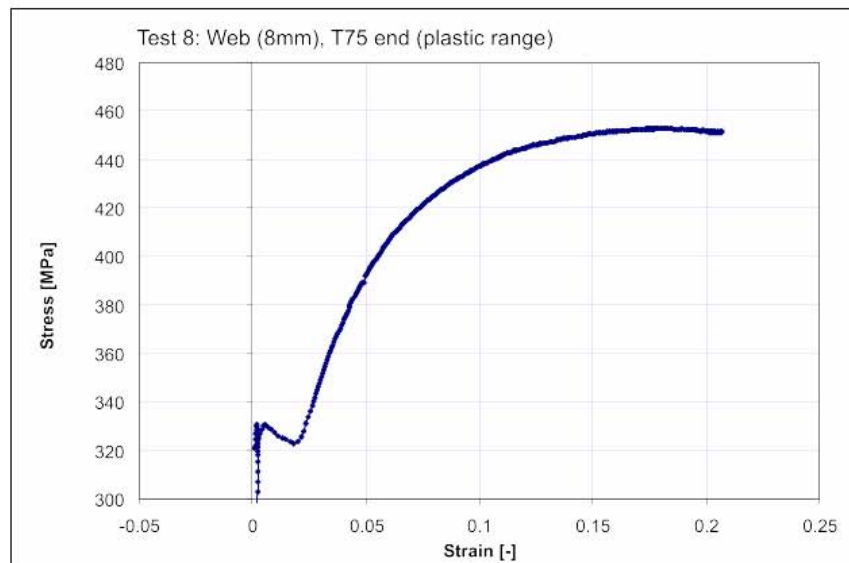
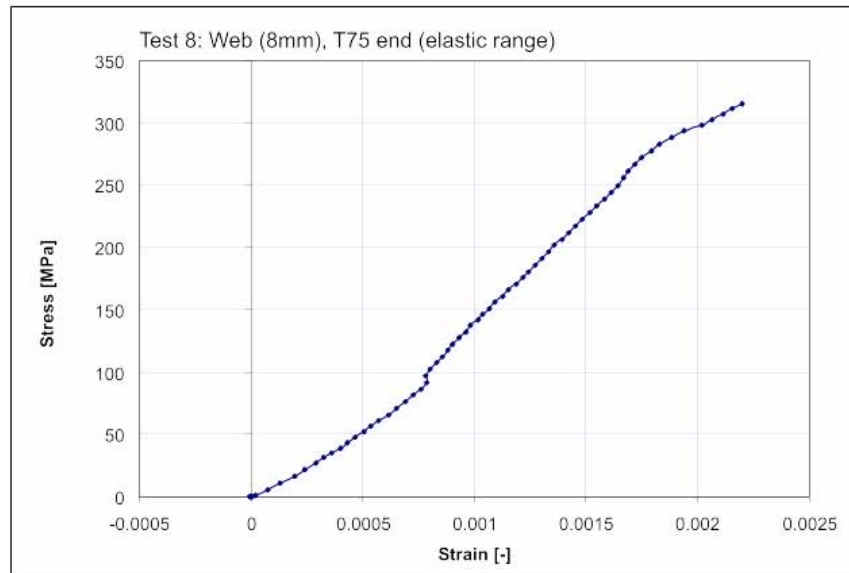
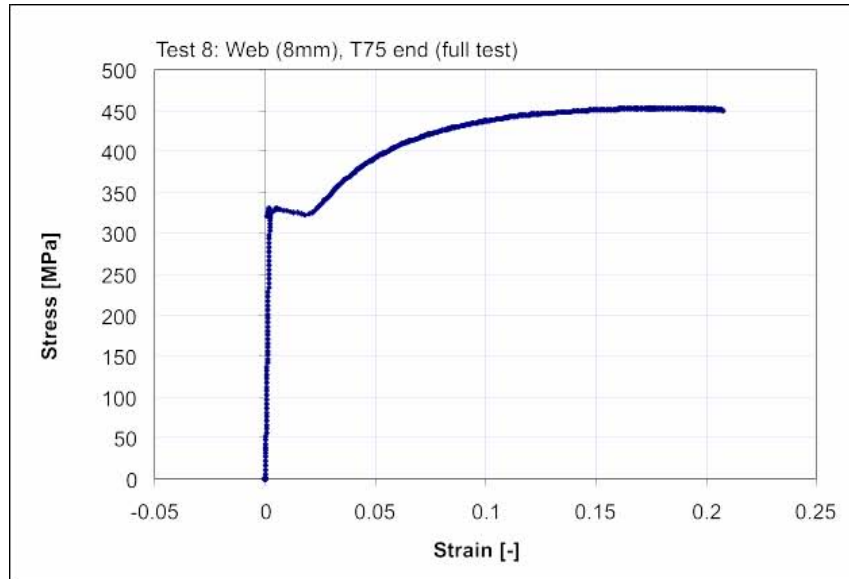


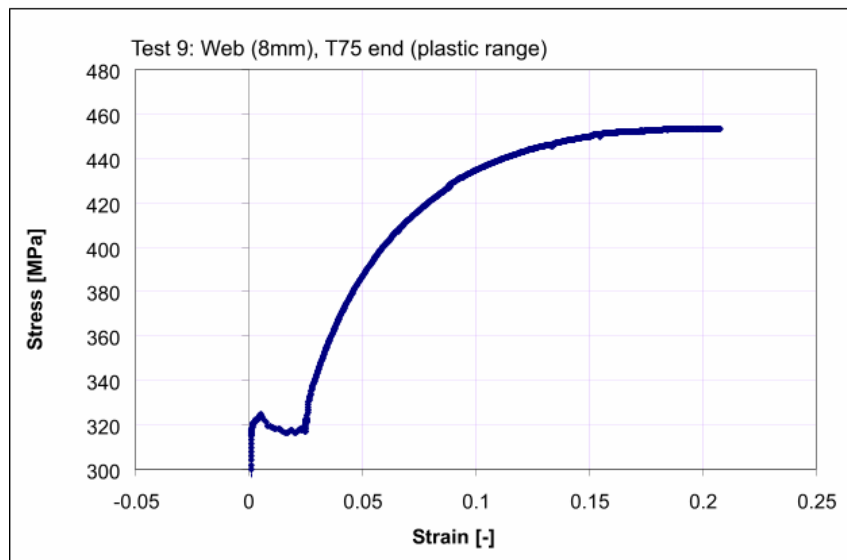
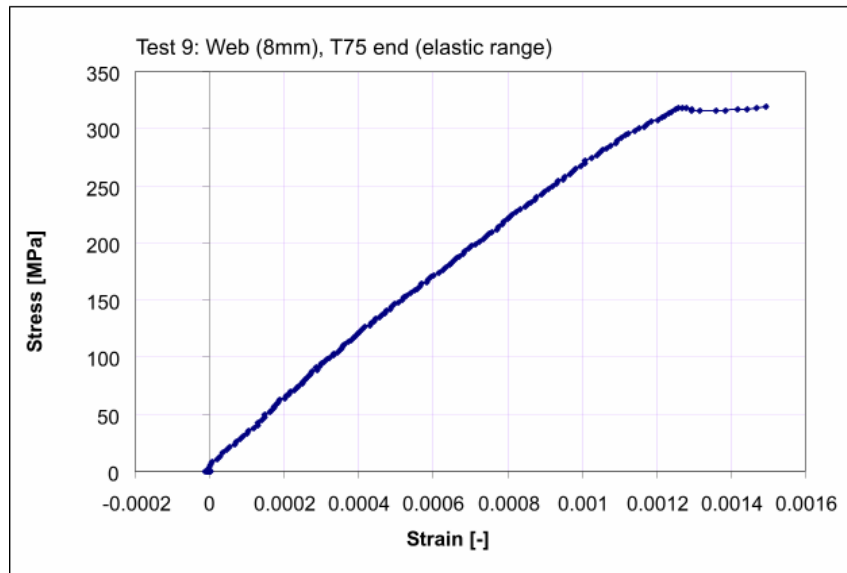
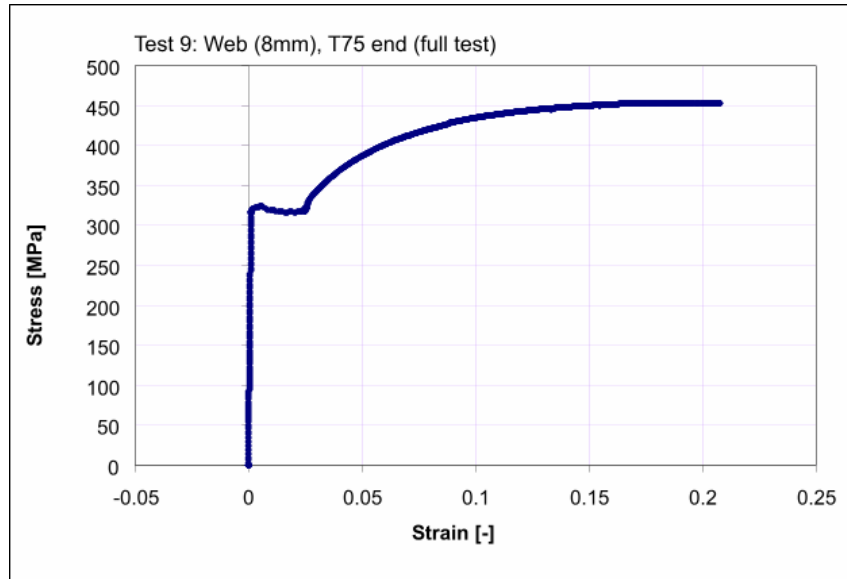


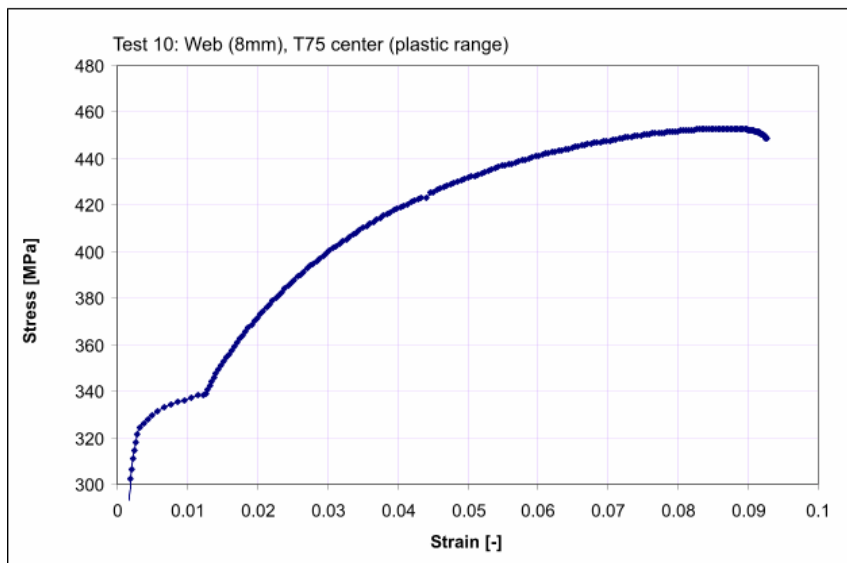
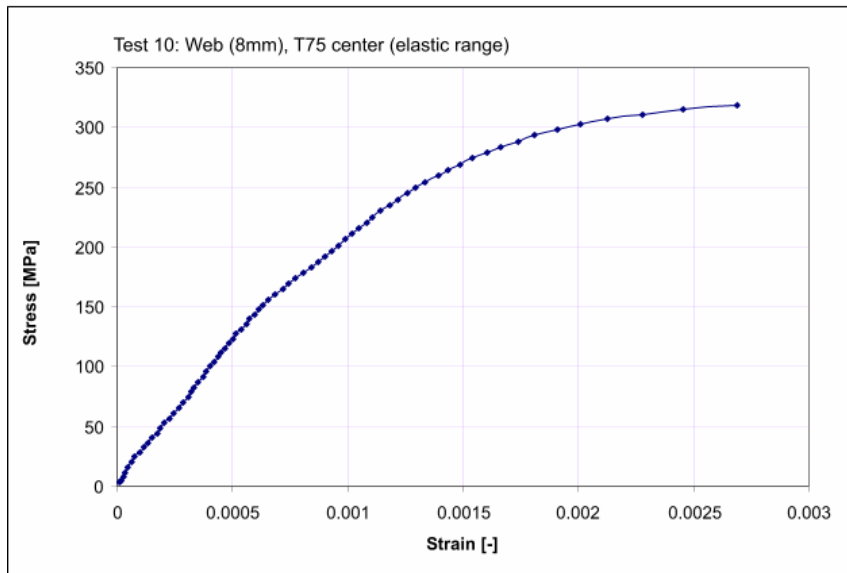
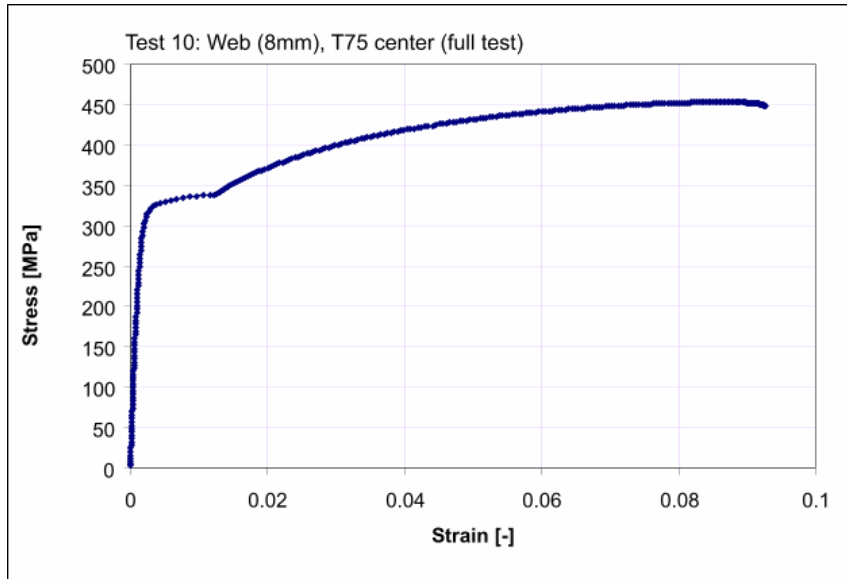


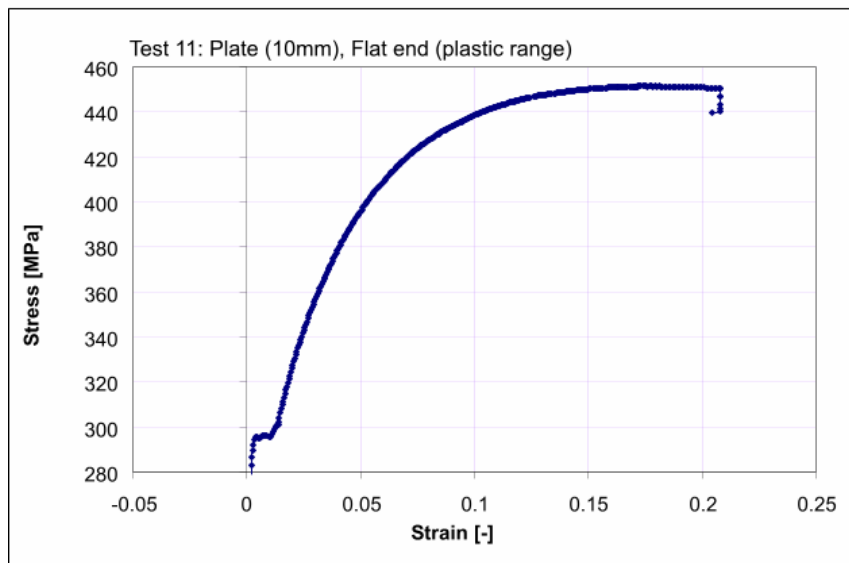
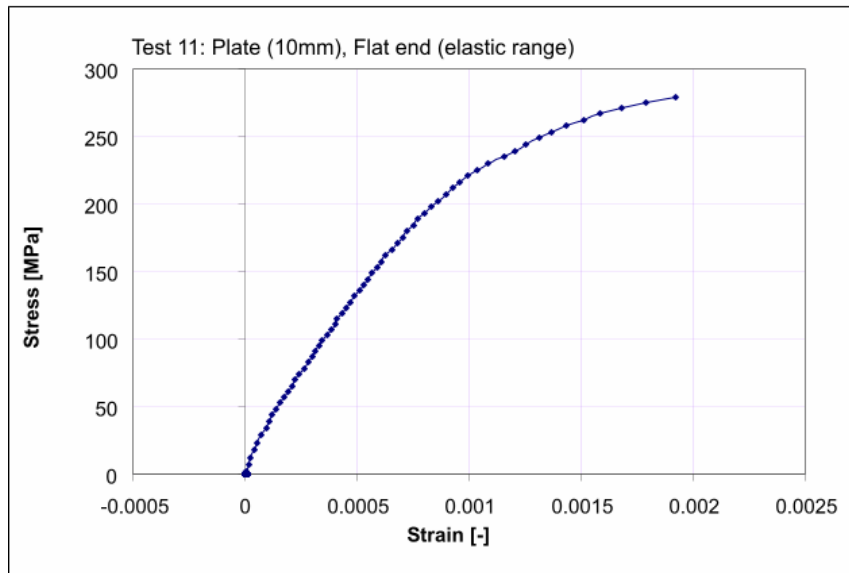
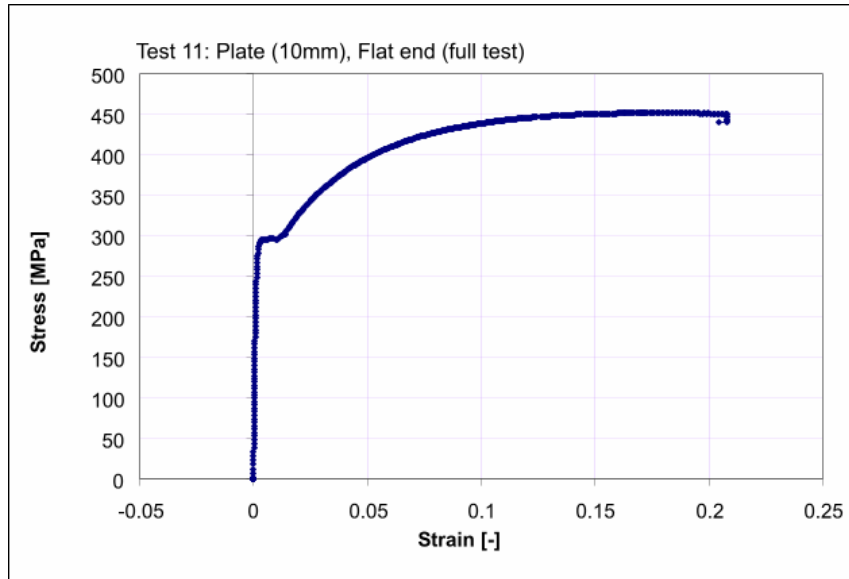


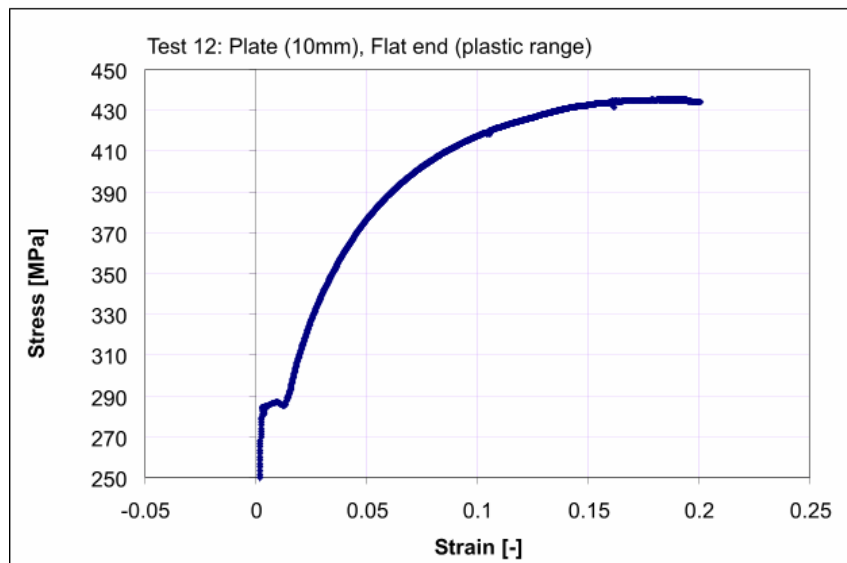
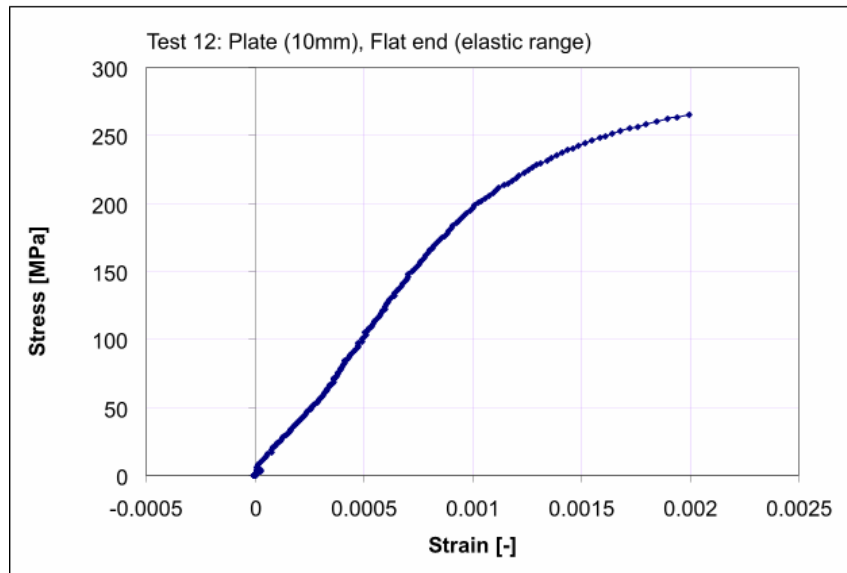
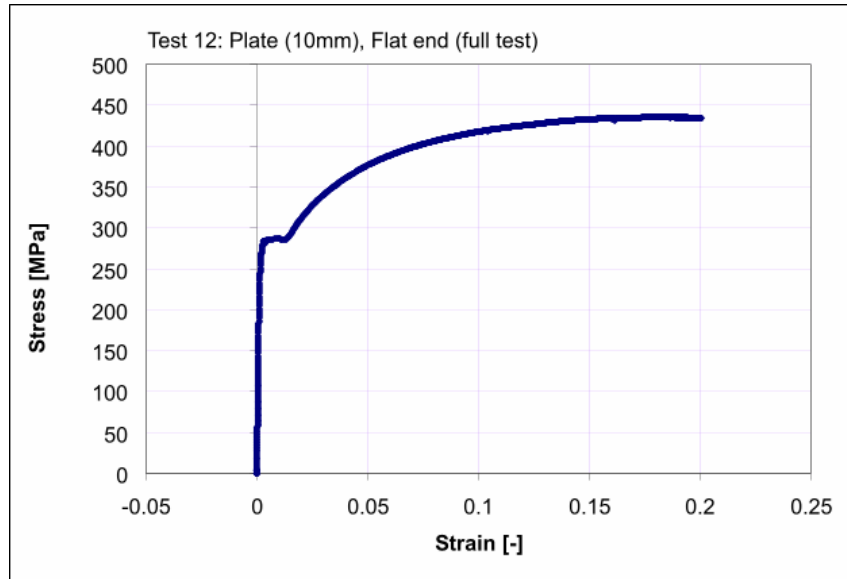


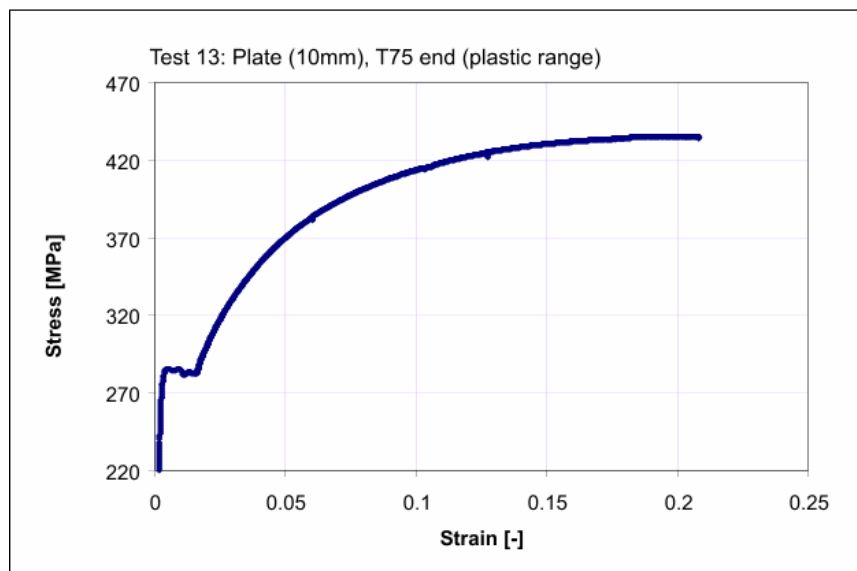
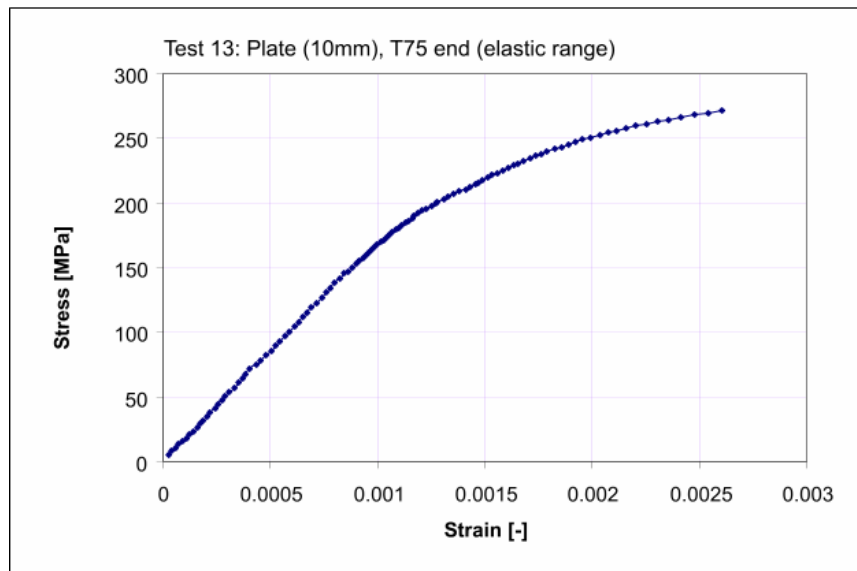
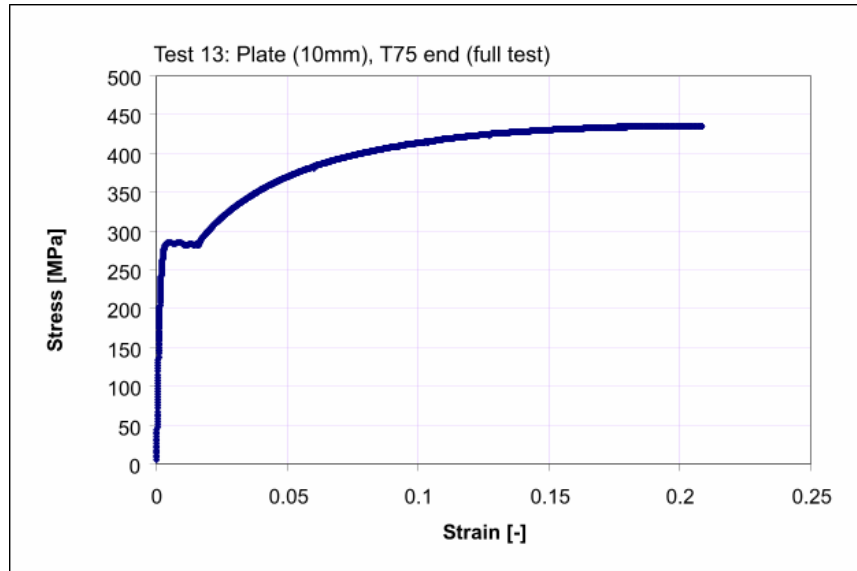


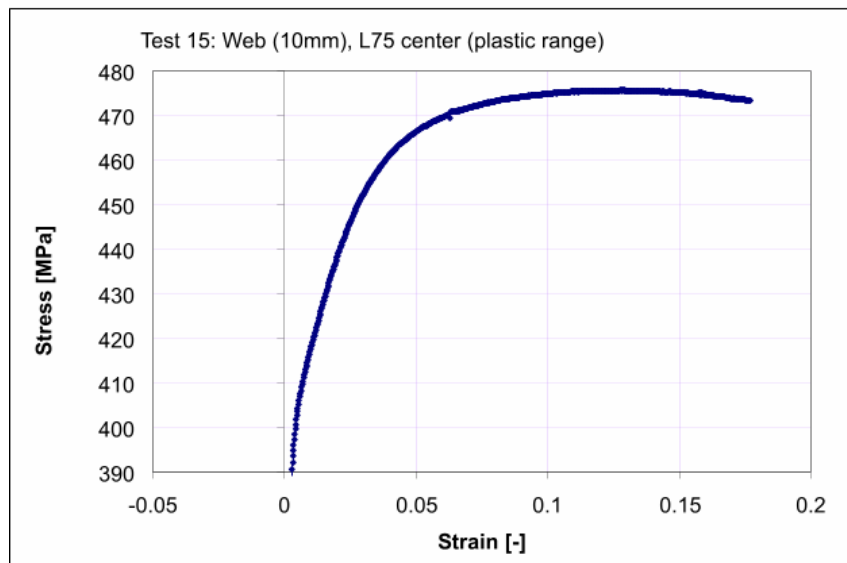
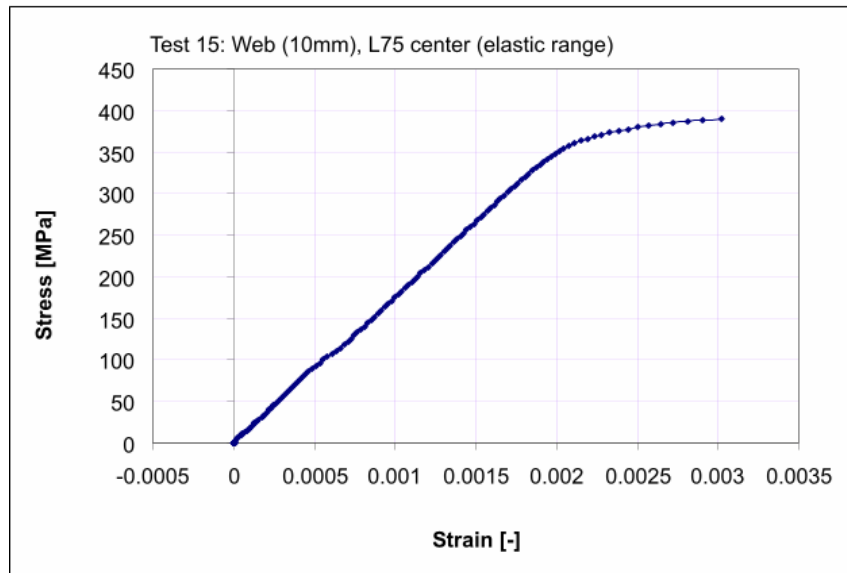
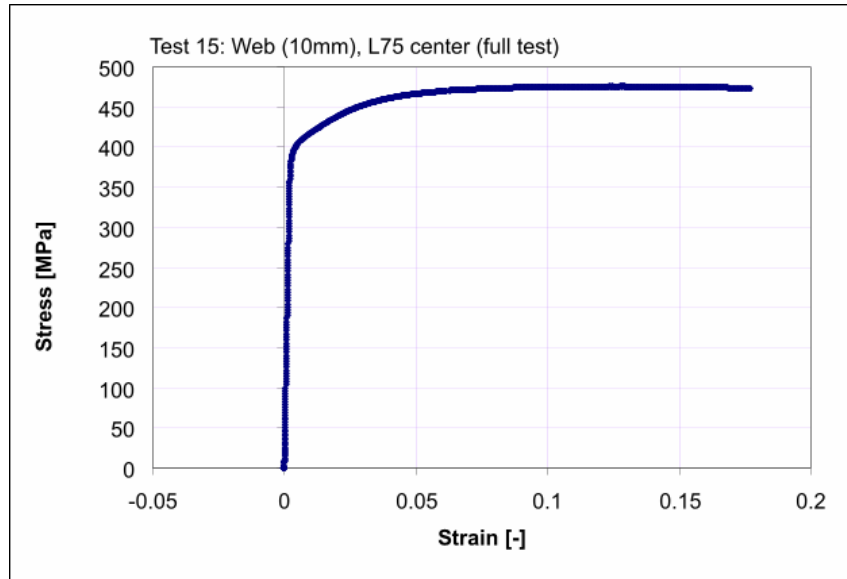












Appendix C – Large Grillage Test Data Tables and Plots



Figure C1 Large Grillage

Table C1 List of test data:

Test Name	Load Position	Test Date	Frame Description*
LG1_1	North End	10/26/2006	200x8,75x10 T
LG1_2	South End	11/23/2006	200x8,75x10 T
LG1_3	Center	11/30/2006	200x8,75x10 T
LG2_1	Center	4/20/2007	200x8,75x10 T
LG2_2	South End	5/23/2007	200x8,75x10 T
LG2_3	North End	6/7/2007	200x8,75x10 T
LG2_4	West Center	7/11/2007	200x8,75x10 T

The plots given in the following pages are for the seven large grillage tests, as listed above. The force is determined from the hydraulic ram, and the deflection is the ram deflection. As well, the deflections measured with the micro-scribe are indicated with “mS”.

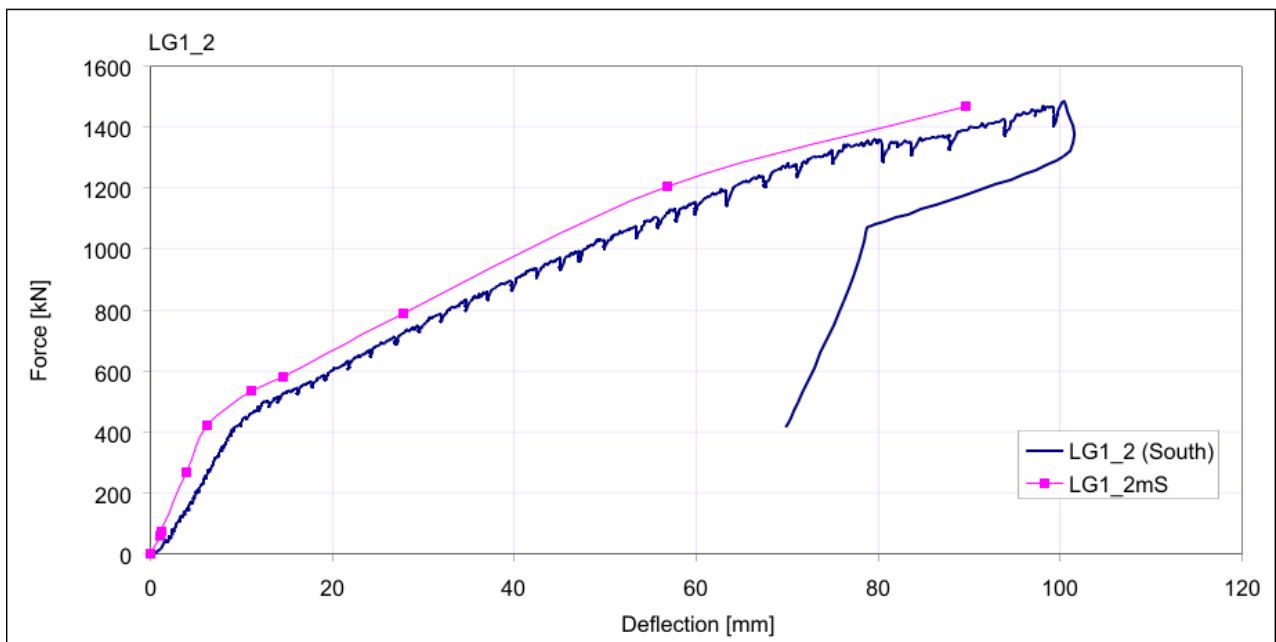
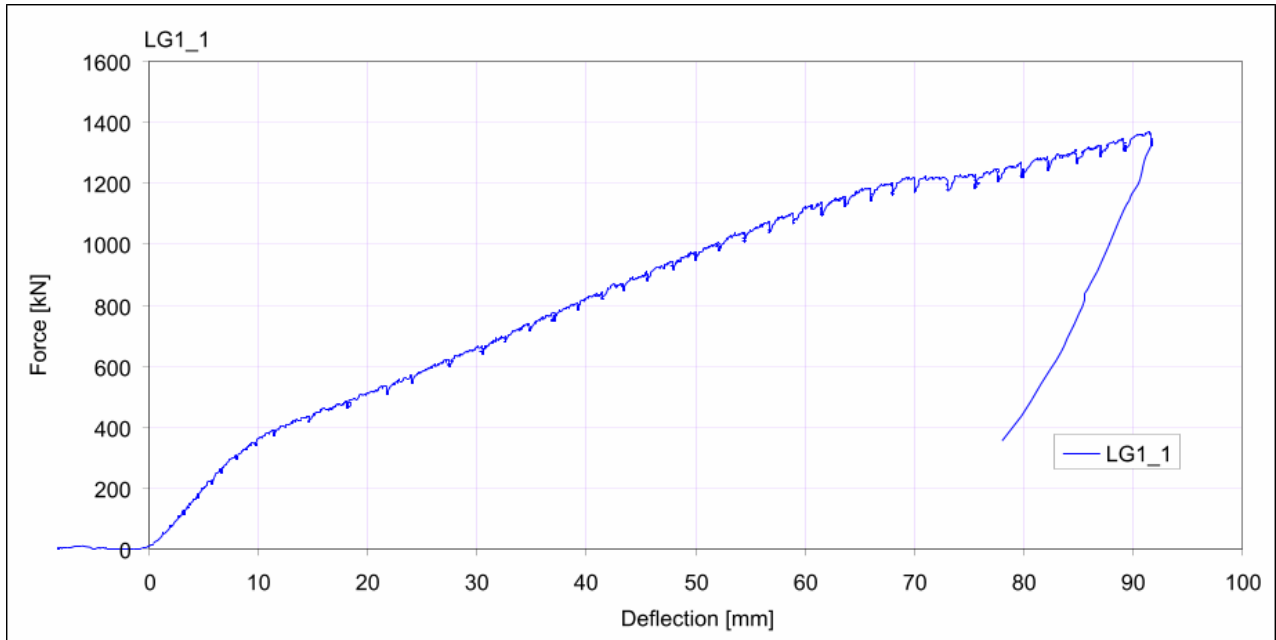
Table C2 Microscribe Load-Deflection Data for Test LG1_2

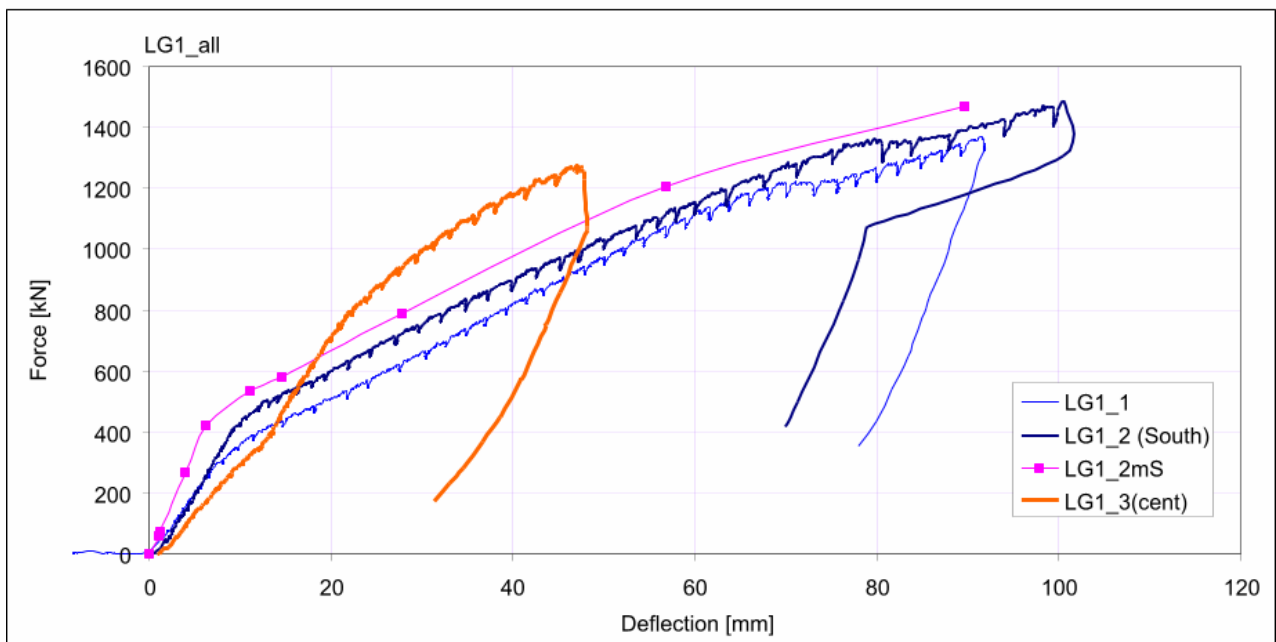
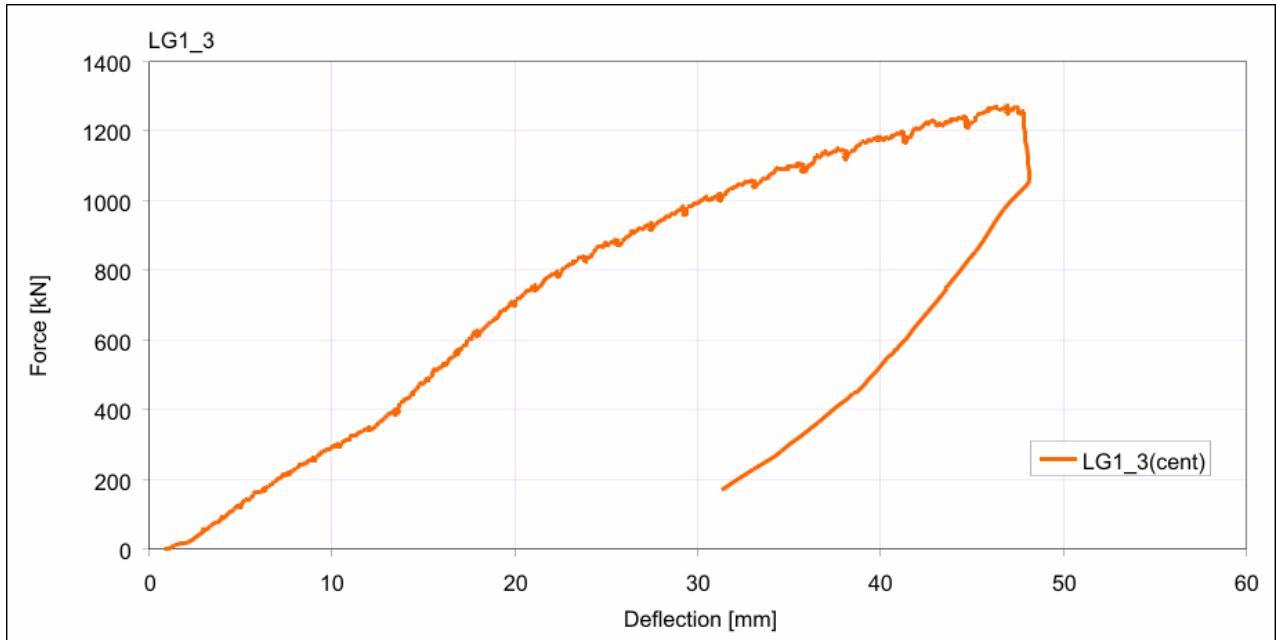
LG1_2: MicroScribe Data

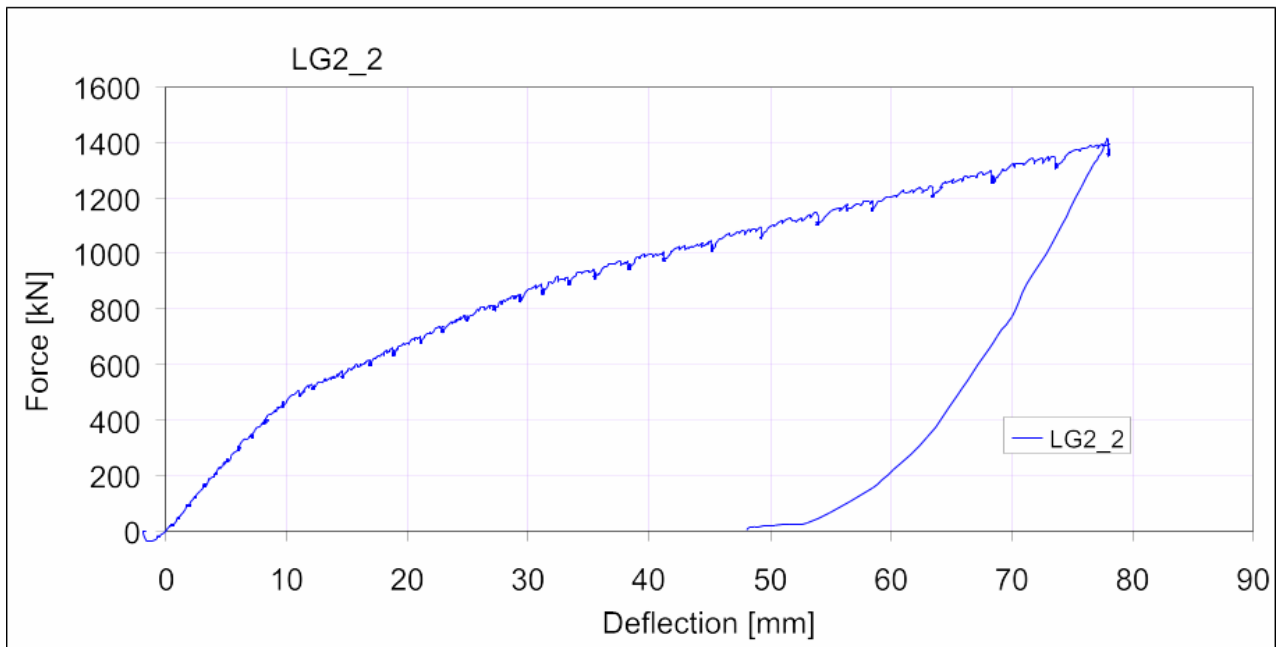
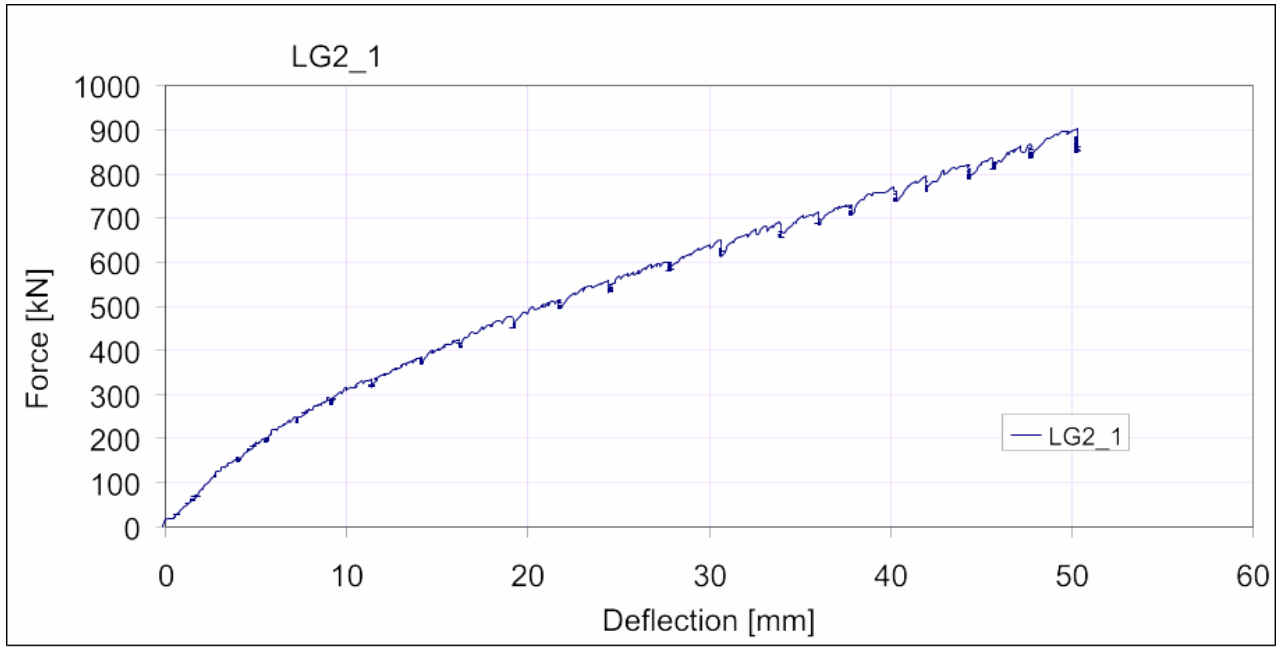
Load kN	Deflection mm
0	0
58.19	1.07
71.94	1.28
267.42	4.02
423.19	6.25
533.76	11.02
578.38	14.54
787.74	27.85
1205.41	56.84
1467.84	89.65

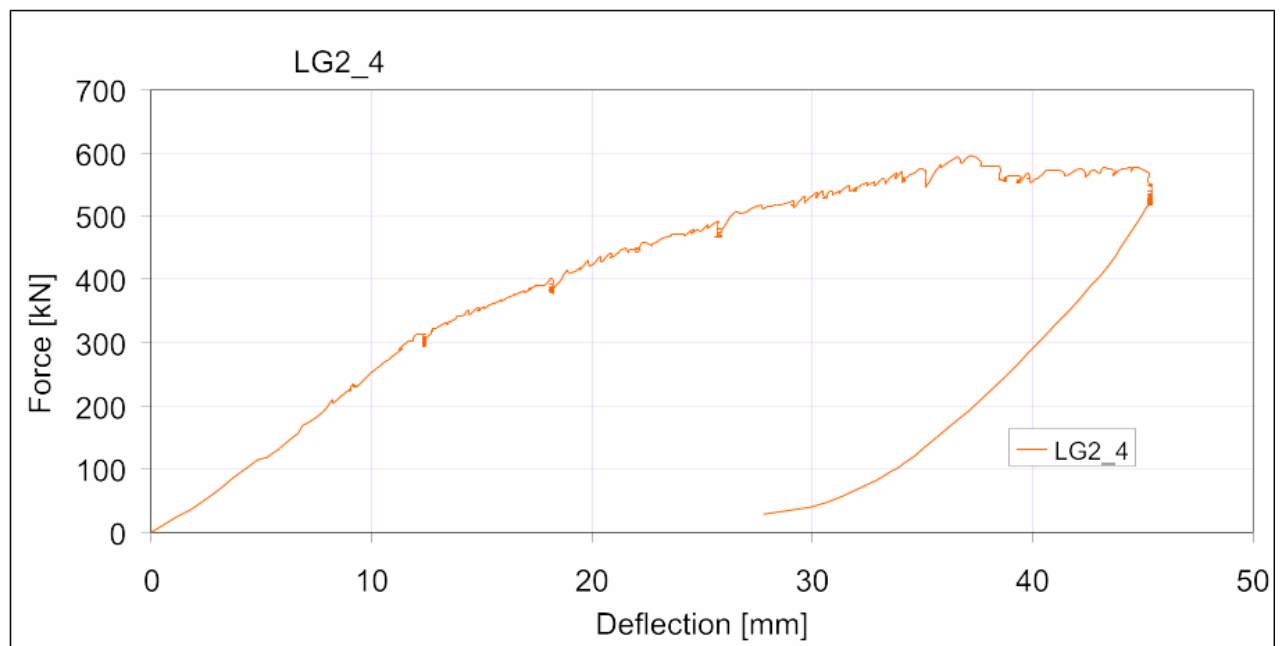
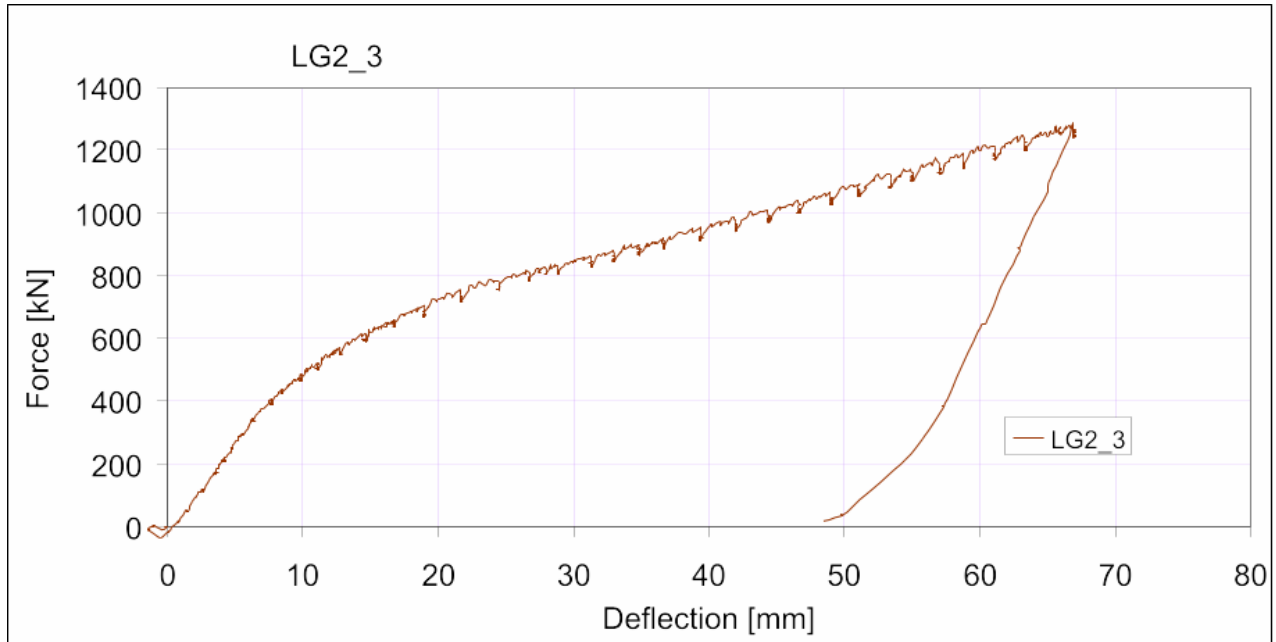
Table C3 Microscribe Load-Deflection Data for Test LG2_1,2,3

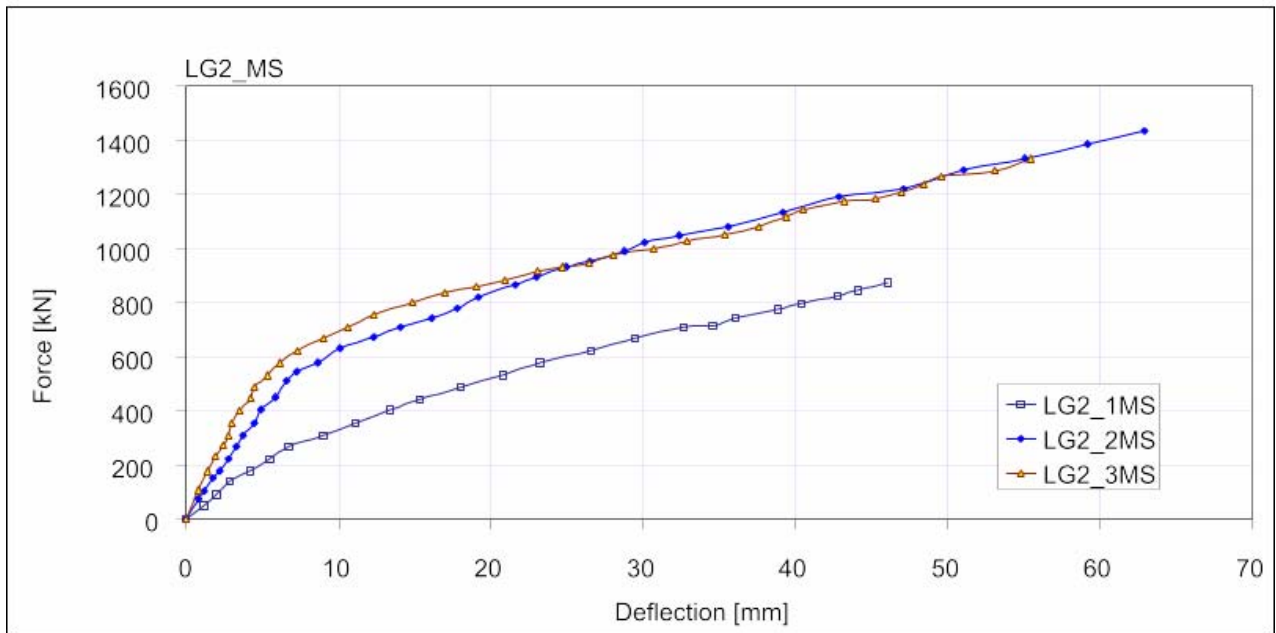
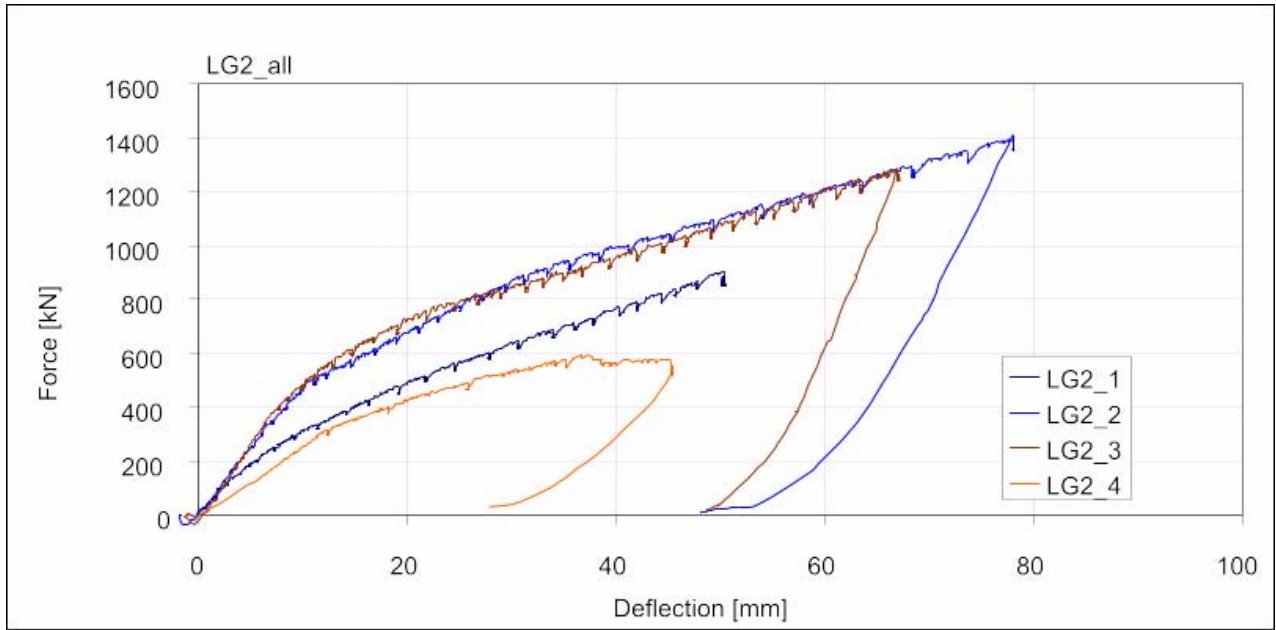
LG2_1M S		LG2_2M S		LG2_3M S	
Deflection [mm]	Force (kN)	Deflection [mm]	Force (kN)	Deflection [mm]	Force (kN)
0	0	0.0	0	0.0	0.0
1.14	50.5	0.8	75.5	0.8	106.6
1.99	90.1	1.2	102.1	1.4	177.6
2.86	138.9	1.8	151.0	1.9	230.9
4.18	178.5	2.2	177.6	2.4	270.8
5.49	222.7	2.8	222.0	2.8	310.8
6.74	266.9	3.3	266.4	3.0	355.2
9.04	311.1	3.7	310.8	3.5	399.6
11.14	355.2	4.5	355.2	4.3	444.0
13.38	402.6	4.9	404.0	4.5	488.4
15.3	440.7	5.9	448.4	5.4	532.8
18.04	486.5	6.6	510.6	6.1	577.2
20.81	533.0	7.2	546.1	7.3	621.6
23.22	577.4	8.6	577.2	9.0	666.0
26.58	622.1	10.1	630.5	10.6	710.4
29.46	670.0	12.3	670.4	12.3	754.8
32.65	710.6	14.1	710.4	14.8	799.2
34.58	715.1	16.1	741.5	17.0	839.2
36.04	742.6	17.8	781.4	19.1	856.9
38.82	774.6	19.2	821.4	20.9	883.6
40.33	797.5	21.6	865.8	23.0	914.6
42.73	824.9	23.0	896.9	24.7	932.4
44.09	843.6	25.0	932.4	26.4	945.7
46.07	873.7	26.5	954.6	28.1	976.8
		28.8	990.1	30.7	999.0
		30.1	1021.2	32.9	1025.6
		32.4	1047.8	35.4	1052.3
		35.6	1078.9	37.5	1078.9
		39.2	1132.2	39.4	1118.9
		42.9	1189.9	40.5	1141.1
		47.1	1221.0	43.2	1176.6
		51.1	1292.0	45.2	1185.5
		55.1	1332.0	46.9	1207.7
		59.2	1385.3	48.4	1238.8
		62.9	1434.1	49.6	1265.4
				53.1	1287.6
				55.4	1332.0

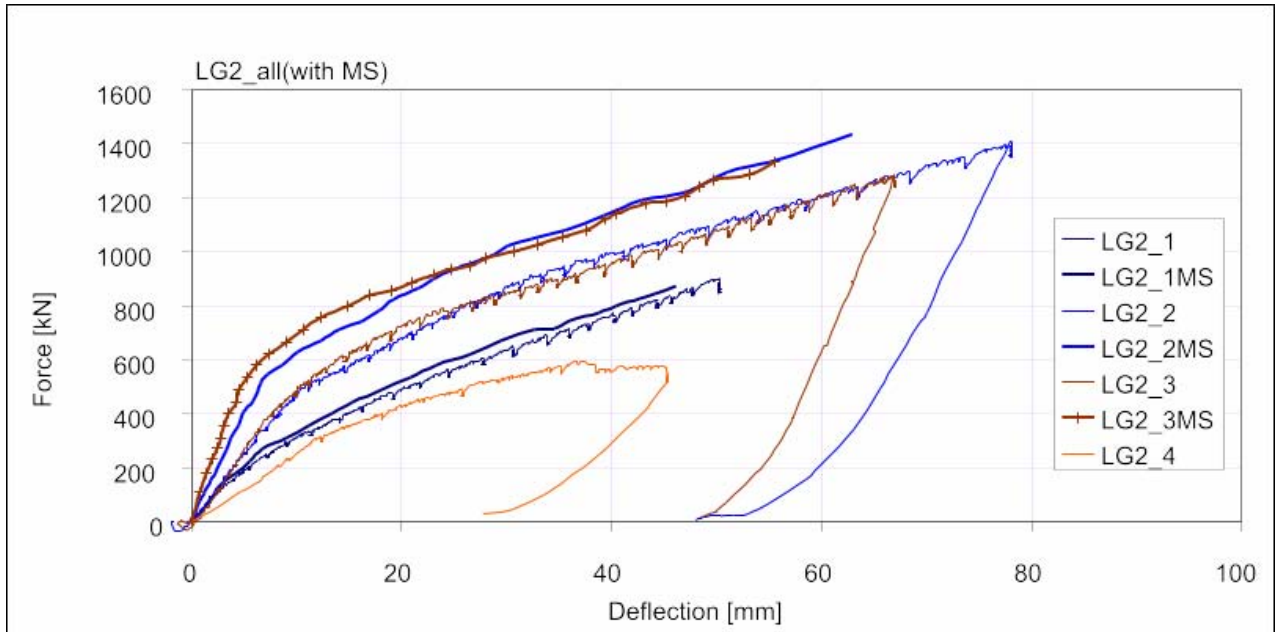












SHIP STRUCTURE COMMITTEE LIAISON MEMBERS

LIAISON MEMBERS

American Society of Naval Engineers	Captain Dennis K. Kruse (USN Ret.)
Bath Iron Works	Mr. Steve Tarpay
Colorado School of Mines	Dr. Stephen Liu
Edison Welding Institute	Mr. Rich Green
International Maritime Organization	Mr. Igor Ponomarev
Int'l Ship and Offshore Structure Congress	Dr. Alaa Mansour
INTERTANKO	Mr. Dragos Rauta
Massachusetts Institute of Technology	
Memorial University of Newfoundland	Dr. M. R. Haddara
National Cargo Bureau	Captain Jim McNamara
National Transportation Safety Board - OMS	Dr. Jack Spencer
Office of Naval Research	Dr. Yapa Rajapaksie
Oil Companies International Maritime Forum	Mr. Phillip Murphy
Samsung Heavy Industries, Inc.	Dr. Satish Kumar
United States Coast Guard Academy	Commander Kurt Colella
United States Merchant Marine Academy	William Caliendo / Peter Web
United States Naval Academy	Dr. Ramswar Bhattacharyya
University of British Columbia	Dr. S. Calisal
University of California Berkeley	Dr. Robert Bea
Univ. of Houston - Composites Eng & Appl.	
University of Maryland	Dr. Bilal Ayyub
University of Michigan	Dr. Michael Bernitsas
Virginia Polytechnic and State Institute	Dr. Alan Brown
Webb Institute	Prof. Roger Compton

RECENT SHIP STRUCTURE COMMITTEE PUBLICATIONS

Ship Structure Committee Publications on the Web - All reports from SSC 1 to current are available to be downloaded from the Ship Structure Committee Web Site at URL:

<http://www.shipstructure.org>

SSC 445 – SSC 393 are available on the SSC CD-ROM Library. Visit the National Technical Information Service (NTIS) Web Site for ordering hard copies of all SSC research reports at

URL: <http://www.ntis.gov>

SSC Report Number	Report Bibliography
SSC 456	Buckling Collapse Testing on Friction Stir Welded Aluminum Stiffened Plate Structures, Paik J.K. 2009
SSC 455	Feasibility, Conceptual Design and Optimization of a Large Composite Hybrid Hull, Braun D., Pejicic M. 2008
SSC 454	Ultimate Strength and Optimization of Aluminum Extrusions, Collette M., Wang C. 2008
SSC 453	Welding Distortion Analysis Of Hull Blocks Using Equivalent Load Method Based On Inherent Strain, Jang C.D. 2008
SSC 452	Aluminum Structure Design and Fabrication Guide, Sielski R.A. 2007
SSC 451	Mechanical Collapse Testing on Aluminum Stiffened Panels for Marine Applications, Paik J.K. 2007
SSC 450	Ship Structure Committee: Effectiveness Survey, Phillips M.L., Buck R., Jones L.M. 2007
SSC 449	Hydrodynamic Pressures and Impact Loads for High Speed Catamaran / SES, Vorus W. 2007
SSC 448	Fracture Mechanics Characterization of Aluminum Alloys for Marine Structural Applications, Donald J.K., Blair A. 2007
SSC 447	Fatigue and Fracture Behavior of Fusion and Friction Stir Welded Aluminum Components, Kramer R. 2007
SSC 446	Comparative Study of Naval and Commercial Ship Structure Design Standards, Kendrick A., Daley C. 2007
SSC 445	Structural Survivability of Modern Liners, Iversen R. 2005
SSC 444	In-Service Non-Destructive Estimation of the Remaining Fatigue Life of Welded Joints, Dexter R.J., Swanson K.M., Shield C.K. 2005
SSC 443	Design Guidelines for Doubler Plate Repairs on Ship Structures Sensharma P.K., Dinovitzer A., Traynham Y. 2005